

# PHASE 2 INITIAL BOREHOLE DRILLING AND TESTING, IGNACE AREA

*Thin Section Petrography and Lithogeochemical  
Analysis of Core Samples from IG\_BH02 and  
IG\_BH03*

APM-REP-01332-0376

June 2020

**Nuclear Waste Management Organization**

**nwmo**

NUCLEAR WASTE  
MANAGEMENT  
ORGANIZATION

SOCIÉTÉ DE GESTION  
DES DÉCHETS  
NUCLÉAIRES

**Nuclear Waste Management Organization**

22 St. Clair Avenue East, 4<sup>th</sup> Floor

Toronto, Ontario

M4T 2S3

Canada

Tel: 416-934-9814

Web: [www.nwmo.ca](http://www.nwmo.ca)

**Phase 2 Initial Borehole Drilling and Testing, Ignace Area.**

**Thin Section Petrography and Lithogeochemical Analysis of Core Samples from IG\_BH02 and IG\_BH03**

**APM-REP-01332-0376**

June 2020

**Nuclear Waste Management Organization**

## Document History

Title:	Phase 2 Initial Borehole Drilling and Testing, Ignace Area. Thin Section Petrography and Lithogeochemical Analysis of Core Samples from IG_BH02 and IG_BH03		
Report Number:	APM-REP-01332-0376		
Revision:	R000	Date:	June 2020
Author Company(s)	Nuclear Waste Management Organization		
Authored by:	Nuclear Waste Management Organization (NWMO)		
Accepted by:	Sarah Hirschorn (Geoscience Director)		

<b>Revision Summary</b>		
<b>Revision Number</b>	<b>Date</b>	<b>Description of Changes/Improvements</b>
R001	2022-12	Initial issue

## 1. INTRODUCTION

Lithogeochemistry and optical petrography provides important information about the composition, petrogenesis, alteration, and deformation of the host and accessory rock types of the Revell batholith. Whole rock (major element) and trace element analyses are performed on each sample, in addition to a detailed qualitative optical petrographic description. The goal of this work is to further understand and classify the host and accessory rock types of the batholith, to identify outlier or unusual rock types, and to better understand the types and locations of alteration throughout the rock mass

In general, whole rock geochemistry provides a breakdown of the major cations present in the sample (Si, Ti, Al, Fe, Mn, Mg, Ca, Na, K, and P) which aid in rock classification and understanding the conditions of melting and/or the subsequent crystallization history of the batholith. Trace element geochemistry provides a breakdown of elements in the sample in concentrations less than 0.1 wt. %. Most commonly, these trace elements substitute for major elements (listed above) in the rock-forming minerals. Trace elements can help identify geological processes and combined with major elements, can identify the original tectonic setting of igneous rocks.

Qualitative optical petrography provides a detailed description of the minerals present in each sample, their form, interrelationship, and any deformation they may have undergone. Point-counting provides a relative amount of major minerals, allowing for classification of igneous rocks on a QAPF diagram. Additionally, the presence of accessory minerals and their relationship to the rock-forming minerals provide valuable information on post-cooling processes and fluid movement. The petrographic report and associated high-quality thin section photographs are an essential part of understanding the host and subordinate rock types present in the Revell batholith.

This report documents the results of Thin Section Petrography and Lithogeochemical Analysis of Core Samples from IG\_BH02 and IG\_BH03. This work was complete as part of Phase 2 Initial Borehole Drilling and Testing, Ignace Area. The analyses and reporting were completed by ACTLABS.

Results documented within this report are divided into two parts:

- A) Thin Section Petrographic Analysis
- B) Lithogeochemical Analysis

## **2. SCOPE OF LABORATORY WORK**

The work associated with Phase 2 Geoscientific Preliminary Assessment, Lithochemical analysis of samples from IG\_BH02 and IG\_BH03 in Ignace was undertaken by Activations Laboratories, which is a mineral laboratory with ISO 17025:2017 accreditation.

All samples are prepared on arrival at Activation Laboratories in Thunder Bay using the following methodology: samples are crushed to 80% passing 2 mm, riffle split (250 g) and pulverized using a mild steel mill to 95% passing 105 µm. All samples are then analyzed for 60 major and trace elements using the techniques described below. Note that any analyses listed below with a 4 in their code are added to the 4Lithores suite to account for specific elements.

### ***4Lithores***

Crushed samples are fused with lithium metaborate/tetraborate and the resulting molten bead is digested in a weak nitric acid solution. The liquid is analyzed for major and trace elements using Inductively-Coupled Plasma Mass Spectroscopy (ICP-MS) and Inductively-Coupled Plasma Optical Emission Spectroscopy (ICP-OES). This analysis is intended for non-mineralized samples.

### ***4B1***

4B1 is used to obtain accurate levels of base metals (Cu, Pb, Zn, Ni, and Ag). A 4-acid (near-total) digestion is used, which is a combination of hydrofluoric, nitric, perchloric, and hydrochloric acids. The solution is analyzed with ICP-OES.

### ***4B – INAA***

4B-INAA is recommended for As, Sb, high W, and moderate levels of Cr. Instrumental Neutron Activation Analysis (INAA) is an analytical technique dependent on measuring gamma radiation induced in the sample by irradiation with neutrons. The source of neutrons is (usually) a nuclear reactor. Each element emits a unique signature of gamma radiation which can be measured and analyzed on a high-purity Ge detector.

### ***QOP***

A qualitative optical petrography report is completed for each sample. Thin-sections are prepared by ACTLABS and a petrographic analysis using transmitted and reflective light microscopy (including modal mineralogy, thin section description, and photomicrographs) is completed by a qualified person.

#### **4F – F**

This analysis is specifically to measure fluoride. Samples are fused with lithium metaborate/tetraborate in an induction furnace to release fluoride ions from the sample matrix. An ion selective electrode (ISE, in this case fluoride-selective) is immersed in the solution to measure the fluoride-ion activity directly using an automated fluoride analyzer.

#### **4F – B**

This analysis is specifically to measure boron. Samples are irradiated with neutrons from a nuclear reactor and then measured for the Doppler broadened prompt gamma ray using a high purity Ge detector.

#### **4F – C, S**

This analysis is specifically to measure total carbon and sulphur. An accelerator material is added to the sample, and the inductive elements of the sample and accelerator couple with the high frequency field of the induction furnace, causing the sample to combust. During combustion, sulphur- and carbon-bearing elements are reduced, releasing sulphur and carbon, which bond with oxygen to form SO<sub>2</sub>, CO, and CO<sub>2</sub> (majority CO<sub>2</sub>). Sulphur and carbon dioxide are measured by infrared spectroscopy.

#### **4F – Cl**

This analysis is specifically to measure chlorine. Samples are irradiated with neutrons from a nuclear reactor and then measured for the Doppler broadened prompt gamma ray using a high purity Ge detector.

#### **4F – Hg**

This analysis is specifically to measure mercury. Samples are digested with aqua regia (a mixture of nitric and hydrochloric acids) and the resulting solution is oxidized to the stable divalent form. Solution is transported into an absorption cell and the cell is placed in the light path of an Atomic Absorption Spectrophotometer. The maximum amount absorbed (peak height) is directly proportional to the concentration of mercury atoms in the light path. Measurement is performed using a cold vapour flow injection mercury system (FIMS).

#### **1B1**

To analyze the platinum group elements (PGE), fire-assay and INAA are used. Samples are fire assayed using a nickel sulphide (NiS) procedure. The nickel sulphide button is dissolved in concentrated HCl and the resulting residue is collected. The residue undergoes INAA to measure the PGE and gold.

**5S – I, Re**

This analysis is for short-lived isotopes and is used to measure iodine and rhenium. Samples are sent to the source of irradiation and then back to the lab for analysis and are counted sequentially based on the analyte(s) of interest.

## **1. Thin Section Petrographic Analysis**



Petrographic Report  
on Polished Thin Sections  
(work order: A20-05149)

Reviewed By:  
Dr. Mahdi Ghobadi

Date:  
June, 2020

This report is subject to the following terms and conditions:

1. This report relates only to the specimen provided and there is no representation or warranty that it applies to similar substances or materials or the bulk which this specimen is a part of 2. The contents of this report is for the information of the customer identified above only and it shall not be represented or published in whole or in part or disclosed to any other party without prior consent of ACTLABS 3.The name ACTLABS shall not be used in connection with the specimens reported or any substance or materials similar to that specimen without prior written consent of ACTLABS 4. Neither ACTLABS nor its employees shall be responsible for any claims, loss or damages arising in consequence of reliance on this report or any error or omissions in its preparation or the test conducted 5.Specimens are retained for 90 days. Samples which are critical or the subject of litigation should be retrieved as soon as possible. Actlabs will not be responsible for loss or damage however caused. Test reports and test data are retained 10 years from date of final test report and then disposed of, unless instructed otherwise in writing. 6. Micrograph magnification based on a photo size of approximately 3.5"x5" unless otherwise noted. QA Forms Revision 4.2 Effective Date: March 22, 2006.

## ***EXECUTIVE SUMMARY***

---

The present “Petrographic Descriptions” provides the following information for each sample:

- (i) the petrographic rock classification;**
- (ii) a brief microstructural description;**
- (iii) a table with the modal percentage and average grain size for each mineral; and**
- (iv) a detailed description of the minerals in decreasing order of abundance.**

Samples were cut and prepared as  $\sim 20 \times 40$  mm polished thin sections.

The petrographic classification follows the recommendations of Gillespie and Styles (1999).

The microstructural terminology used in this report follows the recommendations and definitions of Vernon (2004), Passchier and Trouw (2005), and Ramdohr (1980).

## ***METHODS EMPLOYED***

---

Polished thin sections (PTS) were examined using a petrographic microscope, under both transmitted and reflected light. Both techniques use the properties of polarized light as it travels through, or reflects off of, the mineral sample, respectively.

Within transmitted light petrography, one can look at a sample in either ‘plane polarized light’ (ppl), or ‘crossed polars’ (xp). Plane polarized light is when the light coming through the microscope is traveling in only one direction. This state most closely resembles what the naked eye would see, just magnified. Some minerals show a slight difference in color as the microscope stage is rotated under ppl, and this is called ‘pleochroism’. It happens because the light travels faster along one of the three axial planes in the mineral compared to another. Some minerals show a high degree of pleochroism (such as amphiboles), while others are not pleochroic at all.

When a second polarizer is inserted into the light path at a right angle to the first polarizer, the incoming light is now polarized in two directions. This other polarizer is called the ‘analyzer’, and this state is called ‘crossed polars’ (or ‘xp’ for short). The colors that we now see down the microscope are the result of the refraction of two light paths coming through the mineral, and the interaction or ‘interference’ between them. One light ray comes through the mineral faster than the other, and that is why the colors are called ‘interference colors’. They are only seen under a petrographic microscope, and in many cases provide diagnostic information to identify minerals. When there is a large difference between the speeds of the two light rays coming out of the mineral, we can say that there is a high degree of ‘birefringence’, and therefore higher ‘orders’ of interference colors will result. This is particularly true for minerals such as carbonates that display anomalously high orders of interference colors, almost resembling a rainbow.

Opaque minerals such as sulfides and oxides appear black in transmitted light, and are identified instead under ‘reflected light’. This is achieved using the same petrographic microscope, in reflected mode, where the light is now shining on the sample, instead of through it. A mineral is said to be highly ‘reflective’ if it appears light white or light yellow. A good example of this reflectance is arsenopyrite (white) and pyrite (light butter yellow). Other sulfides are distinguished mainly by their reflectance, from brassy yellow (chalcopyrite), to a golden yellow color (native gold). Pentlandite has a slightly more pinkish reflectance. Oxides such as hematite and magnetite have a light grey reflectance. Silicates are usually dark grey under reflected light and only the crystal shapes and maybe cleavage traces are visible.

Specific tests are performed using both optical techniques with high powered objectives (2.5x, 5x, 10x, 20x, 50x, and 100x), and specialized petrographic accessories to identify all mineral phases present to the best of the ability of the petrographer. Note that the oculars (eyepieces) also apply a magnification of 10x, therefore the total magnification is the objective magnification multiplied by 10. Images displaying most of the pertinent mineral phases and overall textures are captured using a digital camera mounted on top of the microscope. Scale bars are included in each image, and this scale is calibrated to a micrometer prior to analysis.

**PETROGRAPHY DESCRIPTION****IG\_BH02\_LG001**

*Rock Type: Foliated plagioclase-phyric andesite*

Sparse subhedral phenocrystals of plagioclase are immersed within a fine-grained groundmass of plagioclase, biotite, and subordinate quartz. The biotite is dispersed within the groundmass as randomly oriented flakes. A small percentage of the biotite concentrates within thin, discontinuous clusters defining a weak magmatic foliation.

Alteration: epidote: after biotite and plagioclase; weak in the groundmass; white mica: subtle after biotite.

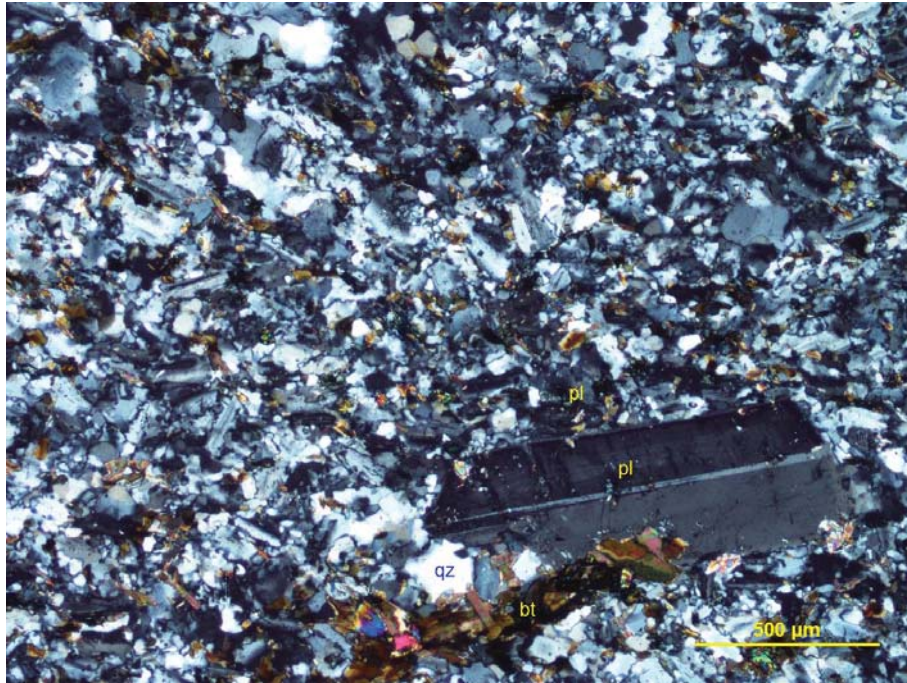
Mineral	Alteration and Weathering Mineral	Modal %	Size Range (mm)
Phenocrystals	Epidote		
Plagioclase		4-5	Up to 1.2 long
Groundmass			
Plagioclase	Epidote	82-84	Up to 0.15
Biotite		6-8	Up to 0.3
Quartz		5-6	Up to 0.01
	Epidote	1-1.5	Up to 0.05
	White Mica	0.2-0.5	Up to 0.05

**Plagioclase** occurs as sparse euhedral phenocrystals (up to 1.2 mm long), which show a weak referred dimensional orientation. The phenocrystals are fresh to weakly altered by epidote and show Albite twinings, and in some cases, a euhedral oscillatory growth zoning.

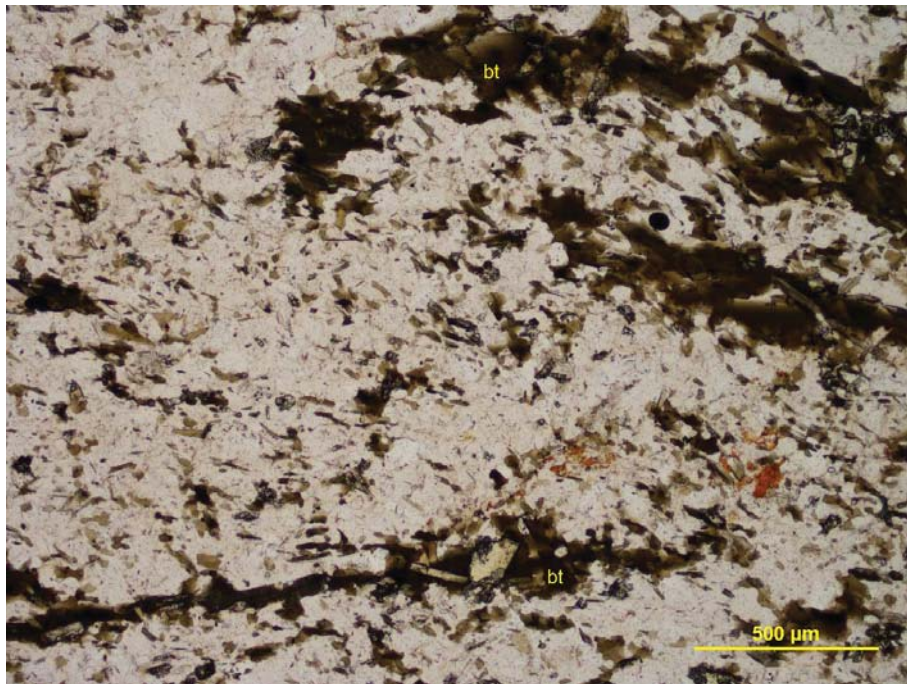
Anhedral crystals of plagioclase (Photomicrograph 1a) prevail over the fine-grained flakes of biotite and the subordinate crystals of quartz in the groundmass.

**Biotite** forms fine-grained flakes, which are randomly oriented within the groundmass. Some of the biotite crystals concentrate within thin, discontinuous and sub-parallel clusters, which define a weak magmatic foliation (Photomicrograph 1b). Very fine- to fine-grained anhedral crystals of epidote are spatially associated and overprinted the biotite flakes, and to a lesser extent, altered the plagioclase phenocrystals.

**Quartz** occurs as fine-grained anhedral crystals (up to 0.1 mm across), which are subordinate to the biotite and the plagioclase in the groundmass. Rare fine-grained lamellae of white mica overprinted some of the biotite lamellae and flakes.



Photomicrograph 1a: Sparse medium-grained phenocrysts of plagioclase (pl) are immersed within a fine-grained groundmass of plagioclase, biotite (bt), and quartz (qz). Crossed polarizers transmitted light.



Photomicrograph 1b: Within the fine-grained groundmass, the biotite is dispersed as randomly oriented flakes and forms irregular, discontinuous and sub-parallel clusters imparting a weak magmatic foliation to this rock. Plane-polarized transmitted light.

*IG\_BH02\_LG002*

*Rock Type: Quartz-plagioclase-phyric microtonalite/microquartz-diorite*

Subhedral phenocrystals of plagioclase and biotite and anhedral phenocrystals of quartz are immersed within a fine-grained groundmass of quartz and subordinate plagioclase. The porphyritic microstructure is relatively homogeneous and isotropic.

Alteration: white mica: weak after plagioclase and biotite; epidote: weak.

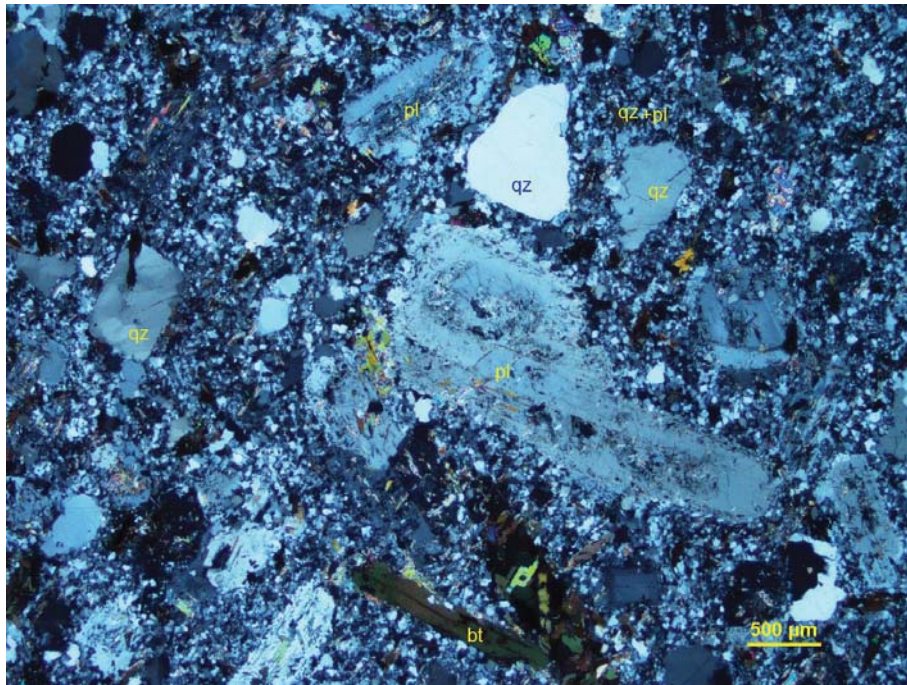
Mineral	Alteration and Weathering Mineral	Modal %	Size Range (mm)
Phenocrystals	Epidote		
Plagioclase	White mica-epidote	10-12	Up to 2.5 long
Quartz		8-10	Up to 1
Biotite (incl. Zircon)	White mica-epidote	0.4-0.5	Up to 1.5 long
Groundmass			
Quartz		66-68	Up to 0.1
Plagioclase		12-14	Up to 0.3
	Biotite	1-1.5	Up to 0.1
	Epidote	0.4-0.6	Up to 0.3
	White Mica	0.3-0.5	Up to 0.2
	Magnetite	Tr	Up to 0.1

Subhedral phenocrystals of **plagioclase** are randomly oriented and homogeneously dispersed within a fine-grained groundmass of quartz and plagioclase. The plagioclase phenocrystals are up to 2.5 mm long and show a continuous subhedral growth zoning in some cases. The plagioclase phenocrystals host very fine-grained flakes of white mica, which tend to be concentrated within the phenocrystal core (Photomicrograph 2b). The plagioclase is fine-grained and subordinate to the quartz in the fine-grained anhedral groundmass.

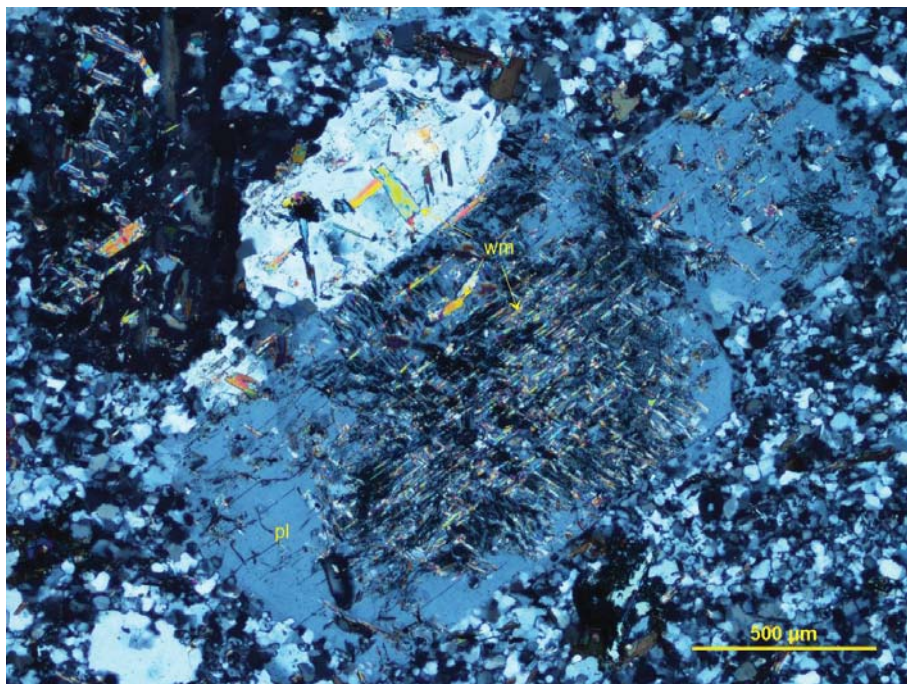
**Quartz** forms anhedral phenocrystals (up to 1 mm), and it is intergrown with fine-grained anhedral crystals of plagioclase within the fine-grained interlobate groundmass. The quartz phenocrystals are homogeneously dispersed within the groundmass, and in some cases, show embayment indicating the disequilibrium of the phenocrystals in the groundmass during the magma crystallization. Some of the phenocrystals show moderate undulose extinction.

**Biotite** forms fine- to medium-grained lamellae (up to 1.5 mm long), which are randomly oriented within the groundmass. The biotite host very fine-grained inclusions of zircon and, in some cases, are overprinted by rare and fine-grained flakes of white mica. Very fine-grained flakes of biotite are dispersed within the groundmass.

**Epidote** forms fine-grained anhedral alteration patches overprinting the groundmass, the biotite, and the plagioclase crystals.



Photomicrograph 2a: Subhedral phenocrysts of plagioclase (pl) biotite (bt), and anhedral phenocrysts of quartz (qz) are immersed within a fine-grained groundmass of quartz and plagioclase (qz+pl). Crossed polarizers transmitted light.



Photomicrograph 2b: Within the plagioclase phenocrystal (pl), the white mica (wm) is concentrated within the phenocrystal core. Crossed polarizers transmitted light.

*IG\_BH02\_LG003*

*Rock Type: Granodiorite*

Subhedral crystals of plagioclase and anhedral crystals of quartz and alkali feldspar define a relatively homogeneous granular microstructure, in which anhedral to subhedral lamellae of biotite are randomly oriented.

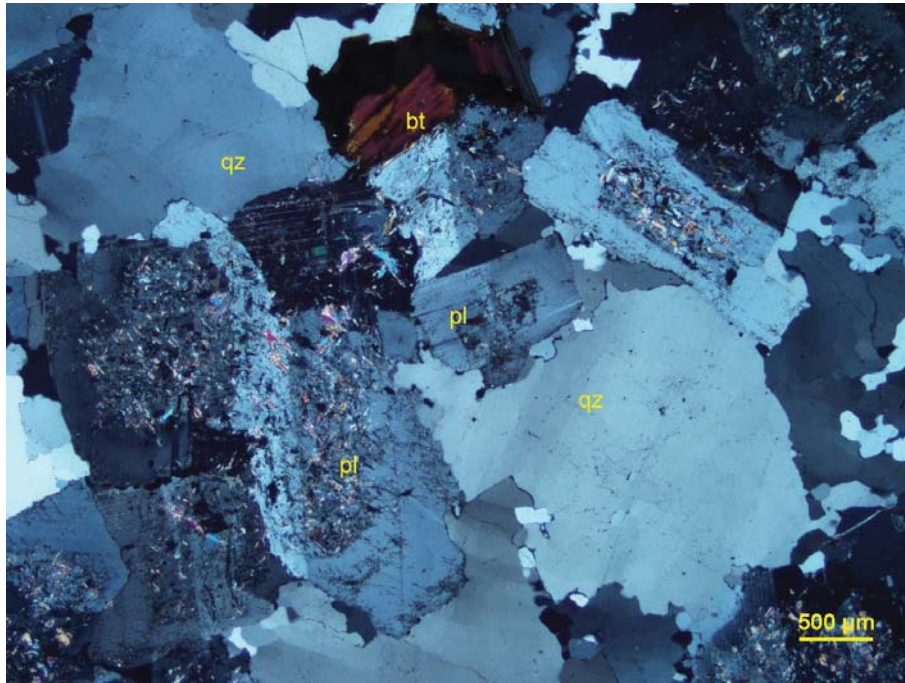
Alteration: white mica: weak after plagioclase and biotite; epidote-iron oxides: subtle.

Mineral	Alteration and Weathering Mineral	Modal %	Size Range (mm)
Plagioclase	White mica	43-45	Up to 2.5
Quartz		41-43	Up to 5
Alkali Feldspar		12-15	Up to 7
Biotite	White mica	2-3	Up to 2
White mica		0.2-0.5	Up to 0.3
	Epidote	Tr	Up to 0.05
?	Iron Oxides + Epidote	Tr	Up to 0.6
Zircon		Tr	Up to 0.01

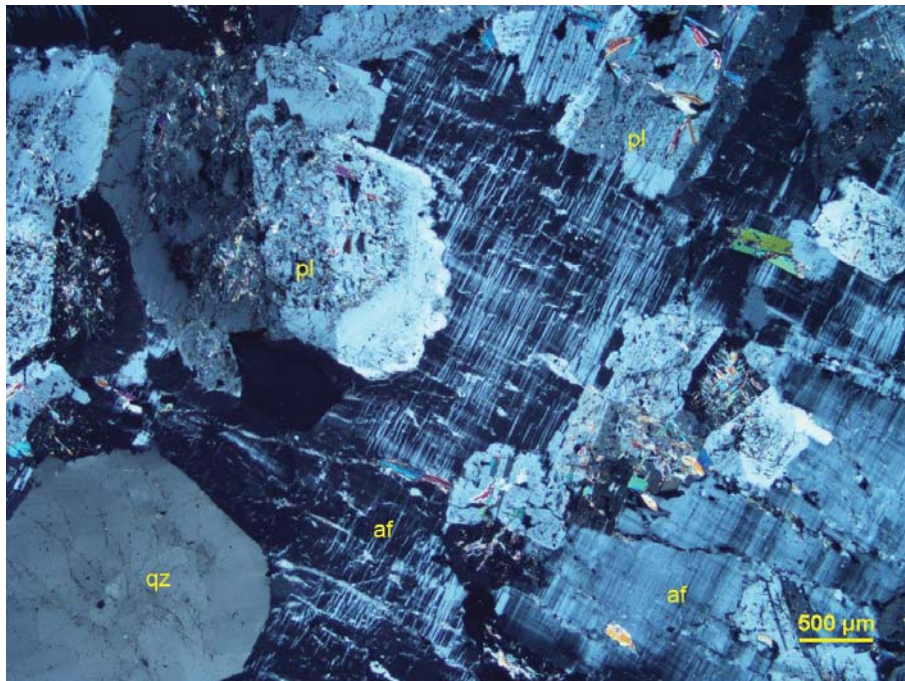
**Plagioclase** forms anhedral to subhedral crystals (up to 2.5 mm across) intergrown with a comparable amount of quartz and subordinate crystals of alkali feldspar. The plagioclase crystals are distinguished by their rare Albite twinnings, and by showing continuous and subhedral growth zoning. In some cases, the core of the crystals are weakly to moderately altered by very fine- to fine-grained flakes of white mica.

**Quartz** forms inequigranular (up to 5 mm across) crystals and domains (up to 7 mm long), which are intergrown with plagioclase and alkali feldspar. Some of the coarse-grained crystals of quartz show moderate undulose extinction. Some of the quartz domains are re-crystallized into interlobate crystal aggregates (Photomicrograph 3a).

**Alkali feldspar** forms anhedral crystals (up to 7 mm across), which tend to occupy the interstitial positions between the plagioclase and the quartz crystals. The alkali feldspar is distinguished by its typical Albite-Pericline twinnings, and it is heterogeneously (at the scale of the thin polished section) dispersed. Its distribution can be observed (please see the corresponding billet photo) of the stained billet, in which the alkali feldspar is stained. Very fine- to fine-grained perthitic blebs are dispersed within the alkali feldspar. Anhedral crystals of biotite are randomly oriented within the quartzofeldspathic rock. The crystals (up to 2 mm across) host very fine-grained crystals of zircon, are weakly oxidized, and in some cases, are overprinted by less abundant lamellae of white mica. An anhedral alteromorph 0.6 mm long is dispersed within the interstices of the plagioclase crystals, and it is made up of probable iron oxides rimmed by fine-grained fibres of epidote.



Photomicrograph 3a: Subhedral crystals of plagioclase (pl) are randomly oriented and associated with quartz crystals and irregularly shaped quartz-only domains (qz). Crossed polarizers transmitted light.



Photomicrograph 3b: Interstitial alkali feldspar (af) is associated with subhedral to anhedral crystals of plagioclase (pl) and anhedral crystals of quartz (qz). Crossed polarizers transmitted light.

*IG\_BH02\_LG005*

*Rock Type: Plagioclase-phyric microdiorite (?)*

Euhedral to subhedral phenocrystals of plagioclase are dispersed within a fine-grained groundmass of plagioclase, quartz, and randomly oriented lamellae of biotite.

Alteration: epidote: weak after biotite; white mica: subtle to weak after biotite and plagioclase

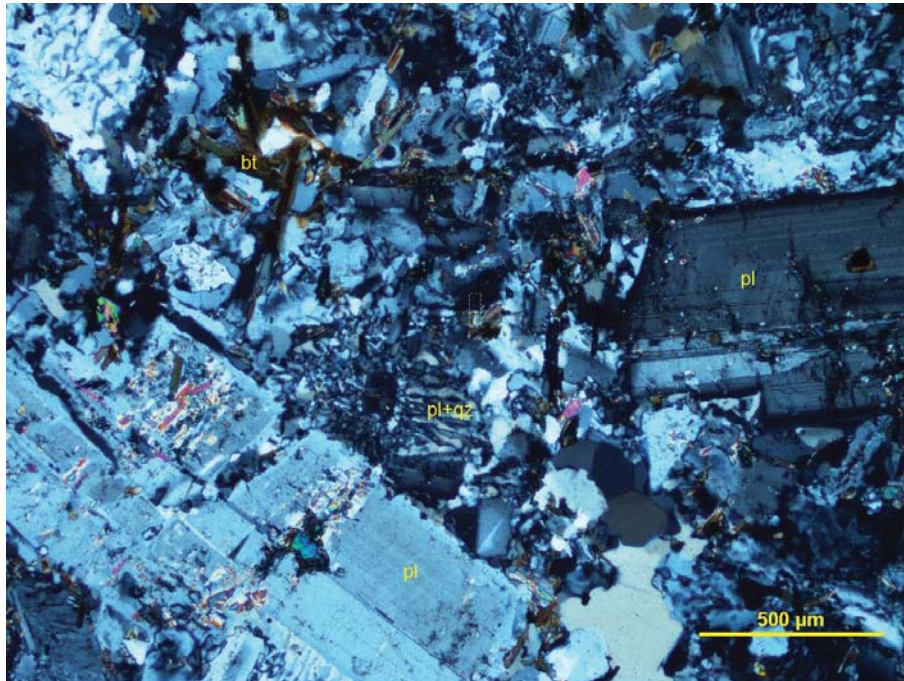
Mineral	Alteration and Weathering Mineral	Modal %	Size Range (mm)
Phenocrystals	Epidote		
Plagioclase		8–10	up to 1
Amphibole?	Biotite	5–7	[up to 3.5 long]
Quartz		tr	up to 0.5
Groundmass			
Plagioclase		48–50	up to 0.5
Quartz		35–37	up to 0.5
Biotite	Epidote-white mica	1.5–2	up to 0.5
Zircon		tr	up to 0.01
Magnetite		tr	up to 0.05
Pyrite		tr	up to 0.01

**Plagioclase** forms euhedral to subhedral phenocrystals (up to 1 mm across). The phenocrystals are fresh to subtly altered by very fine- to fine-grained flakes of white mica, and in some cases (Photomicrograph 4a) are surrounded by a granophyric rim of plagioclase and quartz. Some of the plagioclase phenocrysts show oscillatory growth zoning, and some show Albite-Carlsbad twinnings. The plagioclase occurs in the groundmass as fine-grained anhedral crystals intergrown with the quartz. The granophyric intergrowths of plagioclase and quartz indicate that these two minerals crystallized together during the magmatic phase.

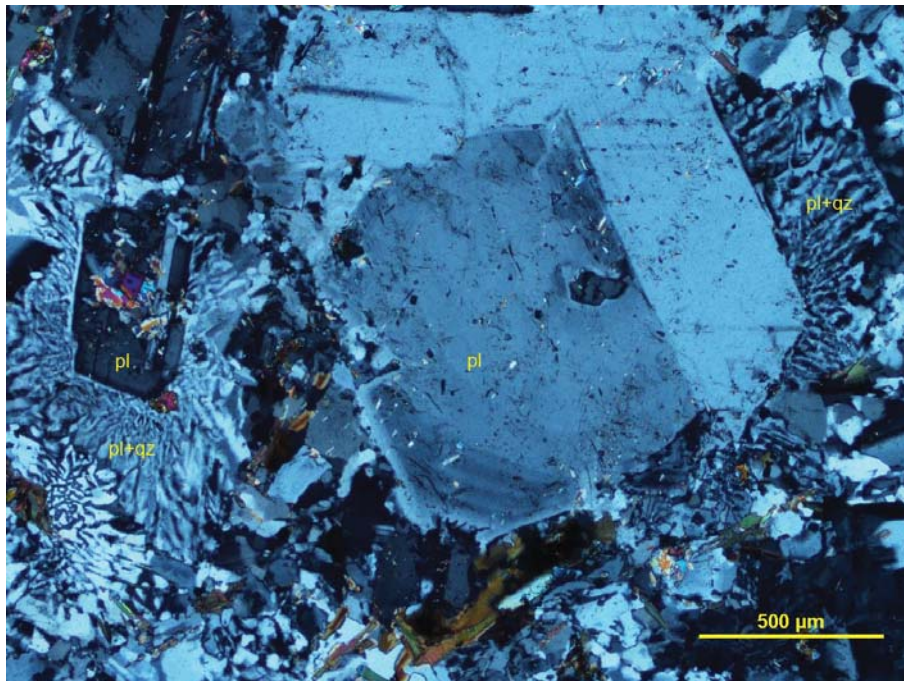
**Quartz** occurs as anhedral granophyric aggregates intergrown with the plagioclase (Photomicrograph 4a). Rare and anhedral crystals of quartz are up to 0.5 mm across, and probably form sparse phenocrystals. In most of its occurrence, the quartz is finely intergrown with the plagioclase in the groundmass.

**Biotite** forms fine-grained flakes and lamellae (up to 0.5 mm long) and fine-grained flakes replacing up to 3.5 mm crystals of probable amphibole. The randomly oriented and elongate pseudomorphs of biotite, together with the abundant granophyric aggregates, indicate that the magma crystallized in the absence of flow.

**Epidote** occurs as very fine- to fine-grained anhedral crystals dispersed within the plagioclase and spatially associated with the biotite flakes. Rare lamellae of **white mica** overprinted some of the biotite lamellae.



**Photomicrograph 4a:** Euhedral phenocrysts of plagioclase (pl) are immersed within a mostly granophyric groundmass of plagioclase and quartz (pl+qz). Crossed polarizers transmitted light.



**Photomicrograph 4b:** In some cases, the plagioclase phenocrysts (pl) are surrounded by micrographic rims of plagioclase and quartz (pl+qz). Crossed polarizers transmitted light.

*IG\_BH02\_LG007*

*Rock Type: Chlorite-epidote-altered foliated magmatic rock  
Alkali feldspar veinlets*

This thin polished section is dominated by a fine-grained aggregate of xenomorphic crystals of albite, quartz, and sub-parallel domains of chlorite and epidote. Within the fine-grained plagioclase-rich groundmass, rare phenocrysts of plagioclase are dispersed and impart a porphyritic microstructure.

Alteration: quartz (?): weak to moderate; chlorite: weak; epidote-calcite-iron oxides: subtle

Mineral	Alteration and Weathering Mineral	Modal %	Size Range (mm)
<b>Albite-quartz-chlorite-altered foliated magmatic rock (~97% of PTS)</b>			
Plagioclase	White mica (?)	77–79	rare up to 1, up to 0.15
Quartz	Quartz	15–25	up to 0.05
	Fe-chlorite	2–2.5	up to 0.2
	Epidote	1–2	up to 0.1
	Calcite	0.5–1	up to 0.5 long
	Iron oxides	tr	up to 0.1
<b>Alkali feldspar veinlets (~3% of PTS)</b>			
Alkali feldspar		3	up to 0.05

**Plagioclase** forms rare relics of phenocrysts (up to 1 mm across), which are immersed within a fine-grained groundmass of xenomorphic crystals of plagioclase (Photomicrograph 5). The fine-grained crystals of plagioclase dominate the composition of the groundmass and are intergrown with subordinate and fine-grained crystals of quartz. The albite crystals are distinguished by their low birefringence, and their refractive index lower than those of the quartz. The albite crystals are weakly altered by a very fine-grained dispersion of white mica (?) and unresolved mineral. The albite crystals are probably crushed and comminuted crystals retaining the weak post-magmatic alteration.

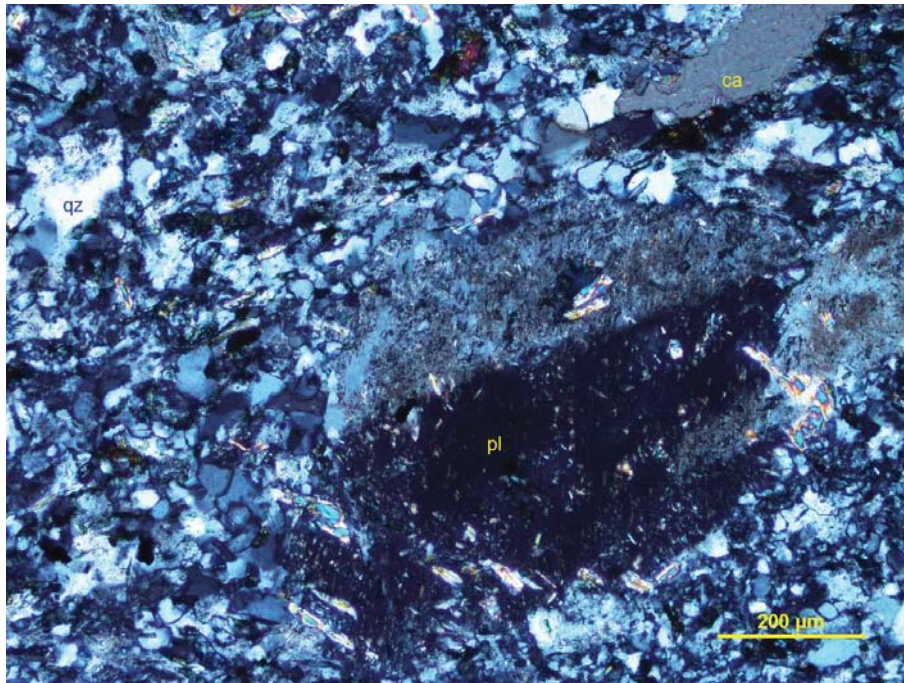
**Quartz** forms very fine- to fine-grained xenomorphic crystals dispersed within the albite-rich aggregate. It is hard to understand if the quartz is a mineral relic from the magmatic stage, or it crystallized during the alteration event. I tentatively interpret its occurrence as derived from both.

**Fe-chlorite** is concentrated within discontinuous and sub-parallel domains, which define a probable relic magmatic foliation. The chlorite flakes are associated with subordinate xenomorphic crystals of

epidote. I tentatively interpret the chlorite and the epidote as generated by the alteration of a ferromagnesian mineral, likely magmatic biotite.

Rare and fine-grained crystals of **calcite** are dispersed within the albite-quartz aggregate, and in some cases, forms irregular infill domains. The calcite is distinguished by its high relief, extreme birefringence. On the billet, the calcite shows a brisk reaction to cold dilute (10%) HCl.

Thin veinlets filled in by **alkali feldspar** define a subparallel and, in some cases, anastomosing set of fracture infill, which is oriented sub-parallel to the foliation of the strongly altered rock.



**Photomicrograph 5:** A rare anhedral phenocrystal of plagioclase is immersed within a groundmass dominated by plagioclase, rare crystals of quartz, and irregular infill domains of calcite (ca). Crossed polarizers transmitted light.

*IG\_BH02\_LG008*

*Rock Type: White mica-altered tonalite*

Subhedral crystals of plagioclase, anhedral crystals of quartz and alkali feldspar, and randomly oriented lamellae of biotite define a coarse-grained granular and isotropic microstructure. The plagioclase is weakly to moderately altered by fine-grained flakes of white mica.

**Alteration: white mica:** weak to moderate after plagioclase; **calcite:** weak after plagioclase and alkali feldspar

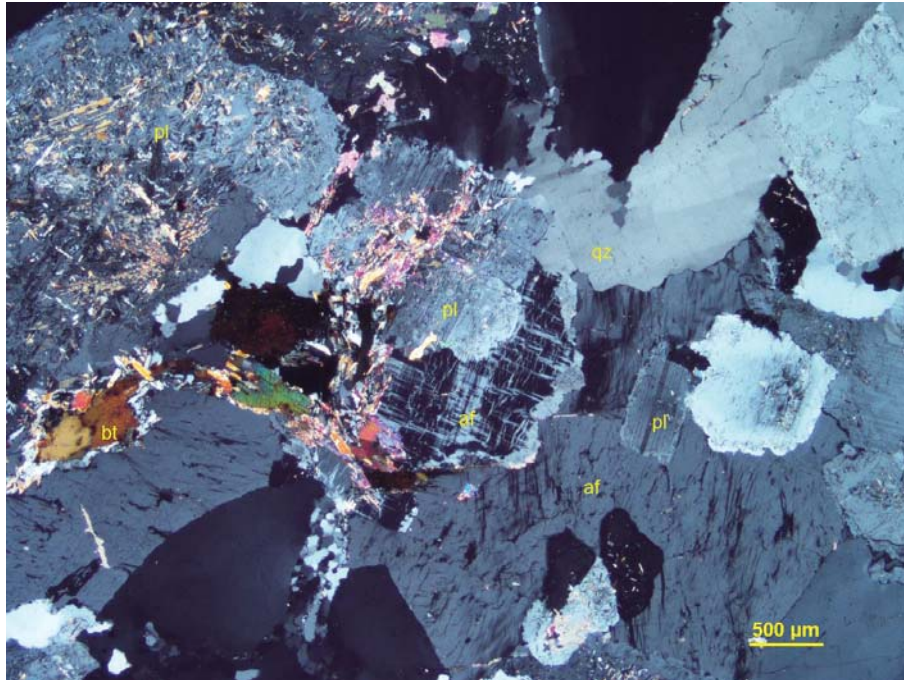
Mineral	Alteration and Weathering Mineral	Modal %	Size Range (mm)
Plagioclase	white mica	45–47	up to 4.5 long
Quartz		42–45	up to 4
Alkali feldspar		8–10	up to 2
Biotite	white mica	2–3	up to 0.6
	calcite	1–1.2	up to 0.15
Ilmenite (?)		tr	up to 0.2

**Plagioclase** occurs as inequigranular (up to 4.5 mm long) subhedral to anhedral crystals. The plagioclase crystals are randomly oriented, and together with the other minerals' random orientation, defines the isotropic granular microstructure. The plagioclase shows refractive indexes smaller than those of the quartz; therefore, it is albite. The plagioclase crystals show Albite twinnings and are overprinted by fine-grained and randomly oriented flakes and lamellae of **white mica**.

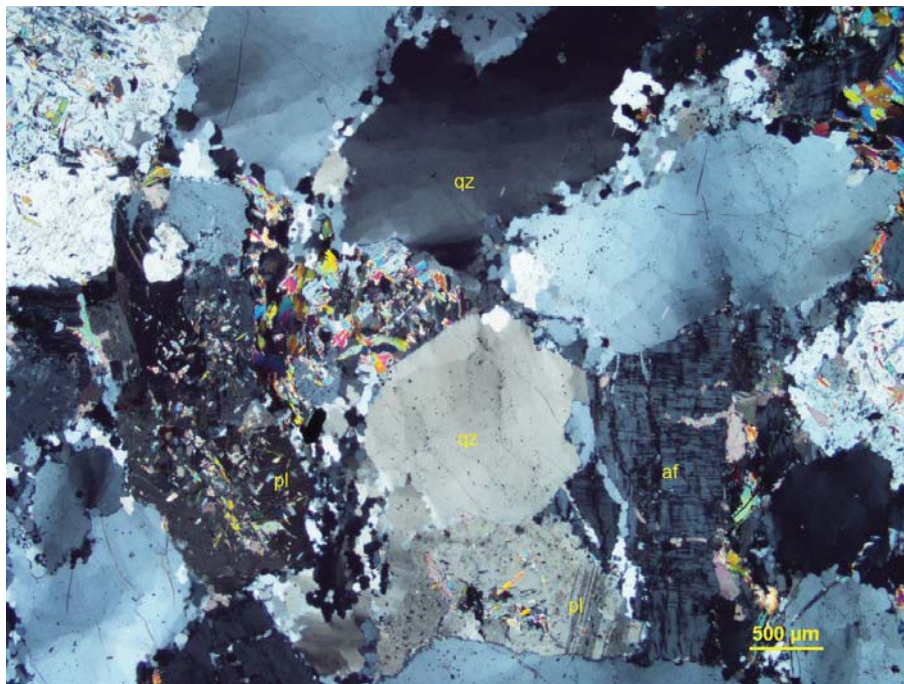
**Quartz** occurs as medium-to coarse-grained crystals (up to 4 mm across) and crystal aggregates. In rare instances, it forms subhedral crystals that I interpret as microstructural relics of phenocrystals. Some of the coarser crystals show a moderate to strong undulose extinction.

**Alkali feldspar** is subordinate to the plagioclase and the quartz, and its anhedral crystals are heterogeneously dispersed within the granular microstructure. The alkali feldspar is subtly to weakly altered by calcite and white mica. In most cases, the alkali feldspar is less altered than the plagioclase, and its Albite-Pericline twinnings, together with its interstitial nature, help to distinguish the alkali feldspar from the plagioclase under crossed Nicols.

**Biotite** is fine- to medium-grained (up to 0.6 mm), and it forms randomly oriented lamellae and clusters of lamellae within the interstices between the quartzofeldspathic minerals. In some cases, the biotite is overprinted by fine-grained flakes of white mica. The biotite encloses very fine-grained crystals of zircon, distinguished by the pleochroic halo they impart to the hosting biotite, and hosts very rare lamellae of ilmenite. Rare and fine-grained patches of **calcite** overprinted the alkali feldspar and the plagioclase.



**Photomicrograph 6a:** Anhedrous crystals of plagioclase (pl) are moderately altered by highly birefringent lamellae of white mica (wm), and are intergrown with less altered interstitial crystals of alkali feldspar, and fresh crystals of quartz (qz). Crossed polarizers transmitted light.



**Photomicrograph 6b:** One of the crystals of quartz (qz) shows a subhedral shape; others are anhedrous and show a strong undulose extinction. The alkali feldspar (af) is subtly altered by calcite, and the plagioclase is weakly to moderately altered by white mica. Crossed polarizers transmitted light.

*IG\_BH02\_LG009*

*Rock Type: Chlorite-white mica-altered granodiorite*

Subhedral crystals of plagioclase, anhedral crystals of quartz, alkali feldspar, and subordinate crystals of biotite define a medium- to coarse-grained isotropic granular microstructure.

**Alteration: chlorite:** subtle to strong after biotite; **white mica±epidote:** weak after plagioclase and biotite; subtle after alkali feldspar; **hematite:** strong after magnetite

Mineral	Alteration and Weathering Mineral	Modal %	Size Range (mm)
Plagioclase (albite)	White mica±epidote	40–42	up to 3
Quartz		37–39	up to 5
Alkali feldspar	White mica	8–10	up to 6
Biotite	Chlorite±white mica±epidote	3–4	up to 1, rare up to 1 long
	Epidote	0.2–0.3	up to 0.2
	Rutile	tr	up to 0.1
Magnetite	Hematite	tr	~0.15
Rutile			up to 0.01

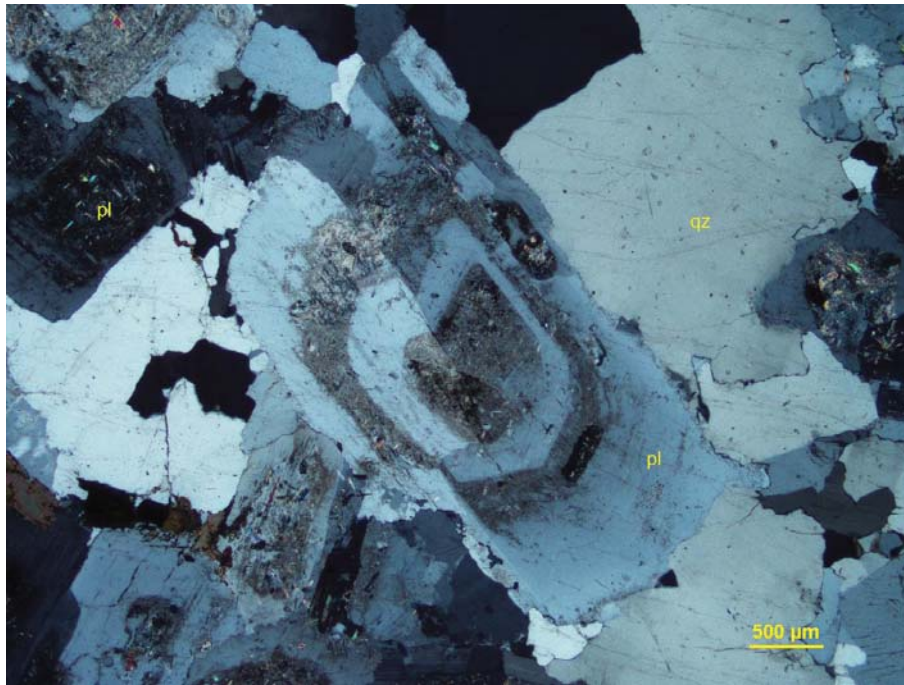
**Plagioclase** occurs as subhedral and inequigranular crystals (up to 3 mm across). The crystals are randomly oriented and are weakly altered by dispersions of very fine- to fine-grained white mica. Some of the crystals show a subhedral oscillatory growth zoning (Photomicrograph 7a and 7c). In these crystals, the white mica is concentrated along some of the growth zones. Very fine- to fine-grained anhedral crystals of epidote are associated with the white mica alteration products. The plagioclase shows refractive indexes smaller than those of the quartz, thus indicating it is Albite. In some cases, the plagioclase host fine- to medium-grained subhedral inclusions of alkali feldspar (Photomicrograph 7c).

**Quartz** is inequigranular (up to 5 mm across), and it is slightly subordinate to the plagioclase. Rare microstructural relics of phenocrystals (Photomicrograph 7d) indicate that some of the quartz re-crystallized phenocrystals up to 5 mm in diameter. Some of the quartz crystals show a moderate undulose extinction.

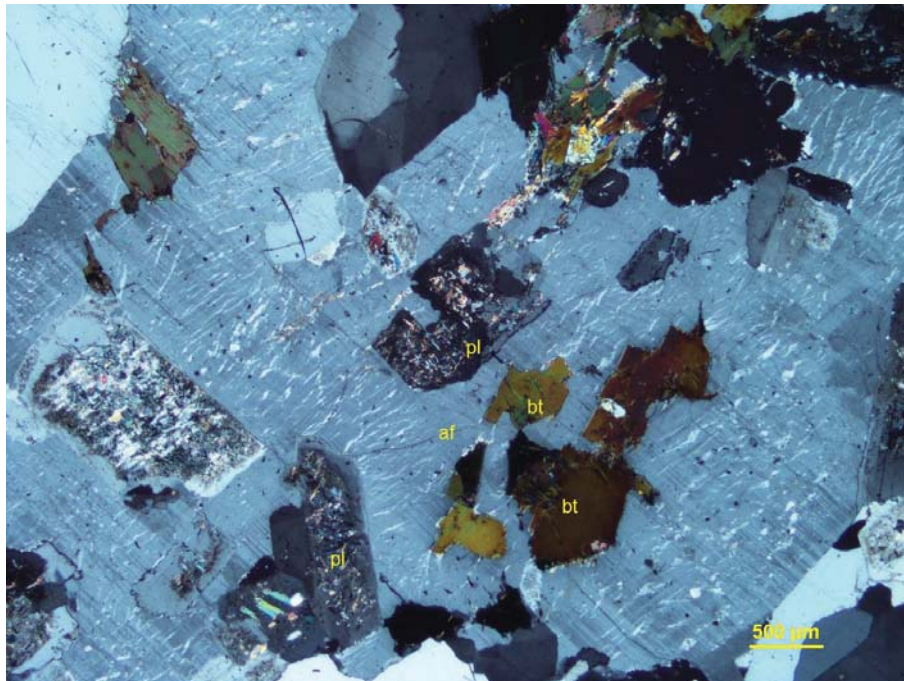
**Alkali feldspar** forms inequigranular and poikilitic crystals up to 6 mm across). The poikilitic crystals crystallized within the interstices between the plagioclase and the biotite and, in some cases, grew until they enclosed the earlier crystallized magmatic minerals (Photomicrograph 7b). The alkali feldspar hosts perthitic blebs and stringlets, and in some cases, show Albite-Pericline twinnings.

**Biotite** forms fine- to medium-grained lamellae, which are randomly oriented within the quartzofeldspathic aggregate. The random orientation of the biotite and plagioclase define the isotropic nature of this thin polished section. The biotite is subtly to strongly altered by chlorite, and this type of alteration varies in different parts of the thin polished section. Fine-grained crystals of epidote preferentially overprinted the biotite, and in some cases, the plagioclase crystals.

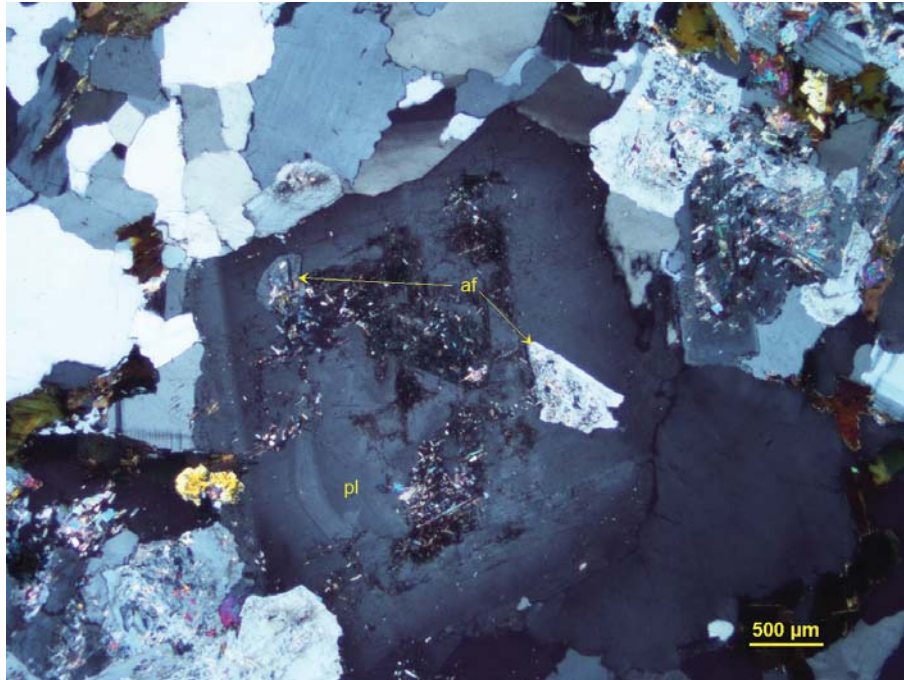
Very rare replacements of hematite after magnetite occurs as fine-grained anhedral crystals within the quartz.



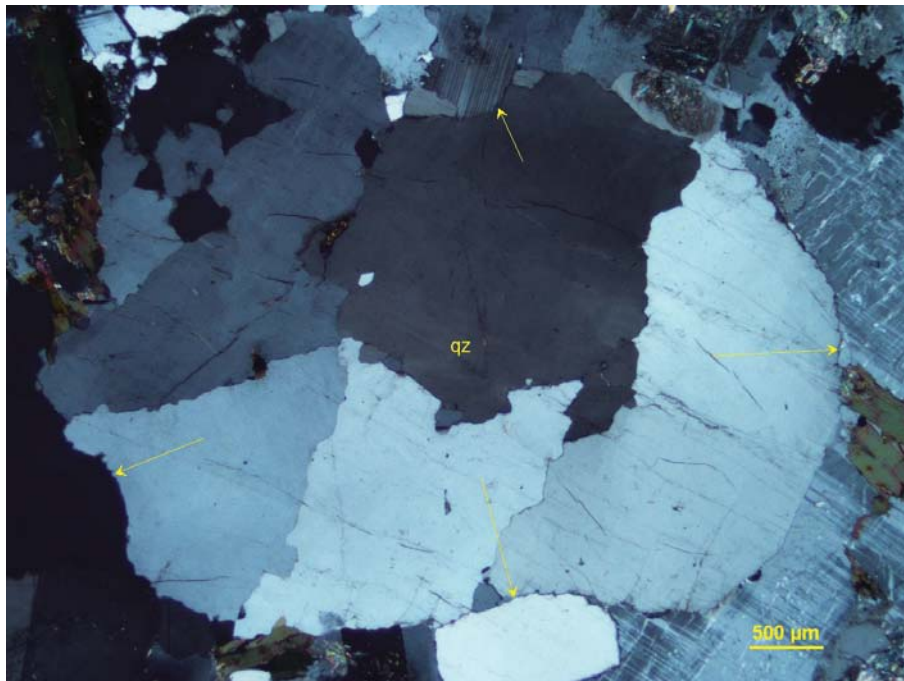
**Photomicrograph 7a:** Subhedral crystals of plagioclase (pl) show euhedral growth zoning, and in some of them, host white mica alteration products. Crossed polarizers transmitted /reflected light.



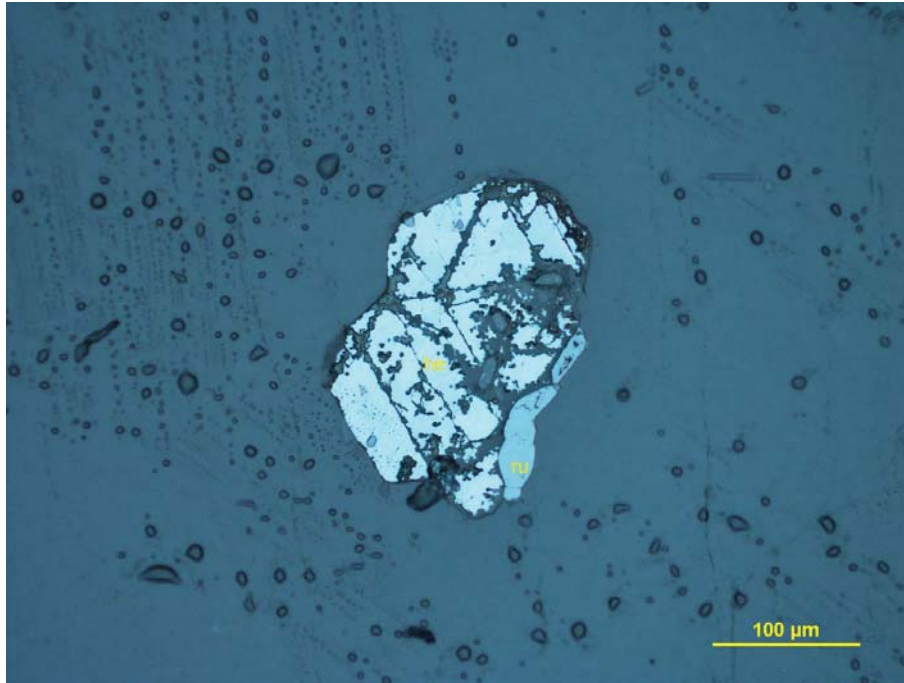
**Photomicrograph 7b:** A poikilitic and interstitial crystal of alkali feldspar (af) is perthitic and hosts medium-grained crystals of plagioclase (pl) and biotite (bt). Crossed polarizers transmitted /reflected light.



**Photomicrograph 7c:** The plagioclase (pl) in the centre of this photomicrograph shows an oscillatory growth zoning and hosts subhedral crystals of alkali feldspar (af). Crossed polarizers transmitted /reflected light



**Photomicrograph 7d:** The yellow arrows suggest that a relic of quartz phenocrystal (yellow arrows) is re-crystallized into smaller crystals (qz). Crossed polarizers transmitted /reflected light



**Photomicrograph 7e:** A magnetite crystal is replaced by hematite (he) and rutile, and occurs within the quartz. Crossed polarizers reflected light

*IG\_BH02\_LG010*

*Rock Type: Foliated plagioclase-phyric microquartz-diorite*

Subhedral phenocrystals of plagioclase are randomly oriented and immersed within a relatively equigranular groundmass of fine-grained plagioclase, quartz, and biotite. Some of the biotite lamellae define discontinuous clusters, which impart to the fine-grained-porphyritic aggregate a subtly foliated microstructure.

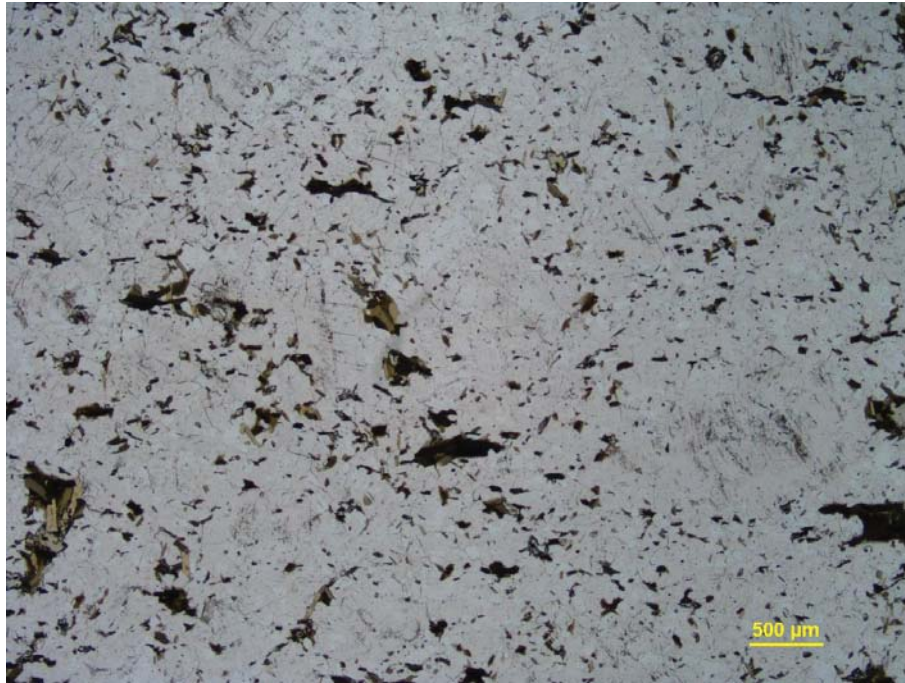
**Alteration: epidote:** subtle after biotite and plagioclase: **white mica:** subtle after plagioclase.

Mineral	Alteration and Weathering Mineral	Modal %	Size Range (mm)
Phenocrystals			
Plagioclase	Epidote-white mica	20–22	up to 1
Groundmass			
Plagioclase	Epidote	55–57	up to 0.2
Quartz		19–21	up to 0.1
Biotite	Epidote	4–5	up to 0.4
Ilmenite		tr	up to 0.1 long

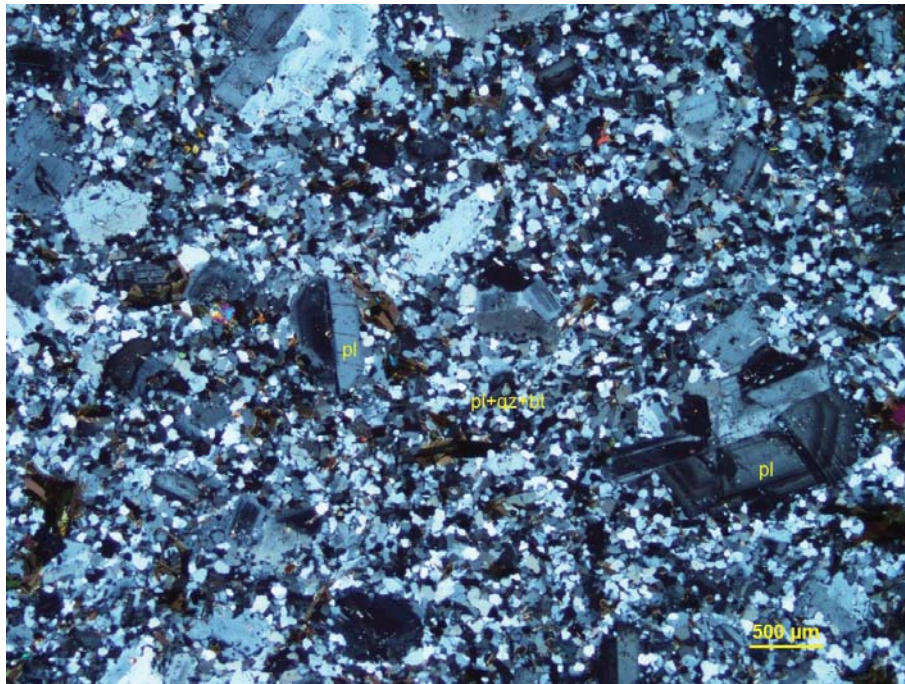
**Plagioclase** occurs as medium-grained (up to 1 mm across) phenocrystals, and it is slightly more abundant than the quartz in the fine-grained anhedral groundmass (Photomicrograph 8b). The phenocrystals are randomly oriented, and their fresh nature allows the observation of euhedral oscillatory growth zoning. The phenocrystals' rims show refractive indexes smaller than those of the quartz, thus indicating that the zonation is normal, and the plagioclase's rim is albitic. The fine-grained anhedral crystals of plagioclase in the groundmass are intergrown with slightly subordinate quartz and less abundant biotite. In some cases, the relic zonation can also be observed in the fine-grained crystals.

**Quartz** is fine-grained, and it forms a relatively homogeneous groundmass in association with plagioclase and biotite. The quartz is relatively well distributed in the groundmass, and I interpret it as a magmatic mineral.

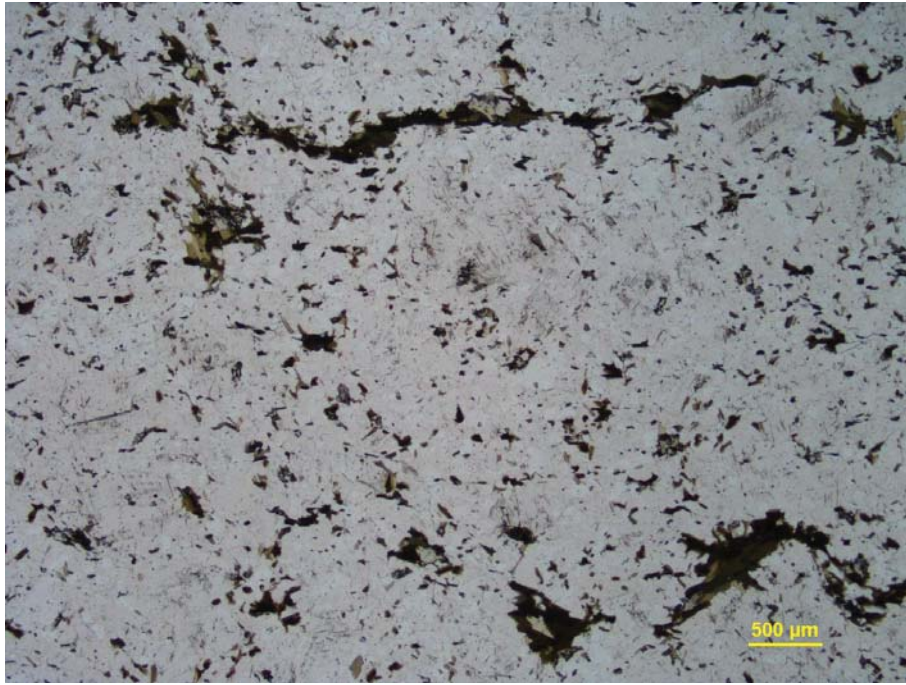
**Biotite** occurs as fine-grained randomly oriented flakes (Photomicrograph 8a) and less abundant medium-grained lamellae defining thin, discontinuous, and sub-parallel clusters. In some cases, these clusters wrap the plagioclase phenocrystals and define a subtle magmatic foliation. Rare anhedral crystals of epidote preferentially overprint the biotite lamellae and cluster. Very rare and anhedral crystals of a low reflective and anisotropic mineral (**ilmenite?**) are spatially associated and, in some cases, are intergrown with the biotite lamellae.



**Photomicrograph 8a:** In most of its occurrence, the biotite is randomly oriented as fine-grained and strongly pleochroic flakes (brown) in a plagioclase and quartz aggregate. Plane-polarized transmitted light



**Photomicrograph 8b:** Under crossed polarizers transmitted light, the same area shown in Photomicrograph 8a, shows the porphyritic microstructure defined by subhedral phenocrysts of plagioclase and a fine-grained groundmass of plagioclase, quartz, and biotite (pl+qz+bt).



**Photomicrograph 8c:** Thin, discontinuous, and sub-parallel clusters of biotite define a subtle magmatic foliation. Plane-polarized transmitted light.

*IG\_BH02\_LG011*

*Rock Type: Granodiorite*

Subhedral crystals of plagioclase are intergrown with a comparable amount of anhedral crystals of quartz, subordinate anhedral crystals of alkali feldspar and randomly oriented lamellae of biotite. The alkali feldspar is heterogeneously dispersed within a relatively homogeneous and isotropic granular microstructure.

**Alteration: clay (?)**-white mica: weak after plagioclase; **epidote**-white mica: subtle to weak after biotite.

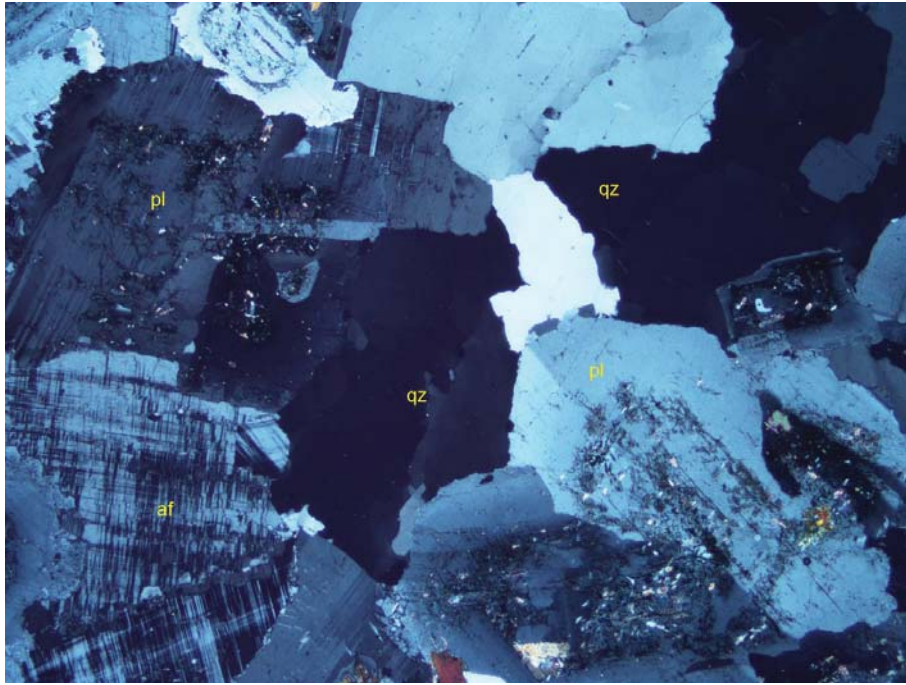
Mineral	Alteration and Weathering Mineral	Modal %	Size Range (mm)
Plagioclase	Clay (?)	42–44	up to 2.5
Quartz		38–40	up to 5 long
Alkali feldspar		15–18	up to 5
Biotite	Epidote	3–5	up to 2.5 long
	Iron oxides	tr	up to 0.05
Apatite		tr	up to 0.05
Zircon		tr	up to 0.01

**Plagioclase** forms subhedral inequigranular crystals (up to 2.5 mm across). The plagioclase crystals are randomly oriented and are fresh to weakly altered by very fine-grained unresolved material (clay?) and, in some cases by fine-grained flakes of white mica. The alteration is concentrated within the anhedral to subhedral crystal cores. Rare Albite and Albite-Carlsbad twinings occur.

**Quartz** occurs as inclusion-free crystals and crystal aggregates occupying the interstitial position between the plagioclase, the alkali feldspar and the biotite. The crystals of quartz show interlobate boundaries and a weak to moderate undulose extinction within the monomineralic and interstitial crystal aggregates (Photomicrograph 9a).

**Alkali feldspar** forms coarse-grained interstitial crystals (up to 5 mm across), which are heterogeneously dispersed within the granular microstructure. In some cases, the alkali feldspar forms poikilitic crystals hosting inclusions of quartz and plagioclase, and in some cases fine-grained perthitic beads. In other cases, the alkali feldspar shows Albite-Pericline twinings. Both these types of alkali feldspar are derived from the magmatic crystallization.

**Biotite** forms randomly oriented lamellae and anhedral crystals, which are randomly oriented and contribute to the isotropic nature of the granular microstructure. The biotite crystals host abundant and very fine-grained crystals of zircon, which are distinguished by their typical pleochroic halo generated in the biotite host. Rare fine-grained crystals of epidote and rare fine-grained crystals of apatite overprinted some of the biotite lamellae. In some cases, the rim of the biotite is weakly altered by fine-grained white mica



**Photomicrograph 9:** Subhedral crystals of plagioclase (pl), interstitial crystals of quartz (qz), and anhedral crystals of alkali feldspar (af) define an isotropic granular microstructure. Crossed polarizers transmitted light.

*IG\_BH02\_LG012*

*Rock Type: Chlorite-altered granodiorite*

Subhedral crystals of plagioclase, anhedral to interstitial crystals of quartz and alkali feldspar, and randomly oriented lamellae of biotite define an isotropic granular microstructure.

**Alteration: chlorite:** weak to moderate after biotite; epidote: subtle after biotite; **clay and/or white mica:** weak to moderate after plagioclase

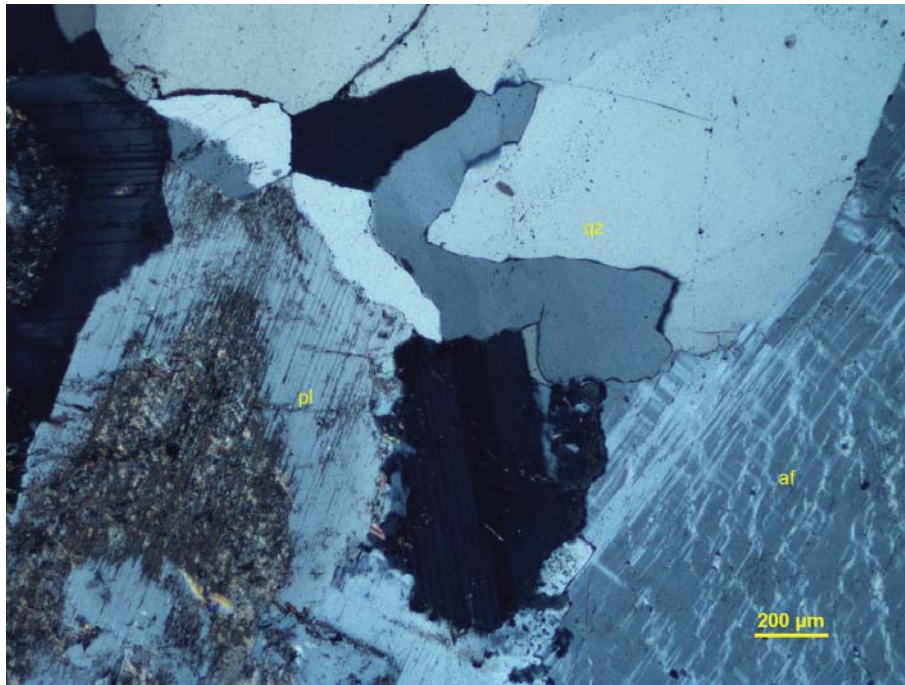
Mineral	Alteration and Weathering Mineral	Modal %	Size Range (mm)
Plagioclase	Clay and/or white mica	49–51	up to 3.5
Quartz		36–38	up to 3
Alkali feldspar		10–12	up to 5
Biotite	Chlorite-epidote	3–4	up to 2 long
	Iron oxides	tr	up to 0.05
Zircon		tr	up to 0.01

**Plagioclase** forms medium-grained subhedral crystals, which are randomly oriented within an interstitial aggregate of quartz. The plagioclase crystals are weakly to moderately altered by very fine-grained flakes of clay and/or white mica. The alteration products are concentrated within the subhedral crystal cores (Photomicrograph 12).

**Quartz** occurs as inequigranular (up to 3 mm long) crystals and crystal aggregates occupying the interstitial position between the plagioclase, the alkali feldspar and the biotite. Within the monomineralic and interstitial aggregates of quartz, the quartz crystals show interlobate to jig-saw boundaries.

**Alkali feldspar** forms anhedral and up to 5 mm across crystals, which are heterogeneously dispersed within the thin polished section. The alkali feldspar hosts very fine- to fine-grained perthitic stringlets and beads, and in some cases, shows Albite-Pericline twinnings. Similarly, to Sample 11, the alkali feldspar crystallized during the latest stages of the magmatic crystallization. The alkali feldspar distribution can be observed on the image of the stained billet (please see the corresponding billet photo), in which it shows a yellow staining colour.

**Biotite** forms fine- to medium-grained lamellae, which are randomly oriented within the interstitial positions between the plagioclase. Most of the lamellae are epitaxially replaced by chlorite. The occurrence of biotite is indicated by the abundant inclusions of **zircon**.



**Photomicrograph 10:** Subhedral crystals of plagioclase (pl) and anhedral crystals of quartz (qz) and alkali feldspar (af) define a granular microstructure. Crossed polarizers transmitted light.

*IG\_BH02\_LG013*

*Rock Type:* White mica-altered tonalite

Anhedral to subhedral crystals of plagioclase, anhedral crystals of quartz, alkali feldspar, and biotite define an isotropic granular microstructure, in which the plagioclase and the biotite are moderately to strongly altered by white mica.

**Alteration:** **white mica:** weak to moderate after plagioclase and biotite; **pyrrhotite:** subtle in the pseudomorphs after biotite; **epidote-calcite:** subtle.

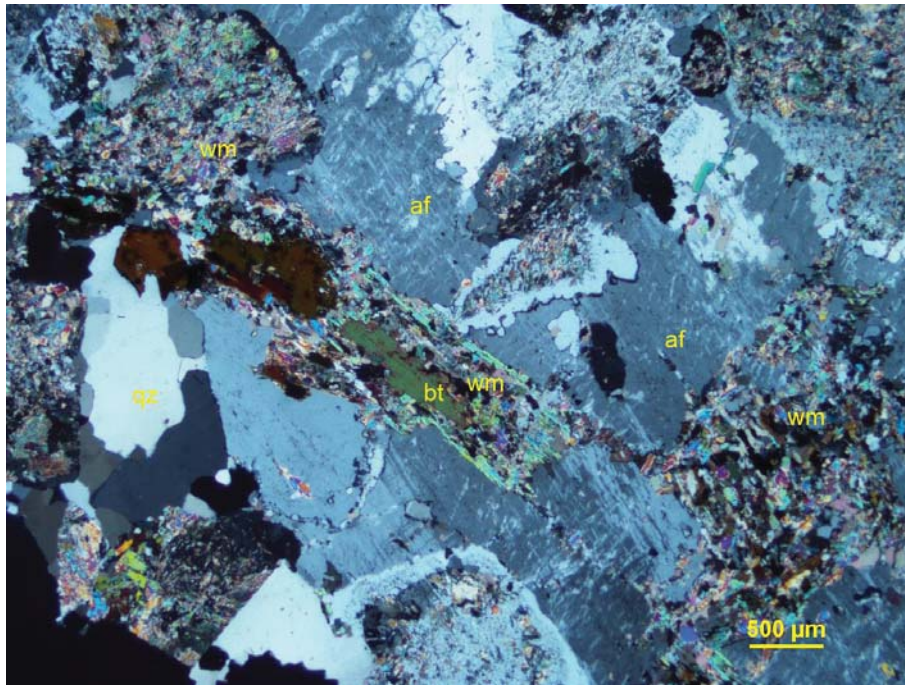
Mineral	Alteration and Weathering Mineral	Modal %	Size Range (mm)
Plagioclase (albite)	white mica	51–53	up to 3.5
Quartz		40–45	up to 2.5
Alkali feldspar		6–8	up to 2.5
[Biotite]	White mica	1–1.2	up to 2
	Pyrrhotite	tr	up to 0.1
	Calcite	tr	up to 0.1

**Plagioclase** occurs as anhedral to subhedral crystals (up to 3.5 mm long). The plagioclase is inequigranular, and it is moderately altered by fine-grained dispersions of randomly oriented flakes of white mica. The amount of alteration distinguishes the inequigranular crystals of plagioclase from the quartz and the alkali feldspar. Some of the crystals show Albite twinnings. The plagioclase is albite, as indicated by its refractive indexes smaller than those of the quartz.

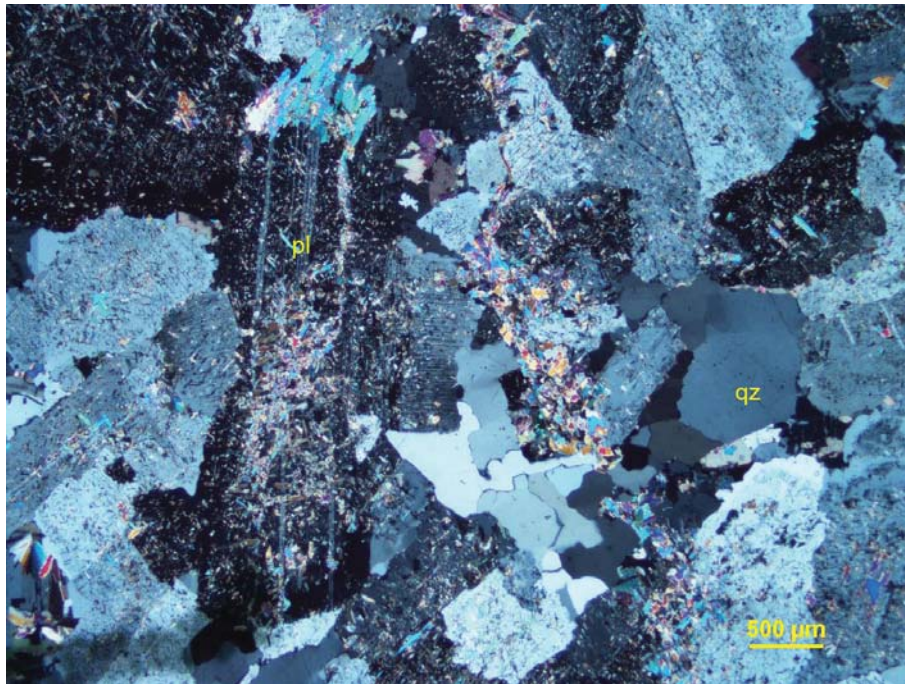
**Quartz** is anhedral and inequigranular, and occupy the interstitial positions left by the more abundant crystals of plagioclase. In some cases, the quartz crystals define structural relics of probable phenocrystals with a maximum diameter of 5 mm. The crystal boundaries between the quartz are interlobate. Some of the quartz crystals show moderate to strong undulose extinction, and sub-grain boundaries along some of the intergranular boundaries indicate that the quartz is re-crystallized because of a strained environment. This interpretation is also supported by the occurrence of Albite-Pericline twinnings within the alkali feldspar.

**Alkali feldspar** forms inequigranular interstitial crystals up to 2.5 mm across. The alkali feldspar is perthitic, twinned, and in some rare cases, host subhedral inclusions of plagioclase.

**Biotite** forms medium-grained anhedral relics dispersed within the quartzofeldspathic rock. The randomly oriented crystals of biotite and plagioclase impart the isotropic nature to this sample. In some cases, the biotite is an anhedral relic within subhedral pseudomorphs of euhedral crystals of biotite up to 2 mm long, which are partially replaced by white mica. Rare **pyrrhotite** is dispersed within the white mica in the pseudomorphs after biotite.



**Photomicrograph 11a:** The interstitial crystal of alkali feldspar (af) is perthitic and is intergrown with subhedral pseudomorphs of white mica (wm) after biotite (bt). Crossed polarizers transmitted light.



**Photomicrograph 11b:** Subhedral to anhedral crystals of plagioclase are weakly to moderately altered by white mica and are associated with interstitial crystal aggregates of quartz (qz). Crossed polarizers transmitted light.

*IG\_BH02\_LG014*

*Rock Type: Plagioclase-quartz-alkali feldspar felsitic granitoid*

This thin polished section consists of two granular domains. The two domains are mostly made up of anhedral crystals of plagioclase, alkali feldspar, quartz and subordinate lamellae of biotite with a high aspect ratio. The main difference between the two domains is the grain size of the quartzofeldspathic aggregate: it is medium-grained (up to 2.5 mm across) and fine-to medium-grained (0.2–0.5 mm) in the upper right of the thin polished section.

Alteration: white mica-epidote: subtle after biotite

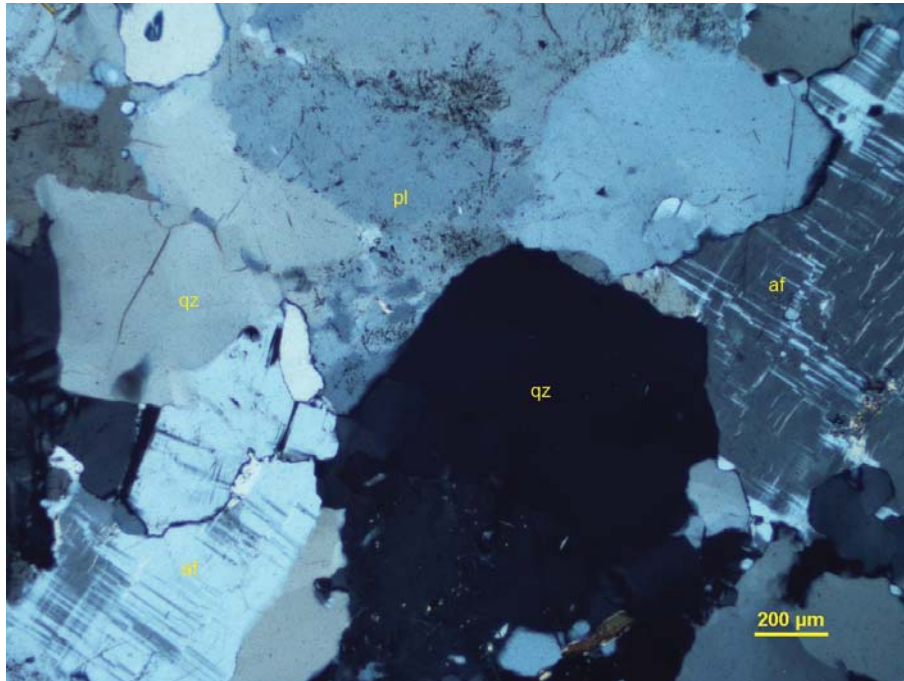
Mineral	Alteration and Weathering Mineral	Modal %	Size Range (mm)
<b>Domain A: medium-grained felsitic rock (~85% of PTS)</b>			
Plagioclase		30–32	up to 1.5
Quartz		28–30	up to 1
Alkali feldspar		24–26	up to 1
Biotite	White mica-epidote	0.2–0.5	up to 1 long
	Epidote	tr	up to 0.2
White mica		tr	up to 0.2
<b>Domain B: fine-grained felsitic rock (~15% of PTS)</b>			
Plagioclase		5	up to 0.5
Quartz		5	up to 0.5
Alkali feldspar		4.8	up to 0.4
Biotite	White mica-epidote	0.2	up to 1 long
	Epidote	tr	up to 0.1
White mica		tr	up to 0.2

**Plagioclase** forms anhedral crystals prevailing over the quartz and the alkali feldspar in the two domains. The crystals are relatively fresh and show Albite twinnings. In Domain A, the plagioclase crystals are anhedral and range from 0.3 to 1.5 mm across. In Domain B, the plagioclase is finer-grained, and it is mostly fine-grained and in some cases up to 0.5 mm across.

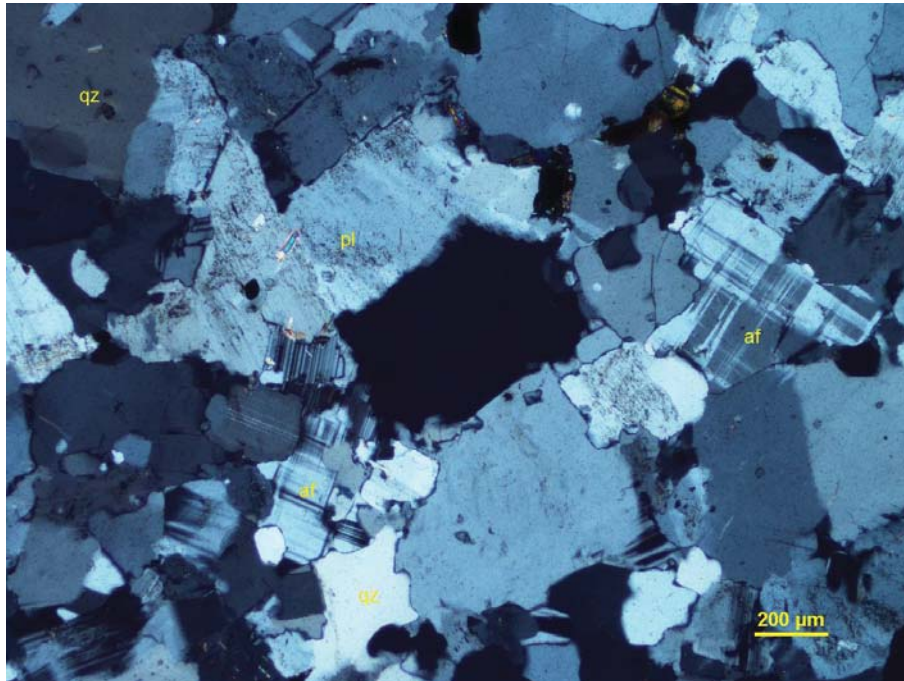
**Quartz** forms anhedral crystals intergrown with the feldspar. It is coarser-grained (up to 1.5 mm across) in Domain A, and finer-grained (up to 0.5 mm across) in Domain B.

**Alkali feldspar** is heterogeneously dispersed within the two domains. Its anhedral crystals are distinguished by the typical Albite-Pericline twinnings (a.k.a. tartan pattern) as shown in Photomicrograph 12a and 12b. The coarser crystals of alkali feldspar host fine-grained perthitic stringlets.

**Biotite** occurs as randomly oriented lamellae, which are characterized by an aspect ratio up to 0.05 to 1 mm (Photomicrograph 12c). This feature indicates that the biotite likely crystallized in a liquid. Rare crystals of epidote and flakes of white mica are spatially associated with the biotite.



**Photomicrograph 12a:** Domain A—Anhedral crystals of plagioclase (pl), quartz (qz) and alkali feldspar (af) define a medium-grained granular microstructure. Crossed polarizers transmitted light.



**Photomicrograph 12b:** Domain B—Anhedrals crystals of plagioclase (pl), quartz (qz) and alkali feldspar (af) define a fine-grained granular microstructure. Crossed polarizers transmitted light.



**Photomicrograph 12c:** The biotite (bt) forms elongate lamellae with a high aspect ratio. Plane polarized transmitted light.

*IG\_BH02\_LG015*

*Rock Type: Tremolite-calcite-biotite granofels*

Xenoblastic and inequigranular crystals of calcite, amphibole, plagioclase, chlorite, and biotite define a granular isotropic microstructure.

Mineral	Alteration and Weathering Mineral	Modal %	Size Range (mm)
Amphibole (tremolite?)		55–57	up to 1
Calcite		22–24	up to 0.8
Biotite		15–15	up to 1
Plagioclase		4–5	up to 0.7
Chlorite	Chlorite-rutile	2–5	up to 0.5
Epidote		0.2–0.3	up to 0.2
Titanite		tr	up to 0.1
Pyrite		tr	up to 0.1

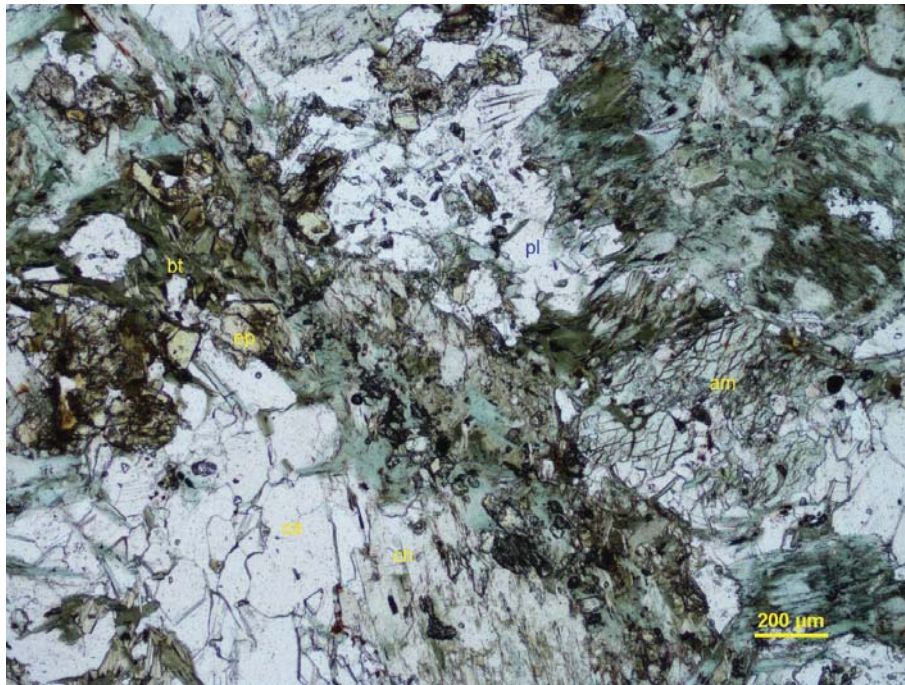
Xenoblastic and inequigranular crystals of **amphibole** are randomly oriented and variably intergrown with fine-grained flakes of biotite and chlorite. The amphibole shows a very subtle pleochroism with pale green tints and an extinction angle up to 20°. These optical features suggest that the amphibole belongs to the tremolite-actinolite series.

**Calcite** forms medium-grained crystal aggregates, which are heterogeneously dispersed within the xenoblastic microstructure. The calcite is distinguished by its high relief, extreme birefringence, and brisk reaction to cold dilute (10%) HCl.

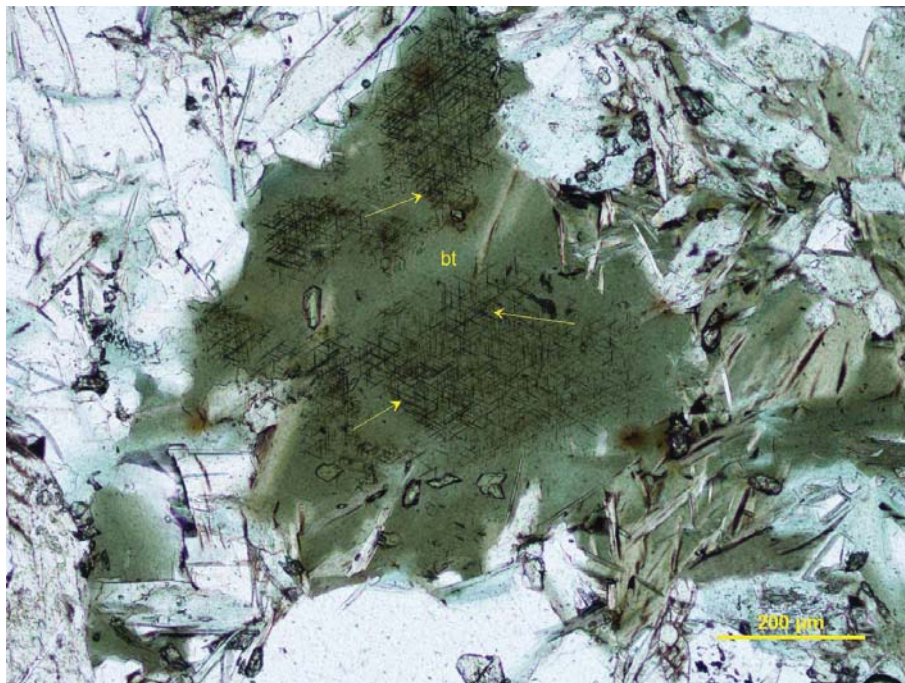
**Biotite** is xenoblastic, and it occurs as inequigranular lamellae and flakes. In some cases, the biotite is partially to completely replaced by chlorite, and in some of its crystals, sagenitic rutile occurs (Photomicrograph 13b).

**Plagioclase** is dispersed as relict anhedral crystals, which I interpret as the only magmatic relic from the mafic magmatic rock. The plagioclase is relatively fresh. It shows Albite twinnings, and in some cases it is overprinted by fine-grained crystals of biotite and epidote. In rare instances, the plagioclase forms relict magmatic microstructures. In one example (Photomicrograph 13c) the plagioclase forms interstitial crystals surrounding a subhedral crystal of amphibole, which is partially replaced by biotite and chlorite.

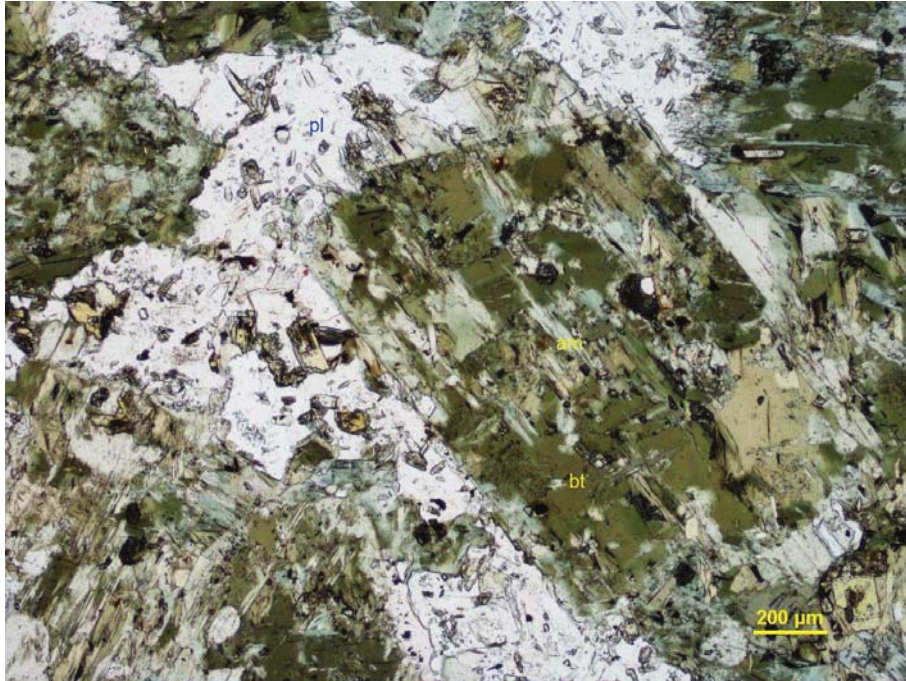
Very rare and fine-grained crystals of **pyrite** are heterogeneously dispersed within this thin polished section and are spatially associated with the biotite-chlorite crystals.



**Photomicrograph 13a:** Xenoblastic crystals of amphibole (am), crystal aggregates of calcite (ca), biotite (bt), chlorite (ch), and epidote (ep). Plane-polarized transmitted light.



**Photomicrograph 13b:** The biotite crystal (bt) hosts very fine-grained sagenitic rutile (yellow arrows). Plane-polarized transmitted light.



**Photomicrograph 13c:** Plagioclase (pl) crystals surround a subhedral crystal of amphibole (am), which is partially replaced by biotite. Plane-polarized transmitted light.

*IG\_BH02\_LG017*

*Rock Type: Foliated microtonalite*

Medium-grained crystals of plagioclase are randomly oriented and associated with anhedral and interstitial crystals of quartz and subordinate crystals of biotite. The biotite shows a subtle preferred dimensional orientation and defines a subtle foliation.

**Alteration: white mica:** weak after plagioclase; **epidote:** subtle

Mineral	Alteration and Weathering Mineral	Modal %	Size Range (mm)
Plagioclase		50–52	0.5–2.5
Quartz		43–45	up to 0.5, rare up to 2 long
Biotite	Epidote	4–5	up to 0.8, rare up to 2 long
Alkali feldspar		1–2	up to 0.2
Zircon		tr	up to 0.01

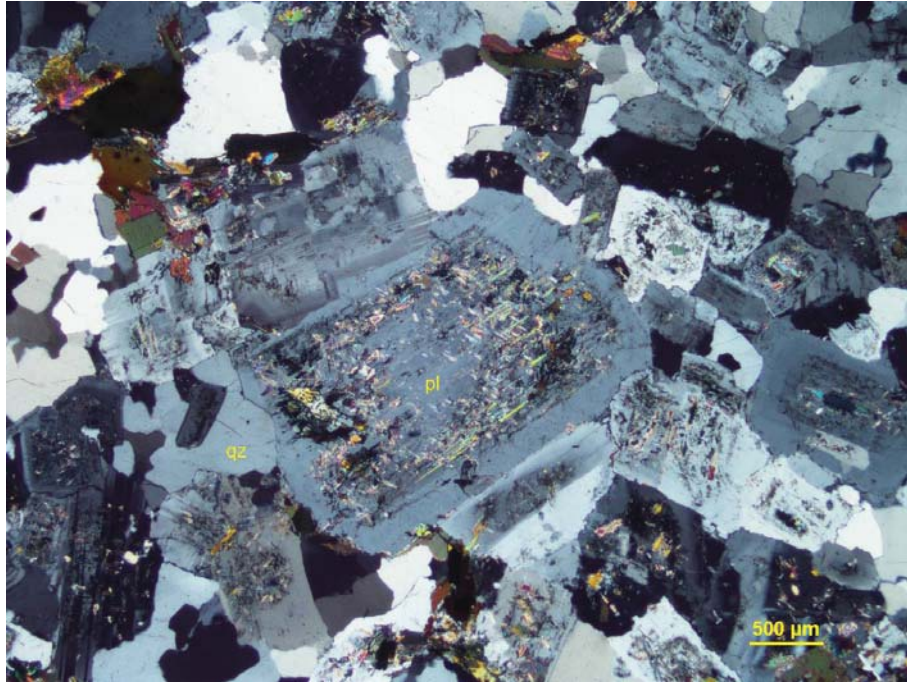
**Plagioclase** forms medium-grained (0.5–2.5 mm) subhedral and randomly oriented crystals showing Albite twinnings and subhedral oscillatory zoning. The plagioclase grain size distribution is seriate and defines a mostly inequigranular microstructure. In some cases, some of the growth zones host very fine-grained white mica alteration products.

**Quartz** forms anhedral crystals and crystal aggregates occupying the interstitial positions between the plagioclase (Photomicrograph 14).

**Biotite** is dispersed within the granular microstructure dominated by plagioclase and quartz. Its lamellae show a subtle preferred iso-orientation imparting to the rock a subtle foliation. I interpret this foliation as having been generated during the latest stages of magmatic crystallization.

Rare and mostly fine-grained crystals of **alkali feldspar** occupy the interstices between the plagioclase and the quartz. The alkali feldspar crystals are fresh and show Albite-Pericline twinning.

Fine-grained lamellae of **white mica** overprinted and are spatially associated with the biotite lamellae, and in some cases, are associated with fine-grained (up to 0.2 mm across) crystals of epidote.



**Photomicrograph 14:** Subhedral crystals of plagioclase (pl) show a subhedral growth zone and a selective white mica alteration in some of the growth zones. The plagioclase crystals are associated with interstitial and anhedral crystals of quartz (qz) and subordinate biotite. Crossed polarizers transmitted light.

*IG\_BH02\_LG018*

*Rock Type: Chlorite-altered granodiorite (?)  
Alkali feldspar-quartz brecciated veinlets  
Calcite veinlets*

Anhedral to subhedral crystals of plagioclase, anhedral crystals and crystal aggregates of quartz, anhedral crystals of alkali feldspar, and randomly oriented clusters of chlorite replacing magmatic biotite define a granular microstructure, which is crosscut by irregular veinlet hosting angular crystals of quartz and alkali feldspar-rich matrix. The alkali feldspar-quartz infills are crosscut by calcite-rich veinlets.

Alteration: chlorite: strong after biotite; clay and/or epidote: weak to moderate after plagioclase.

Mineral	Alteration and Weathering Mineral	Modal %	Size Range (mm)
<b>Granodiorite (?) (~98% of PTS)</b>			
Plagioclase	Clay and/or epidote	46–48	up to 2
Quartz		31–33	0.05–2
Alkali feldspar		15–20	up to 2
[biotite]	Chlorite	4–5	up to 1.5 long
	Epidote	tr	up to 0.3
Zircon		tr	up to 0.01
<b>Alkali-feldspar- quartz veinlets (~2% of PTS)</b>			
Alkali feldspar		1.5	up to 0.01
Quartz		0.5	up to 0.1
<b>Calcite veinlets</b>			
Calcite		tr	up to 1 long

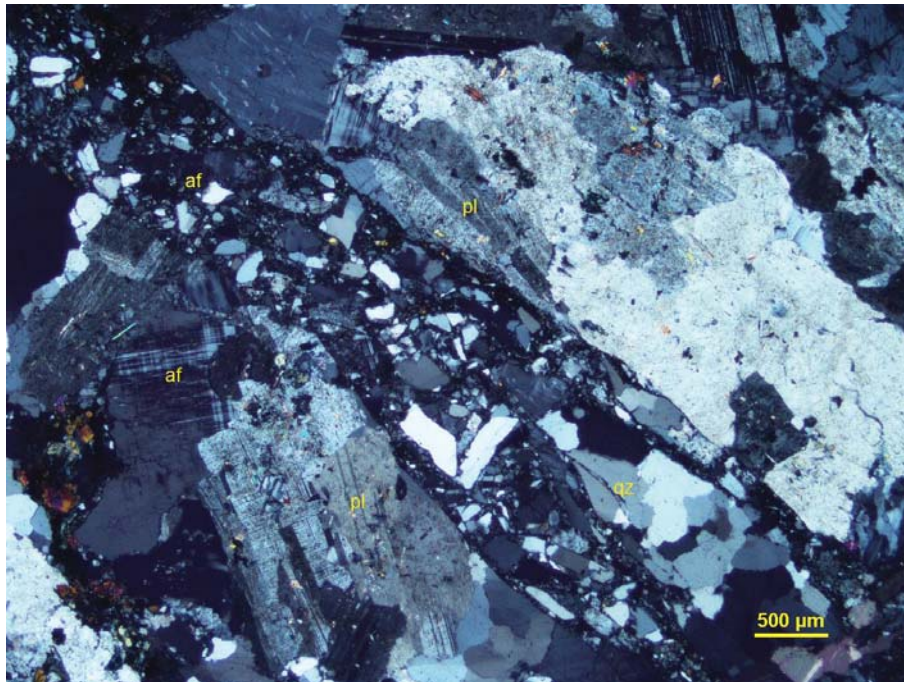
**Plagioclase** occurs as anhedral to subhedral crystals (up to 2 mm across). The plagioclase crystals are randomly oriented and are moderately altered by very fine-grained and unresolved material, which I tentatively interpret as clay and/or epidote.

**Quartz** forms inequigranular anhedral crystals and crystal aggregates occupying the interstitial positions between the prevailing plagioclase. Angular crystal fragments of quartz are rotated and immersed within a very fine-grained matrix in the irregular veinlets crosscutting the granular magmatic microstructure (Photomicrograph 15). I interpret these veinlets as generated during a brittle event triggered by fluid overpressure at the end of the magmatic crystallization.

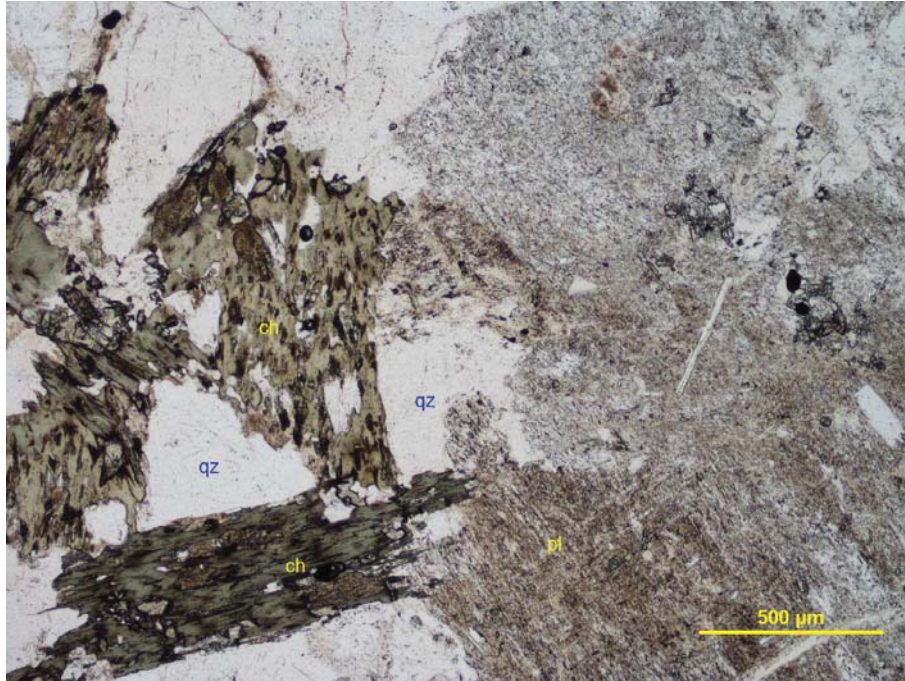
**Alkali feldspar** forms anhedral, inequigranular (up to 2 mm across) and fresh crystals dispersed within the granular magmatic rock. Very fine-grained alkali feldspar forms the matrix of brecciated veinlets crosscutting the magmatic rock. The distribution of the alkali feldspar can be observed in the image of the stained billet (please see the corresponding billet photo), in which the alkali feldspar is stained yellow.

**Chlorite** epitaxially replaced fine- to medium-grained lamellae of magmatic biotite. The chlorite lamellae are randomly oriented and form irregular clusters, which impart to the granular microstructure and isotropic nature.

**Calcite** filled in thin veinlets crosscutting the granular microstructure and the brecciated alkali feldspar-quartz veinlets.



**Photomicrograph 15a:** An irregular brecciated veinlet is made up of angular fragments of quartz (qz), and crosscuts a granular microstructure defined by plagioclase (pl), quartz, and alkali feldspar (af). Crossed polarizers transmitted light.



**Photomicrograph 15b:** Subhedral and weakly altered crystals of plagioclase (pl), epitaxial replacements of chlorite after biotite (ch) and interstitial crystals of quartz define a granular isotropic microstructure within the host rock. Plane-polarized transmitted light.

*IG\_BH02\_LG020*

*Rock Type: Plagioclase-phyric andesite*

Subhedral phenocrystals of plagioclase are randomly oriented within a fine-grained interlobate groundmass of quartz and plagioclase. Fine-grained lamellae of biotite are dispersed within the groundmass.

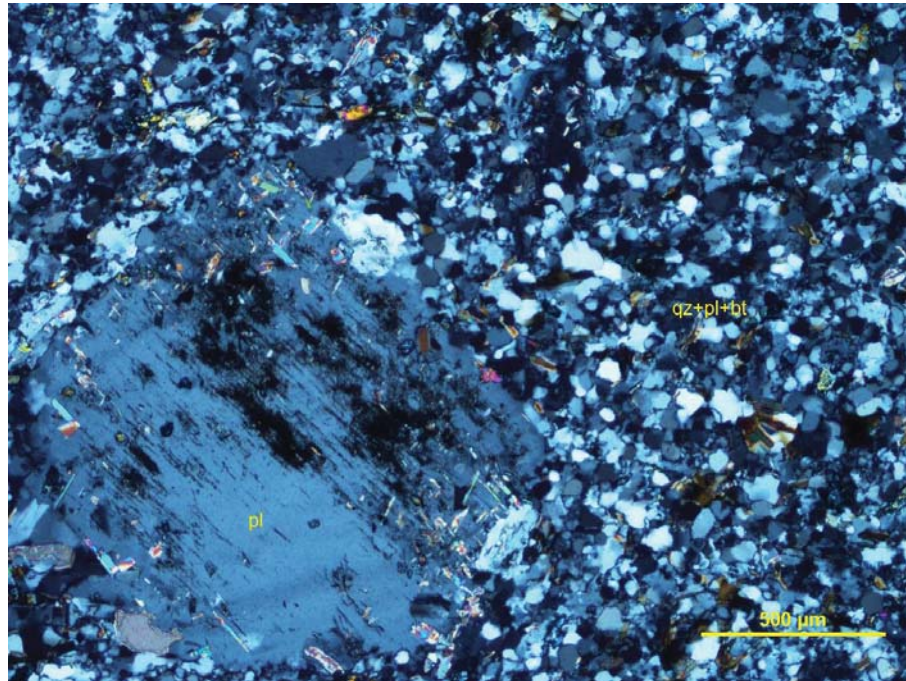
Alteration: white mica: weak after plagioclase and within the groundmass; epidote: subtle to weak after biotite; chlorite-iron oxides: subtle.

Mineral	Alteration and Weathering Mineral	Modal %	Size Range (mm)
Phenocrystals			
Plagioclase		7–8	up to 2
Biotite		0.2–0.4	up to 0.8 long
Groundmass			
Plagioclase (albite)		51–53	up to 0.1
Quartz		38–40	up to 0.1
Biotite		1–2	up to 0.2
	White mica	0.5–1	up to 0.2
	Epidote	0.3–0.5	up to 0.2
	Chlorite	tr	up to 0.1
Ilmenite (?)		tr	up to 0.15
	Iron oxides	tr	up to 0.1

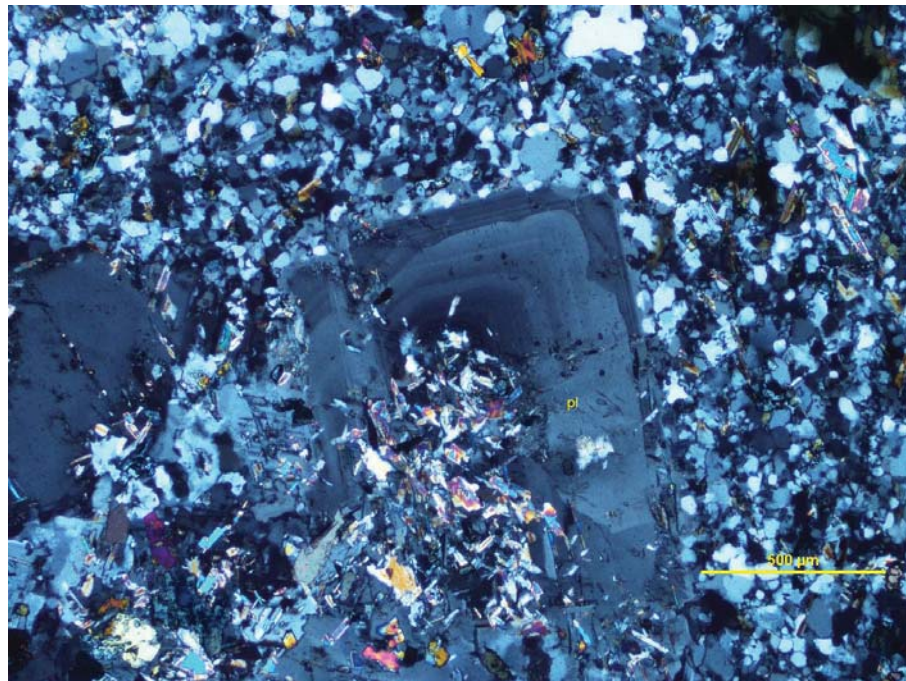
**Plagioclase** forms subhedral phenocrystals (up to 2 mm across), which are randomly oriented within the groundmass, and in some cases (Photomicrograph 16b), shows euhedral growth zoning. The plagioclase is weakly altered by very fine-grained flakes of white mica. The alteration products are concentrated within the phenocrystal core (Photomicrograph 16b). Fine-grained plagioclase (albite) is intergrown with the quartz in the groundmass. The albitic composition of the plagioclase is determined by its refractive indexes, which are lower than those of the quartz.

**Quartz** forms fine-grained interlobate crystals intergrown with the plagioclase and the biotite in the groundmass. In some cases, the quartz, in association with flakes of chlorite and fine-grained anhedral crystals of epidote, define lenticular to irregular replacement patches or fillings dispersed within the groundmass.

**Biotite** is dispersed as fine-grained flakes within the quartz and plagioclase groundmass. Rare phenocrystals of biotite (up to 0.8 mm long) are randomly oriented. Fine-grained anhedral crystals of **epidote** are spatially associated and overprinted the medium-grained phenocrystals and the fine-grained flakes of biotite.



**Photomicrograph 16a:** A subhedral phenocrystal of plagioclase (pl) is immersed within a fine-grained groundmass of plagioclase, quartz, and biotite (qz+pl+bt). Crossed polarizers transmitted light.



**Photomicrograph 16b:** Very fine-grained flakes of white mica (highly birefringent) are concentrated within the core of the growth zonation of the plagioclase (pl). Crossed polarizers transmitted light.

*IG\_BH02\_LG021*

Rock Type: *Metabasite*

This thin polished section consists of two domains. In the lower part (Domain A), fine-grained and randomly oriented crystals of actinolite, plagioclase, chlorite, and epidote define a relatively homogeneous and isotropic granular microstructure. In the upper part (Domain B), the chlorite defines irregular and sub-parallel cleavage domains separating the fine-grained granular microlithons of plagioclase, epidote, amphibole, and biotite.

Alteration: iron oxides: intense after probable sulphide

Mineral	Alteration and Weathering Mineral	Modal %	Size Range (mm)
<b>Domain A: metabasite (~55% of PTS)</b>			
Actinolite (and hornblende?)		21–23	up to 0.3 long, rare up to 0.7 long
Plagioclase		20–22	up to 0.2 long
Epidote		7–9	up to 0.1
Quartz		4–5	up to 0.1
Chlorite		1–2	up to 0.1
Titanite		tr	up to 0.05
[?]	iron oxides	tr	[up to 0.2]
<b>Domain B: chlorite schist (~45% of PTS)</b>			
Plagioclase		11–13	up to 0.1
Chlorite		10–12	up to 0.3 long
Epidote		9–11	up to 0.2, rare up to 0.8 long
Amphibole		8–10	up to 0.1
Quartz		5–6	up to 0.1
Biotite		1–2	up to 0.1
[?]	iron oxides	1–2	[up to 0.5 long]
Titanite		tr	up to 0.1

**Plagioclase** occurs in both domains as fine-grained xenomorphic crystals (up to 0.2 mm long in Domain A, and up to 0.1 mm across in Domain B). The plagioclase crystals are fresh and, in some cases, show Albite twinnings. In rare cases, the plagioclase crystals show growth zoning indicative of the magmatic origin of the mineral.

**Actinolite** forms subidiomorphic crystals (up to 0.3 mm long, and in rare instances, up to 0.7 mm long) randomly oriented in Domain A. The actinolite is distinguished by its weak green pleochroism and extinction angles up to 15°. The actinolite partially replaced a more pleochroic (see green to brown crystal cores in Photomicrograph 17a). The green to brown pleochroism of the relics suggests that the pre-existing mineral is probable hornblende. In Domain B, the amphibole is less to non-pleochroic, and it is subordinate to the plagioclase, epidote, and chlorite.

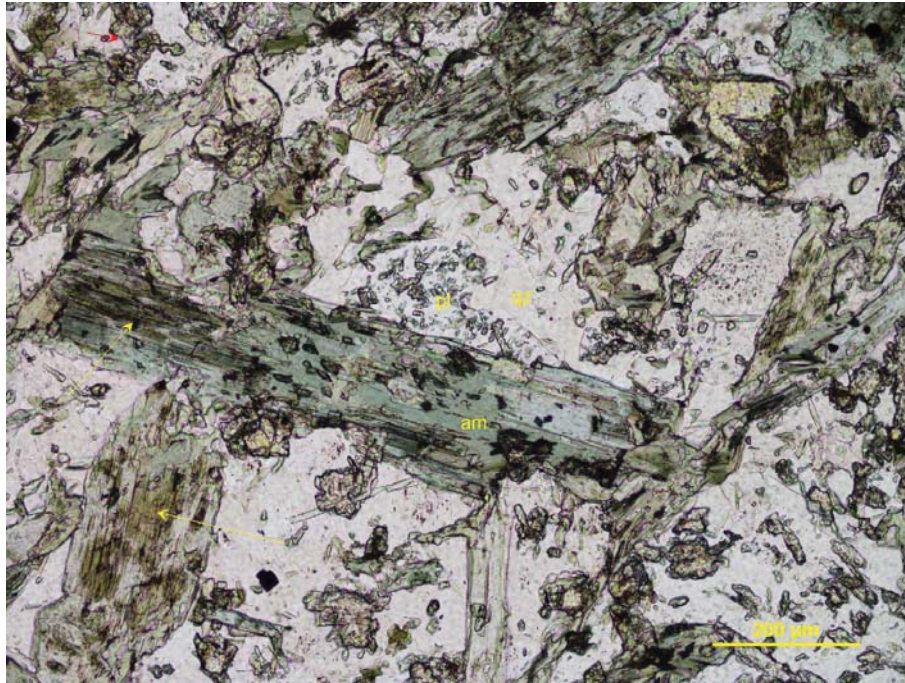
**Chlorite** is concentrated within irregular and sub-parallel cleavage domains defining a spaced schistosity in Domain B. Fine-grained lamellae of biotite partially replaced fine-grained lamellae of biotite outside of the chlorite cleavage domains. In Domain A, the chlorite forms irregular replacement patches and crystal clusters, probably replacing magmatic biotite.

**Epidote** forms fine-grained xenomorphic crystals (up to 0.2 mm across) associated with the plagioclase in the microlithons and forms idiomorphic crystals (up to 0.8 mm long) intergrown with the quartz within lenticular to irregularly shaped domains in Domain B (Photomicrograph 17b). The epidote is fine-grained and subordinate to the actinolite, plagioclase, and chlorite in the granular microstructure of Domain A.

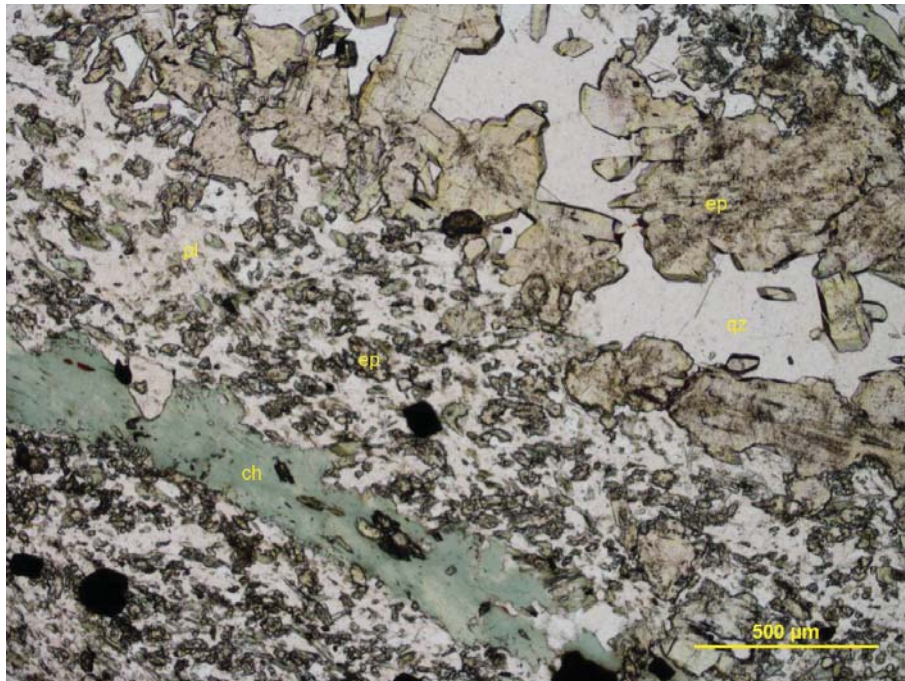
**Quartz** forms fine-grained xenomorphic crystals subordinate and intergrown with the plagioclase in both domains and forms irregular to lenticular domains associated with the epidote in Domain B (Photomicrograph 17b).

**Biotite** occurs as fine-grained relic lamellae, which are partially replaced by the amphibole and the chlorite in Domain B.

**Iron oxides** form layered replacements after probable sulphide (up to 0.5 mm long) preferentially associated and oriented parallel to the chlorite-rich cleavage domains. The iron oxides alteromorphs are fine-grained and less abundant in Domain A



**Photomicrograph 17a:** Subidiomorphic crystals of amphibole are randomly oriented and are associated with interstitial crystals of plagioclase (pl) and quartz (qz). More pleochroic relicts of probable hornblende (see yellow arrows) are overgrown by green-pleochroic crystals (actinolite) Plane-polarized transmitted light.



**Photomicrograph 17b:** The chlorite is concentrated within irregular cleavage domains (ch) wrapping microliths of plagioclase (pl), epidote (ep), and quartz. Quartz (qz) and epidote (ep) also form lenticular domains oriented parallel to the schistosity defined by the chlorite-rich cleavage domains. Plane-polarized transmitted light

*IG\_BH02\_LG022*

*Rock Type: Granodiorite*

Euhedral to subhedral crystals of plagioclase, interstitial to anhedral crystals of quartz and alkali feldspar and randomly oriented lamellae of biotite define a coarse-grained granular and isotropic microstructure.

Alteration: clay and/or epidote-white mica: weak to moderate after plagioclase.

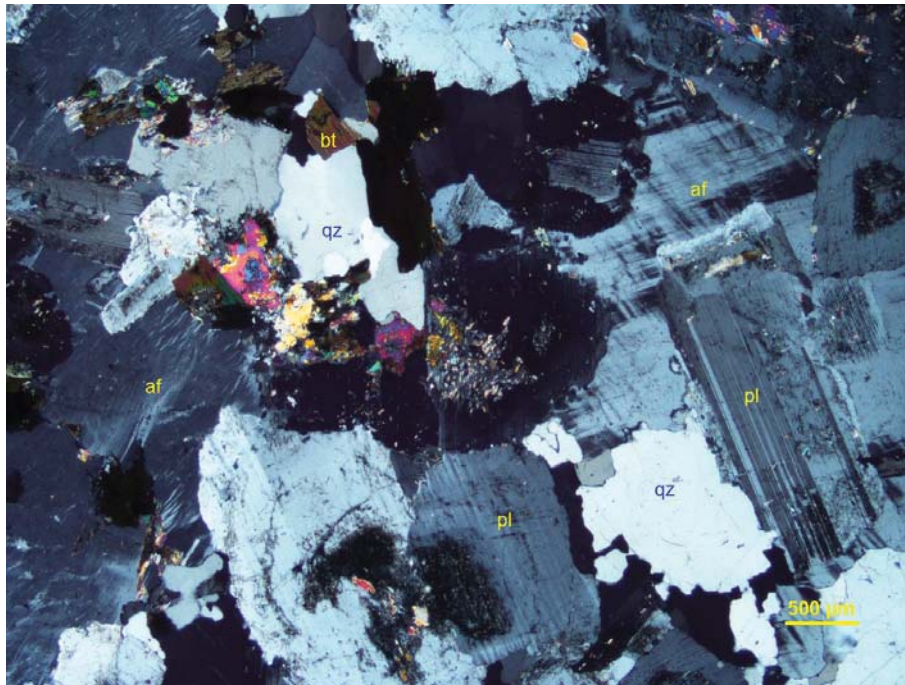
Mineral	Alteration and Weathering Mineral	Modal %	Size Range (mm)
Plagioclase	Epidote-white mica	40–41	up to 4 long
Quartz		39–40	up to 2.5
Alkali feldspar	Epidote	18–19	up to 3.5
Biotite	White mica	1–1.2	up to 2 long
	Epidote	0.1–0.2	up to 0.2
Zircon		tr	up to 0.01

**Plagioclase** occurs as subhedral to euhedral crystals (up to 4 mm long), which are randomly oriented and impart the granular microstructure to this sample. The plagioclase crystals show a subhedral growth zoning, and very fine-grained earthy and unresolved material, probably **epidote**, altered the plagioclase along some of the growth zones. Fine-grained flakes of **white mica** weakly to moderately alter the plagioclase crystals.

**Quartz** defines inequigranular anhedral and inequigranular crystals occupying the interstitial positions between the plagioclase crystals. Some of the crystals show moderate undulose extinction, thus indicating that this rock was subjected to a strain field after its crystallization.

**Alkali feldspar** is heterogeneously dispersed in this thin polished section (see the image of the stained billet). The alkali feldspar is anhedral and forms crystals up to 3.5 mm across, and in most cases, the alkali feldspar is fresh and perthitic.

**Biotite** is medium-grained (up to 2 mm long), and its lamellae are randomly oriented within the granular microstructure. Thin rims of very fine-grained white mica flakes indicate that the biotite is weakly altered. Some of the biotite lamellae are overprinted by fine-grained anhedral crystals of epidote.



**Photomicrograph 18:** Subhedral crystals of plagioclase (pl) anhedral crystals of alkali feldspar (af) and quartz (qz) and subordinate crystals of biotite define a granular isotropic microstructure. Crossed polarizers transmitted light.

*IG\_BH02\_LG023*

*Rock Type: Albite-rich alteration zone (albitite)*

Anhedral to subhedral crystals of plagioclase dominate this thin polished section and define a granular microstructure, in which subordinate clusters of fine-grained chlorite and anhedral crystals of calcite occupy interstitial positions between the plagioclase.

Alteration: albite: intense; calcite-Fe-chlorite: weak; epidote-titanite-tourmaline: subtle.

Mineral	Alteration and Weathering Mineral	Modal %	Size Range (mm)
	Plagioclase → white mica	95–96	0.5–5
	Fe-chlorite	2–2.5	up to 0.15
	Calcite	1–1.1	up to 3
	Epidote	tr	up to 0.8 long
	Titanite	tr	up to 1.2 long
	Tourmaline	tr	up to 0.15

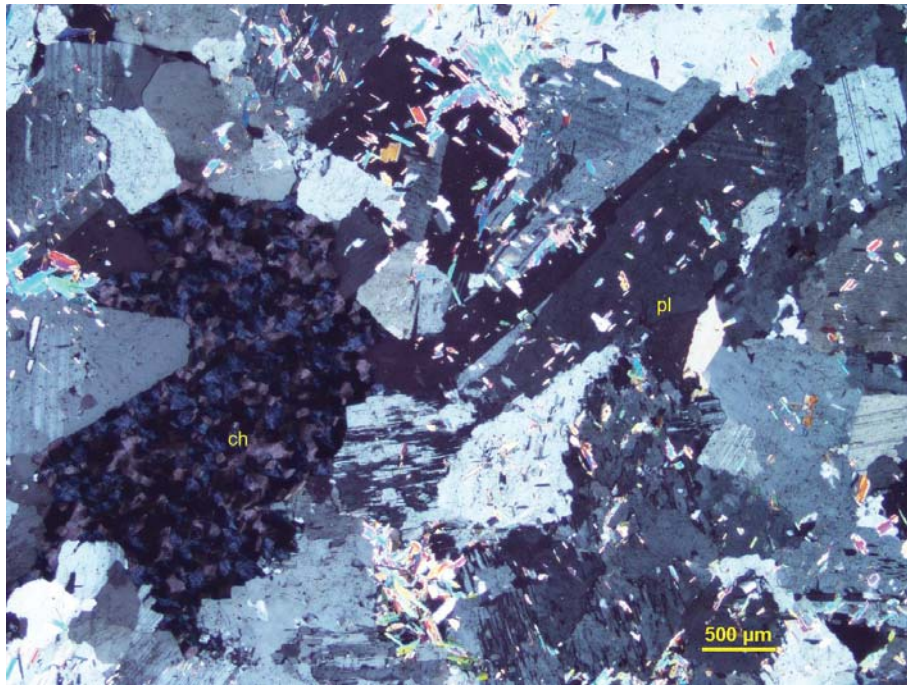
**Plagioclase (albite)** forms inequigranular (0.5–5 mm across) crystals showing anhedral to subhedral shapes. The plagioclase crystals show Albite twinings and are weakly altered by very fine-grained flakes of white mica. The small extinction angle between adjacent Albite twinings indicates that the plagioclase is albite.

**Calcite** occurs as anhedral crystals (up to 3 mm across) occupying the interstices between the plagioclase crystals. The calcite is identified by its strong relief, extreme birefringence under crossed Nicols, and brisk reaction to cold dilute (10%) HCl. Rare and fine- to medium-grained (up to 1.2 mm long) crystals of titanite are spatially associated and intergrown with the calcite crystals.

**Fe-chlorite** forms very fine-grained (up to 0.15 mm across) books concentrated within interstitial domains filling an irregular crack crosscutting the plagioclase crystals (Photomicrograph 19). The anomalous interference colour and the strong green pleochroism indicate that the chlorite is iron-rich. Very rare anhedral crystals of **epidote** (up to 0.8 mm long) are dispersed within the plagioclase and are spatially associated with the fine-grained flakes of white mica.

Very rare and fine-grained crystals of **tourmaline** (up to 0.15 mm long) are dispersed within one crystal of calcite and are distinguished by their strong pleochroism with brown tints and by their typical absorption pattern.

Because of the abundance of plagioclase, the occurrence of typical alteration minerals like chlorite, calcite, and tourmaline, I interpret this rock as an albite-rich alteration zone (albitite).



**Photomicrograph 19:** Anhedral to subhedral crystals of plagioclase (pl) are weakly altered by fine-grained flakes of white mica and are associated with interstitial domains of Fe-chlorite (ch). Crossed polarizers transmitted light.

*IG\_BH02\_LG024*

*Rock Type: Granophyric pegmatite*

Coarse-grained anhedral crystals of alkali feldspar and plagioclase define granophyric intergrowths with subordinate quartz and define a pegmatitic and isotropic microstructure.

**Alteration: white mica:** subtle after alkali feldspar

Mineral	Alteration and Weathering Mineral	Modal %	Size Range (mm)
Alkali feldspar	White mica	60 <sup>1</sup>	up to 25
Plagioclase		30 <sup>1</sup>	up to 13
Quartz		10 <sup>1</sup>	up to 20
Magnetite		tr	up to 0.2, one crystal 0.5 long
Chalcopyrite		tr	0.02

**Alkali feldspar** prevails over the plagioclase in this thin polished section (see the image of the stained billet). It forms anhedral crystals (up to 25 mm in this section). The alkali feldspar is fresh, it shows Albite-Pericline twinnings, and forms granophyric intergrowths with quartz (Photomicrograph 20a). These intergrowths indicate that the alkali feldspar and the quartz crystallized together from the melt.

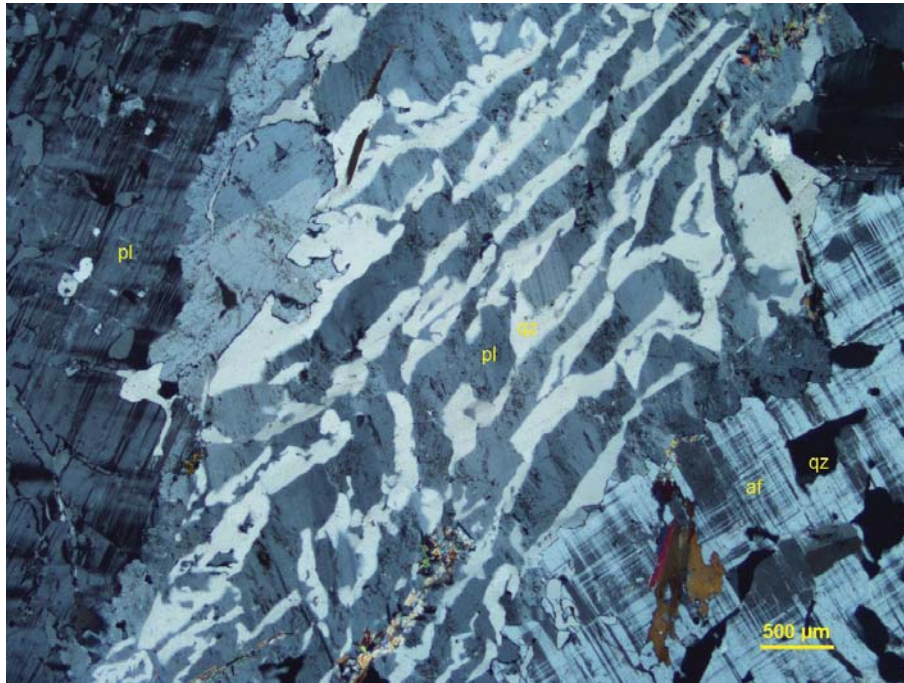
**Plagioclase** is anhedral and, similarly with the alkali feldspar, forms granophyric intergrowths with the quartz (Photomicrographs 20a and 20b). The plagioclase is less abundant than the alkali feldspar, and its crystals are up to 13 mm long in this section.

**Quartz** is graphically intergrown with the feldspars (see Photomicrographs 20a and 20b, and forms anhedral crystals along some of the interstitial spaces left by the feldspars.

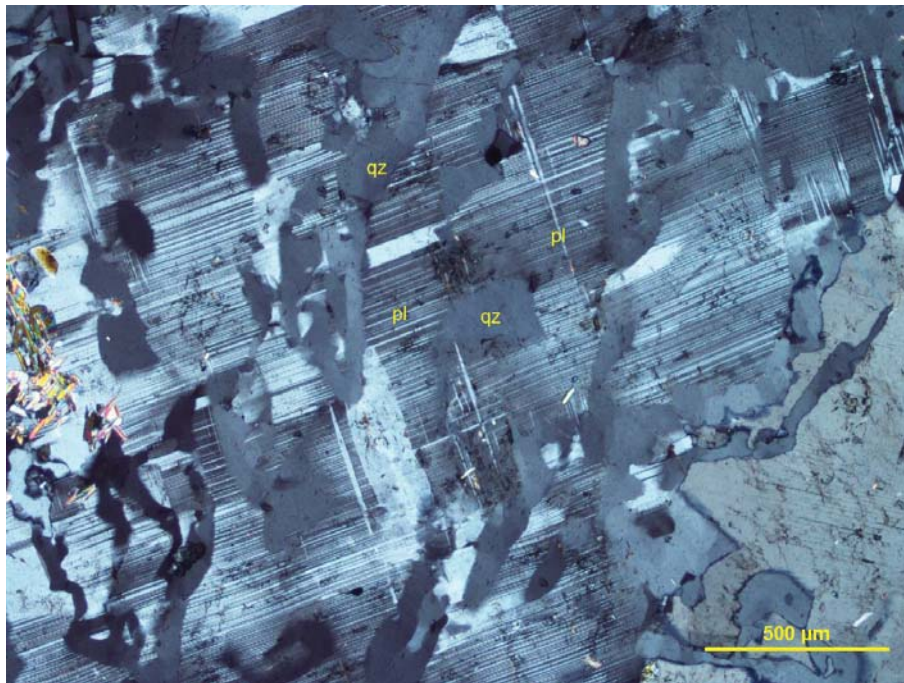
Fine-grained flakes of **white mica** are dispersed within the granophyric alkali feldspar. Rare fine-grained crystals of magnetite are dispersed within alkali feldspar crystals. In one case, a triangular crystal is 0.5 mm long. Other anhedral crystals are 0.2 mm across.

---

<sup>1</sup> The modal percentage is not accurate because of the coarse-grained nature of this rock.



**Photomicrograph 20a:** Anhedral and coarse-grained crystals of plagioclase (pl) and alkali feldspar (af) define granophyric intergrowths with quartz (qz). Crossed polarizers transmitted light.



**Photomicrograph 20b:** The granophyric crystal of plagioclase (pl) is distinguished by the Albite twinnings and is intergrown with quartz (qz). Crossed polarizers transmitted light.

*IG\_BH02\_LG025*

*Rock Type: Chlorite-altered granodiorite*

Subhedral crystals of plagioclase, anhedral to interstitial crystals of quartz, and interstitial to poikilitic crystals of alkali feldspar define a coarse-grained granular microstructure, in which subordinate pseudomorphs of chlorite after biotite are randomly oriented.

Alteration: white mica: weak after plagioclase; subtle after biotite; Fe-chlorite: intense after biotite; epidote: subtle.

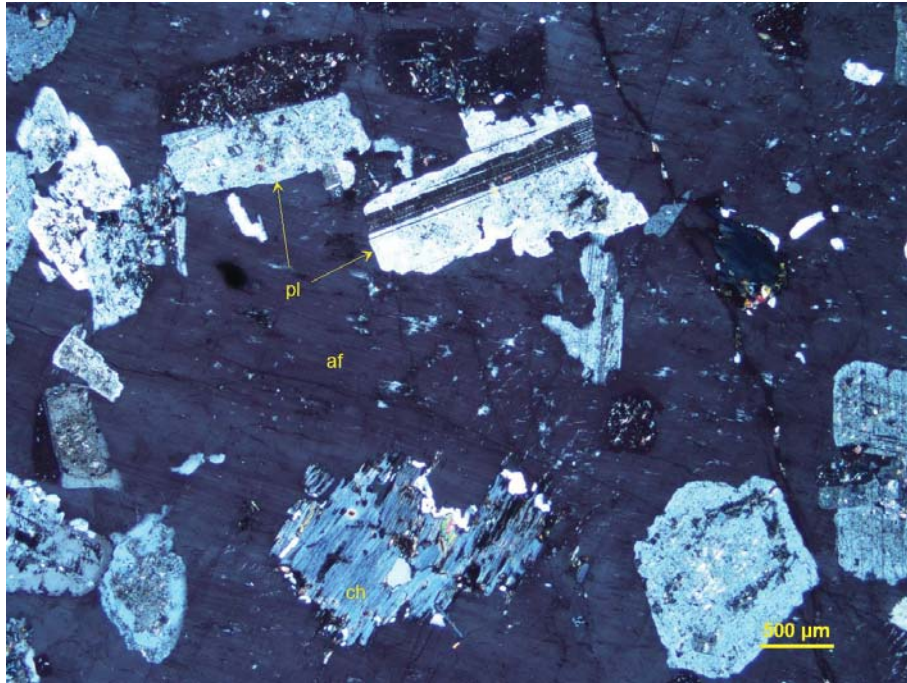
Mineral	Alteration and Weathering Mineral	Modal %	Size Range (mm)
Plagioclase	White mica	51–52	up to 3 long
Quartz		23–24	up to 5
Alkali feldspar		23–24	up to 8
[biotite]	Fe-chlorite>>white mica	1.5–2	up to 1
	Epidote	tr	up to 0.1
Zircon		tr	up to 0.01

**Plagioclase** is the most abundant mineral in this thin polished section; however, it is the finer-grained among the main constituents—plagioclase, quartz, and alkali feldspar. The plagioclase is subhedral to euhedral and its crystals are up to 3 mm long. The plagioclase crystals are weakly altered by a very fine- to fine-grained flakes of white mica. In some cases, the alteration product is selectively concentrated within the subhedral growth zoning of the plagioclase. Most of the plagioclase crystals show Albite twinnings.

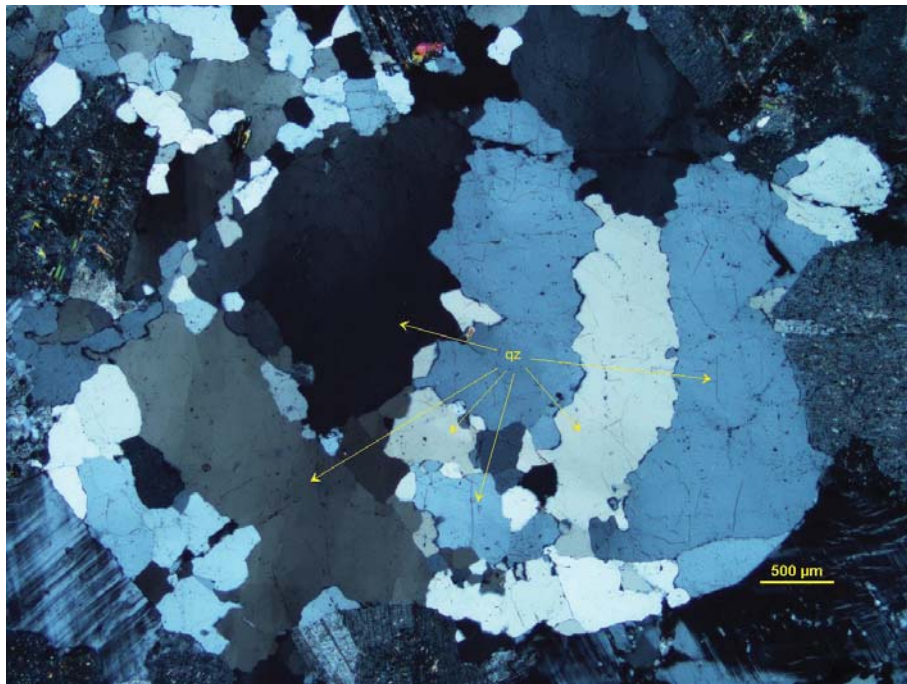
**Quartz** occurs as anhedral and inequigranular crystals occupying the interstices between the plagioclase crystals, and forming anhedral to sub-rounded domains, in which rare crystals reach 5 mm in length, and most of the crystals recrystallized from the magmatic quartz into interlobate crystals. Some quartz crystals show moderate undulose extinction, thus indicating that a strain field may have triggered the recrystallization of the coarser-grained magmatic quartz (Photomicrograph 21b).

**Alkali feldspar** occurs as inequigranular anhedral, interstitial (up to 2.5 mm across), and in some cases, coarse-grained poikilitic crystals (up to 8 mm across) hosting subhedral crystals of plagioclase and pseudomorphs of chlorite (Photomicrograph 21a). The alkali feldspar is fresh. In the medium-grained crystals, it tends to show Albite-Pericline twinnings, and in the coarse-grained crystals, it is perthitic (Photomicrograph 21a). In the thin polished section, the alkali feldspar is heterogeneously distributed (refer the image of the stained billet, in which the alkali feldspar is yellow).

**Fe-chlorite** epitaxially replaced subhedral crystals of biotite (up to 1 mm across). The pseudomorphs are randomly oriented and impart an isotropic nature to the granular microstructure. The Fe-chlorite is distinguished by its moderate to strong green pleochroism and anomalous birefringence colour. Rare and fine-grained crystals of epidote preferentially overprinted the chlorite-rich pseudomorphs. Very fine-grained dispersions of **zircon** within the chlorite further prove, together with the shape of the pseudomorphs, that the chlorite replaced magmatic crystals of biotite.



**Photomicrograph 21a:** A coarse-grained poikilitic and perthitic crystal of alkali feldspar (af) hosts subhedral crystals of plagioclase (pl) and a Fe-chlorite pseudomorph after biotite (ch). Crossed polarizers transmitted light.



**Photomicrograph 21b:** A microstructural relic of a coarse-grained magmatic quartz crystal is recrystallized into finer-grained interlobate crystals of quartz (qz). Crossed polarizers transmitted light.

*IG\_BH02\_LG026*

*Rock Type: Chlorite-altered tonalite  
Alkali feldspar-calcite veinlets*

Subhedral to anhedral crystals of plagioclase, anhedral crystals of quartz, anhedral pseudomorphs of chlorite after biotite, and anhedral to interstitial crystals of alkali feldspar define a granular isotropic microstructure, which is crosscut by irregular veinlets of alkali feldspar and calcite.

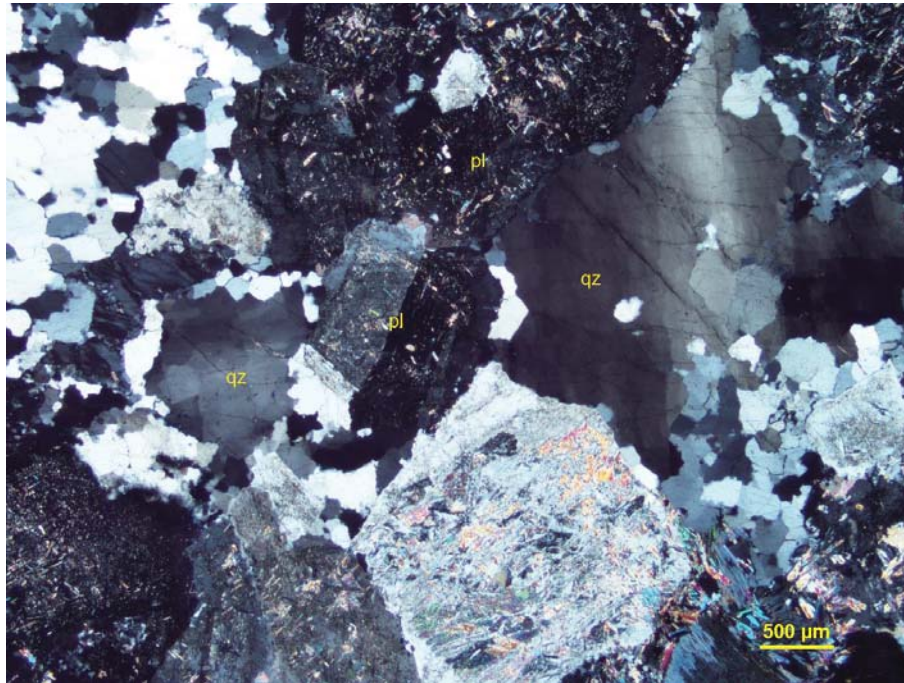
Alteration: Fe-chlorite: intense after biotite; white mica: weak after biotite and plagioclase; calcite-chalcopyrite: subtle.

Mineral	Alteration and Weathering Mineral	Modal %	Size Range (mm)
Tonalite			
Plagioclase	White mica	55–58	up to 5 long
Quartz		38–40	up to 2.5 long
[Biotite]	Fe-chlorite>white mica	2–3	up to 1.5
Alkali feldspar		2–3	up to 2.5
	Calcite	tr	up to 0.1
	Pyrite	tr	up to 0.15
	Chalcopyrite	tr	up to 0.02
<b>Alkali feldspar-calcite veinlets (~1% of PTS)</b>			
Alkali feldspar		1	up to 0.05
Calcite		tr	up to 0.2

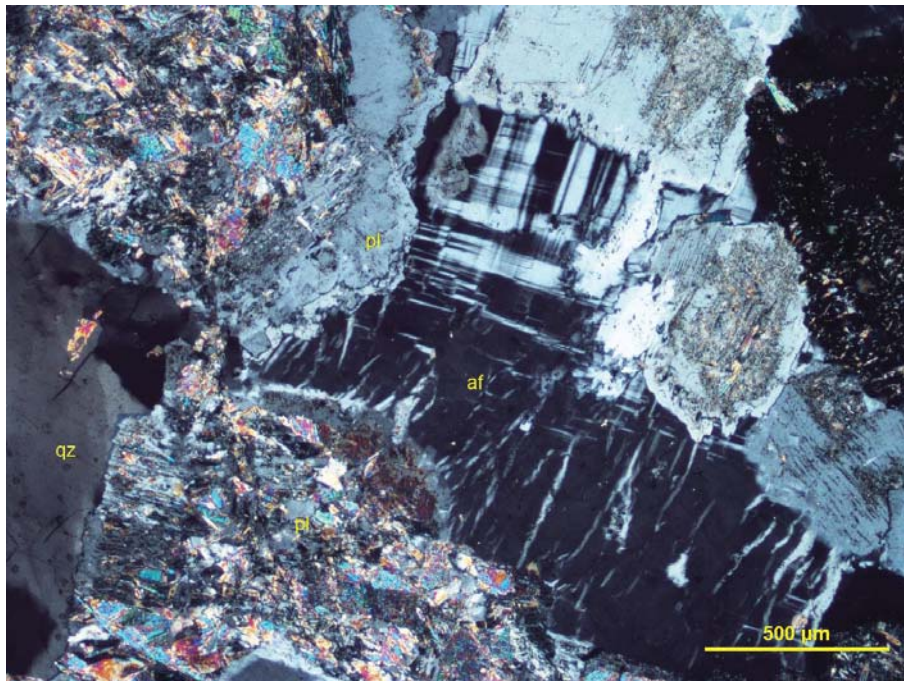
**Plagioclase** is medium- to coarse-grained (1–5 mm long), and its anhedral to subhedral crystals are randomly oriented. The plagioclase crystals are weakly to moderately altered by very fine- to fine-grained flakes of white mica, which in most of the crystals are concentrated within some of the growth zones (Photomicrograph 22a).

**Quartz** forms inequigranular crystals, most of which are concentrated within interstitial monomineralic domains. The quartz shows interlobate shape, and some of the coarser-grained crystals (up to 2.5 mm long) show moderate to strong undulose extinction.

**Alkali feldspar** is subordinate to the plagioclase and the quartz, and forms medium-grained interstitial crystals. The alkali feldspar crystals are fresh and show Albite-Pericline twinings, and these features distinguish them from the more abundant crystals of plagioclase (Photomicrograph 22b). Very fine-grained crystals of alkali feldspar filled in irregular and undulating veinlets (up to 0.8 mm thick). Within the veinlets, the very fine-grained alkali feldspar is associated with fine-grained clusters of calcite. **Fe-chlorite** epitaxially replaced randomly oriented crystals of magmatic biotite, and in most cases, are rimmed by thin coronae of very fine-grained white mica. The random orientation of the pseudomorphs after biotite imparts to the microstructure an isotropic nature. Very rare crystals of **pyrite** are heterogeneously dispersed within the fractured quartz and are associated with the fine-grained crystals of calcite dispersed within the granular microstructure.



**Photomicrograph 22a:** Subhedral crystals of plagioclase (pl) are weakly altered by very fine-grained flakes of white mica, and are associated with inequigranular and interstitial crystals of quartz (qz). Crossed polarizers transmitted light.



**Photomicrograph 22b:** The interstitial crystal of alkali feldspar is fresh and shows Albite-Pericline twinnings, in contrast with the weakly to moderately altered and subhedral crystals of plagioclase (pl). Crossed polarizers transmitted light.

*IG\_BH03\_LG003*

*Rock Type: Tremolite/actinolite-biotite schist*

Preferentially iso-oriented lamellae of biotite and xenoblastic crystals of tremolite/actinolite define a spaced schistosity and are intergrown with xenoblastic crystals of quartz, epidote, and plagioclase.

Mineral	Alteration and Weathering Mineral	Modal %	Size Range (mm)
Amphibole (tremolite/actinolite)		40–42	up to 0.3 long
Biotite		30–32	up to 0.5 long
Quartz		20–25	up to 0.2
Epidote		5–7	up to 0.2
Plagioclase		3–5	up to 0.2
[Pyrite?]	Iron oxides	0.1–0.2	up to 0.2

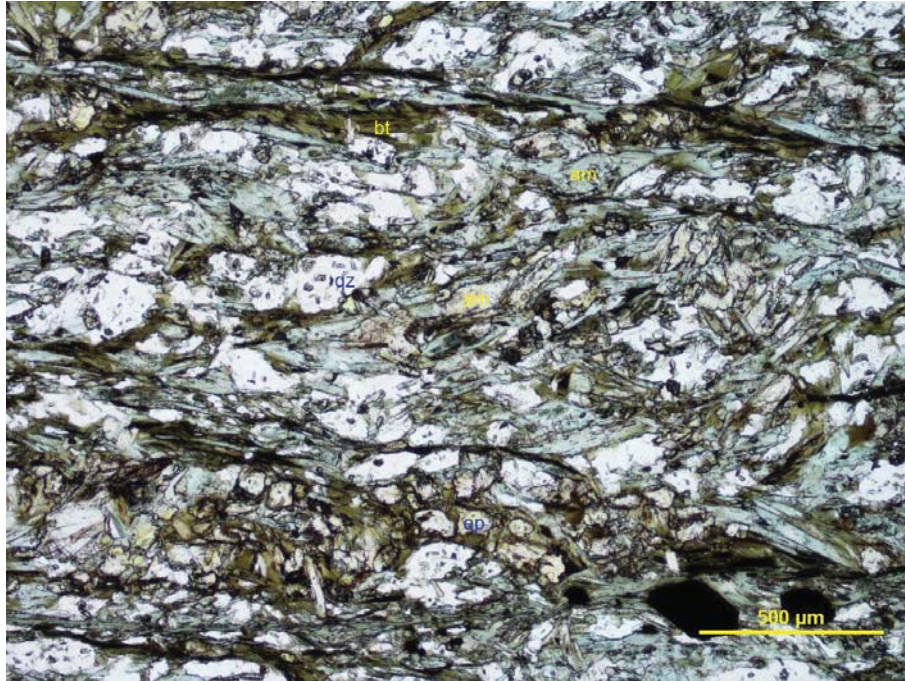
**Amphibole** occurs as xenoblastic elongate prisms (up to 0.3 mm long). The amphibole tends to concentrate along spaced cleavage domains, in which it is iso-oriented and associated with the biotite lamellae. The amphibole shows a very weak pleochroism with green tints and shows extinction angles up to 25°. These optical features suggest that the amphibole belongs to the tremolite/actinolite series.

**Biotite** forms fine- to medium-grained lamellae (up to 0.5 mm long). The lamellae are preferentially iso-oriented and tend to form spaced cleavage domains. The biotite lamellae are intergrown and probably post-dated the crystallization of xenoblastic prisms of amphibole. The amphibole and the biotite are overprinted by fine-grained xenoblastic crystals of epidote.

**Quartz** forms fine- to medium-grained xenoblastic crystals (up to 0.2 mm across) showing weak to moderate extinction and, in some cases, sub-grain boundaries. Most of the quartz is homogeneously dispersed within the schistosity, and only in rare cases tends to form granular microlithons wrapped by the schistosity.

**Plagioclase** forms fine-grained xenoblastic crystals dispersed within the schistosity and distinguished by their low birefringence (up to the first-order white) and rare Albite twinnings.

Rare idioblastic pseudomorphs of **iron oxides** are dispersed as fine-grained (up to 0.2 mm across). The shape of the pseudomorphs suggests that the iron oxides completely replaced pyrite or a cubic mineral.



**Photomicrograph 23:** Preferentially iso-oriented xenoblasts of amphibole (am) and biotite (bt) define a spaced schistosity. The amphibole and the biotite are overprinted by fine-grained epidote (ep) and are intergrown with xenoblastic crystals of quartz (qz). Plane polarized transmitted light.

*IG\_BH03\_LG004***Rock Type:** Granitoid

(The rock is coarse-grained and occurs in a limited area of the polished thin section (13%); therefore, it does not constitute a representative enough sample to be classified according to the BGS Classification Scheme (see Gillespie & Styles, 1999).)

This thin polished section consists of a medium-grained interlobate aggregate of quartz, plagioclase, alkali feldspar, and rare randomly oriented lamellae of biotite. In the upper part of this thin polished section a coarse-grained granular domain of alkali feldspar, quartz, plagioclase, and biotite show an irregular boundary with the fine-grained felsitic rock.

Alteration: white mica: weak after plagioclase in Domain B.

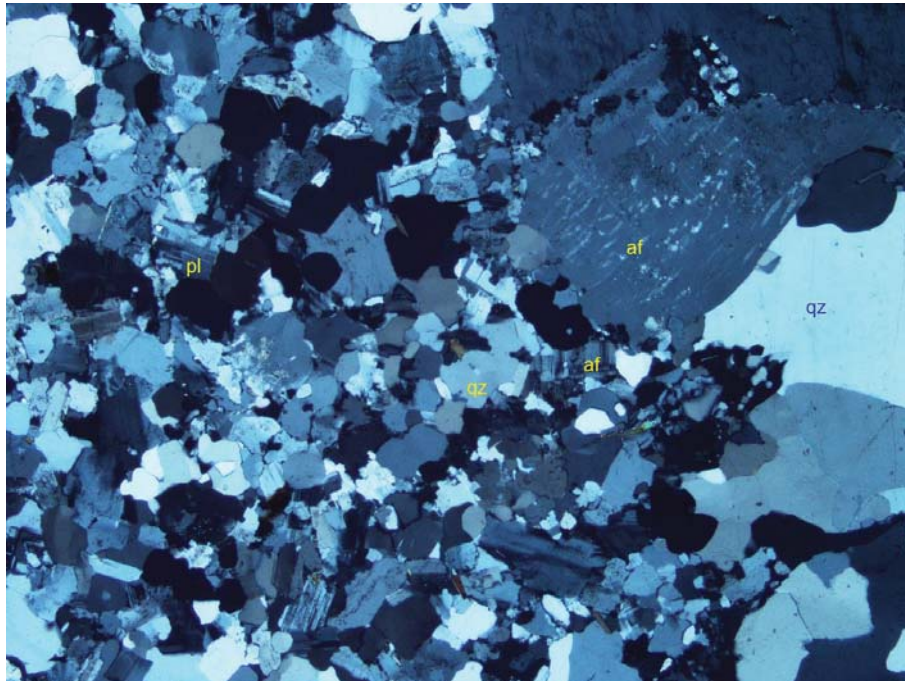
Mineral	Alteration and Weathering Mineral	Modal %	Size Range (mm)
<b>Domain A: felsitic rock (~87% of PTS)</b>			
Quartz		40–42	up to 0.5
Plagioclase (albite)		38–40	up to 0.5
Alkali feldspar		7–10	up to 0.5
Biotite		0.5–0.6	up to 1 long
Ilmenite		tr	0.25
[Magnetite]	Hematite	tr	up to 0.2
<b>Domain B: granitoid (~13% of PTS)</b>			
Alkali feldspar		5	up to 9 long
Biotite		3	up to 15 long
Quartz		3	up to 2.5
Plagioclase (albite)	White mica	2	up to 2

**Quartz** forms anhedral medium-grained crystals (up to 0.5 mm across), which are homogeneously dispersed within the granular microstructure of Domain A. In this domain, the quartz is intergrown with the subhedral to anhedral crystals of plagioclase, anhedral crystals of alkali feldspar, and rare lamellae of biotite. Within Domain B, the quartz forms anhedral crystals (up to 2.5 mm across), and together with the inequigranular crystals of alkali feldspar and plagioclase define a granitic granular microstructure.

**Plagioclase** is medium-grained and anhedral in Domain A. The crystals are fresh and show Albite twinnings. The plagioclase is anhedral and coarser-grained (up to 2 mm across) in Domain B, and in this domain, it is weakly altered by very fine-grained highly birefringent flakes of white mica, which are concentrated within the crystal cores. The refractive indexes of the plagioclase are lower than those of the quartz in both domains, thus indicating that the plagioclase is albite.

**Alkali feldspar** is fine- to medium-grained (up to 0.5 mm across) and occurs as anhedral and interstitial crystals in Domain A. The medium-grained crystals show Albite-Pericline twinings, and are fresh. Within Domain B, the alkali feldspar occurs as a coarse (up to 9 mm long) subhedral crystal hosting fine-grained anhedral inclusion of plagioclase and fine-grained perthitic blebs.

**Biotite** is fine- to medium-grained in Domain A, and in this domain occurs as randomly oriented lamellae showing a high aspect ratio. Similarly with Sample 12, the high aspect ratio indicates that the biotite crystallized within a liquid. A coarse-grained crystal of biotite is 15 mm long, and I interpret this crystal as protruding within Domain A from Domain B; however, the portion of the rock hosting the other end of the crystal is not included in the thin polished section and the billet (please see the corresponding billet photo).



**Photomicrograph 24:** Medium-grained crystals of quartz (qz), plagioclase (pl), and alkali feldspar (af) define a granular microstructure in Domain A (in the left of this photomicrograph). Coarser-grained quartz (qz) and alkali feldspar (af) define a coarser-grained granular microstructure in the granitoid (in the right). Crossed polarizers transmitted light

*IG\_BH03\_LG005*

*Rock Type: Plagioclase-phyric andesitic rock*

Euhedral to subhedral phenocrystals of plagioclase are randomly oriented within a fine-grained groundmass of quartz, plagioclase and biotite. The fine-grained biotite defines elongate clusters defining an irregular magmatic foliation.

Alteration: epidote: weak after biotite and plagioclase; white mica: weak after plagioclase magnetite: subtle.

Mineral	Alteration and Weathering Mineral	Modal %	Size Range (mm)
<b><i>Phenocrystals</i></b>			
Plagioclase	White mica-epidote	10–12	up to 4 long
<b><i>Groundmass</i></b>			
Quartz		38–40	up to 0.1
Plagioclase		21–22	up to 0.1
Biotite	Epidote	12–14	up to 0.1
	Epidote	4–5	up to 0.2
	Magnetite (?)	tr	up to 0.1

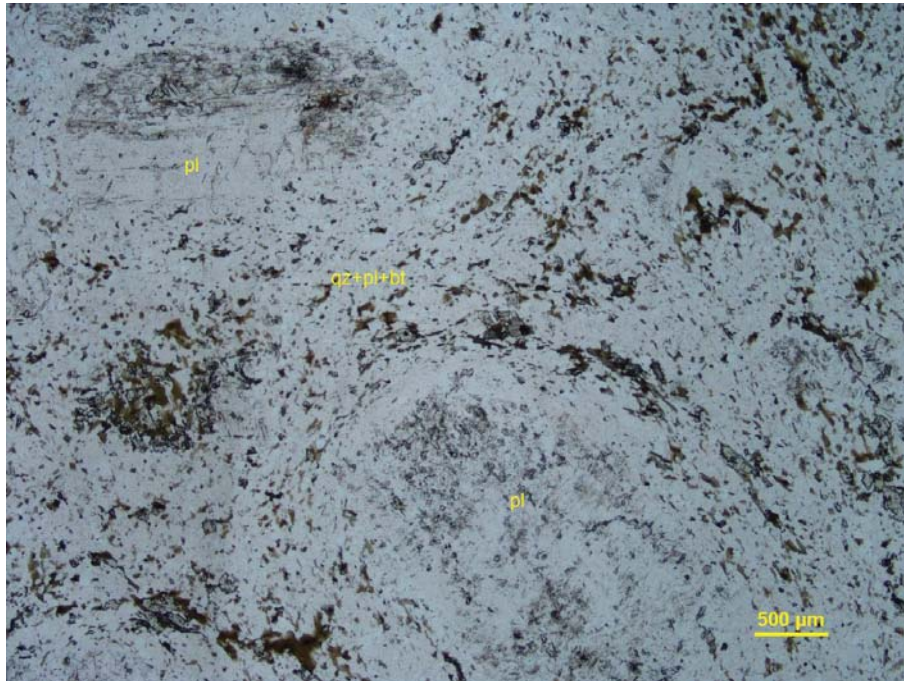
**Plagioclase** forms randomly oriented phenocrystals (up to 4 mm long), which are homogeneously dispersed within the groundmass. The plagioclase phenocrystals are weakly altered by very fine- to fine-grained dispersions of white mica and epidote. Fine-grained anhedral crystals of plagioclase are intergrown with the quartz and the biotite within the fine-grained interlobate groundmass.

**Quartz** is fine-grained and forms, in association with anhedral crystals of plagioclase and biotite, a granular to interlobate crystal aggregate in the groundmass.

**Biotite** forms fine-grained flakes and lamellae, which tend to form elongate clusters defining an irregular magmatic foliation (see Photomicrograph 25a).

Fine-grained anhedral crystals of **epidote** are spatially associated with the biotite lamellae and clusters, and i interpret the epidote as having crystallized during a post-magmatic alteration event.

Very rare crystals of **magnetite** occur within some of the epidote crystals.



**Photomicrograph 25a:** Under plane-polarized transmitted light, the fine-grained crystals of biotite form irregular clusters defining a weak and irregular magmatic foliation wrapping the plagioclase phenocrysts.



**Photomicrograph 25b:** Subhedral phenocrysts of plagioclase (pl) are immersed within a fine-grained groundmass of quartz, plagioclase and biotite (qz+pl+bt). Crossed polarizers transmitted light.

*IG\_BH03\_LG006*

*Rock Type: White mica-epidote-altered granodiorite*

Subhedral crystals of plagioclase, and anhedral crystals of quartz, alkali feldspar, and randomly oriented lamellae of white mica and sparse anhedral crystals of epidote define a medium- to coarse-grained granular and isotropic microstructure.

Alteration: white mica: weak to moderate after plagioclase; intense after biotite; epidote: weak; chlorite: subtle.

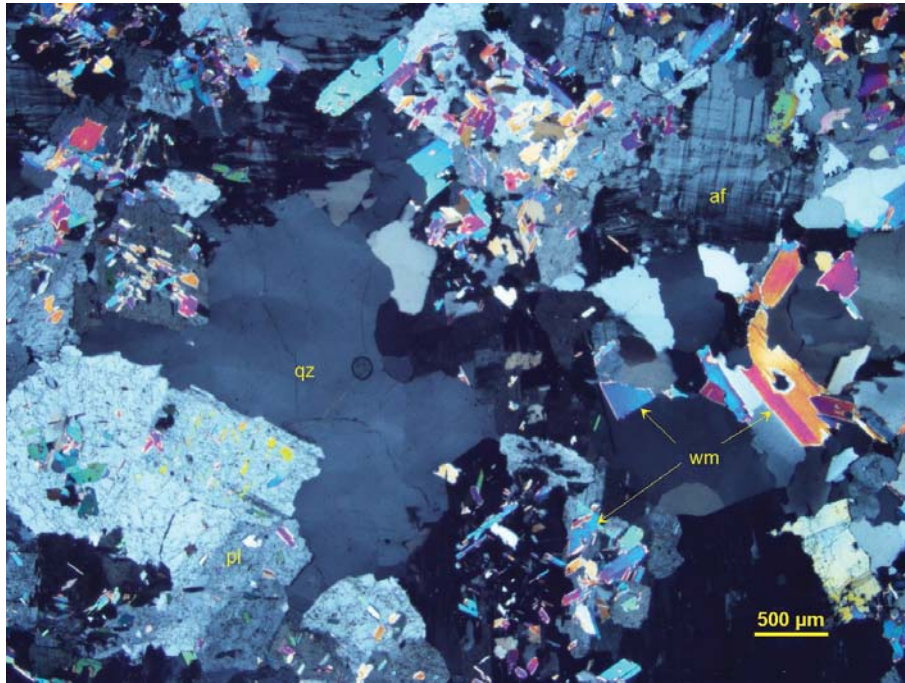
Mineral	Alteration and Weathering Mineral	Modal %	Size Range (mm)
Plagioclase (albite)		44–46	up to 2.5
Quartz		35–37	up to 2.5
Alkali feldspar		12–14	up to 7.5 long
[Biotite]	White mica +epidote+chlorite	6–7	wm: up to 0.7 long
	Epidote	1–2	up to 0.5, rare up to 1
	Chlorite	tr	up to 0.4 long
Zircon		tr	up to 0.01

**Plagioclase (albite)** is fine-grained, and it is dispersed within the granular microstructure as anhedral to subhedral crystals. The plagioclase shows rare Albite twinnings, and it is weakly to moderately altered by fine-grained flakes of white mica. The refractive indexes of the plagioclase are lower than those of the quartz; therefore, the plagioclase is albite.

**Quartz** forms inequigranular anhedral, and in most cases, interstitial crystals and crystal aggregates dispersed within the interstitial positions between the plagioclase.

**Alkali feldspar** is anhedral and forms medium-grained to coarse-grained crystals (up to 7.5 mm long). The alkali feldspar is heterogeneously dispersed in this thin polished section as visible in the image of the stained billet.

**White mica** weakly to moderately altered the plagioclase, and it forms irregular clusters dispersed within the granular microstructure. I interpret these clusters as pseudomorphs after the magmatic biotite. In some cases, fine-grained flakes of chlorite are associated with the white mica in the clusters, and the chlorite host very fine-grained dispersions of zircon. The occurrence of zircon within the chlorite is the main clue that the white mica-chlorite clusters replaced the magmatic biotite.



**Photomicrograph 26:** Subhedral crystals of plagioclase, anhedral crystals of quartz (qz), alkali feldspar (af), and sparse clusters of white mica and epidote define a granular isotropic microstructure. Crossed polarizers transmitted light.

*IG\_BH03\_LG007*

*Rock Type: Microleucogranite*

Anhedral crystals of plagioclase, quartz, and alkali feldspar define a medium-grained granular microstructure, in which rare lamellae of biotite are randomly oriented.

Alteration: clay and/or epidote: weak after plagioclase; chlorite: subtle to strong after biotite; epidote: subtle to weak after biotite; white mica: subtle.

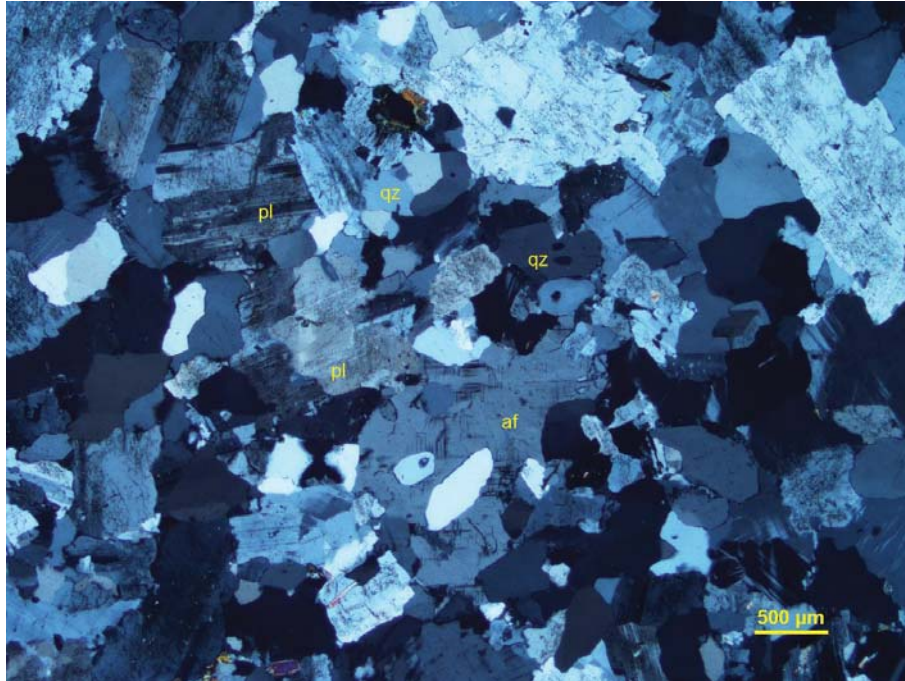
Mineral	Alteration and Weathering Mineral	Modal %	Size Range (mm)
Plagioclase	Clay and/or epidote	38–40	up to 2 long
Quartz		33–35	up to 1
Alkali feldspar		26–28	up to 1
Biotite	Chlorite-epidote	1–1.5	up to 0.5
	Epidote	tr	up to 0.4 long
	White mica	tr	up to 0.4 long

**Plagioclase** is medium-grained, and its anhedral to subhedral (Photomicrograph 27b) crystals define, in association with the quartz and alkali feldspar, a granular microstructure. The plagioclase crystals show Albite twinnings, and are weakly altered by a very fine-grained dispersion of unresolved material (clay and/or epidote). The refractive indexes of the plagioclase are smaller than those of the quartz; therefore, the plagioclase is albite.

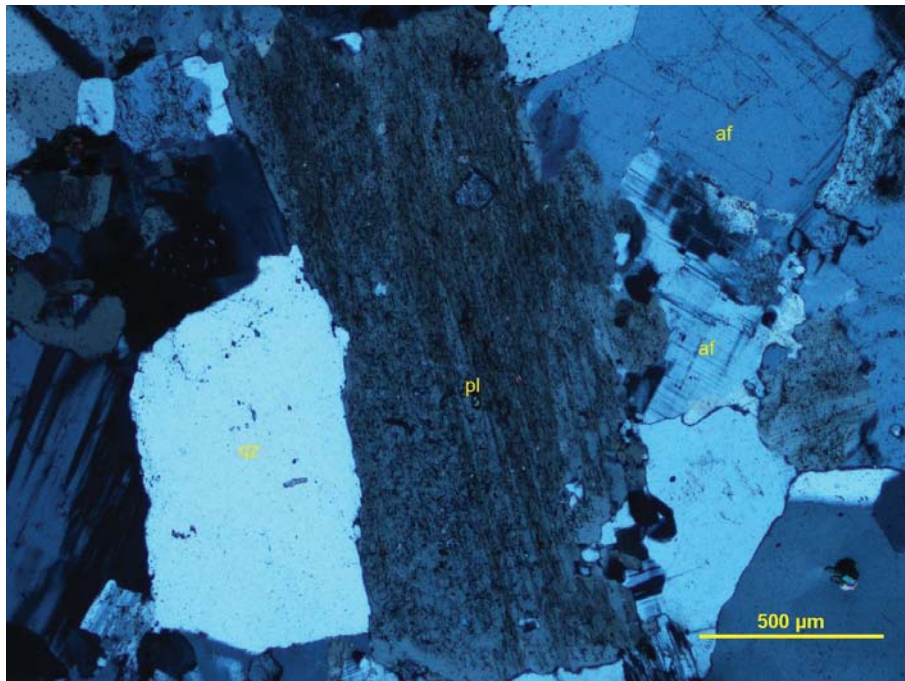
**Quartz** occurs as anhedral to interstitial crystals (up to 1 mm across). The quartz crystals are homogeneously dispersed within the granular microstructure. Between quartz crystals, the crystal boundaries are interlobate.

**Alkali feldspar** forms anhedral to interstitial crystals (up to 1 mm across) distinguished by Albite-Pericline twinnings. In this thin polished section, the alkali feldspar is fresh, and the absence of inclusions and alteration products allows me to easily distinguish the alkali feldspar from the plagioclase, and further, indicates that the alkali feldspar is of magmatic origin.

**Biotite** lamellae are rare and are randomly oriented within the granular microstructure. The biotite lamellae are up to 0.5 mm long, are moderately oxidized, and in some cases, are overprinted by fine-grained anhedral crystals of epidote. In some other cases, the biotite is epitaxially replaced by chlorite. Very rare lamellae of **white mica** occur within the interstices between the quartz and the feldspar.



**Photomicrograph 27a:** A medium-grained granular microstructure is defined by anhedral crystals of plagioclase (pl), quartz, and alkali feldspar (af). Crossed polarizers transmitted light.



**Photomicrograph 27b:** A subhedral crystal of plagioclase is associated with anhedral crystals of quartz (qz) and alkali feldspar (af). Crossed polarizers transmitted light.

*IG\_BH03\_LG008*

*Rock Type: Plagioclase-phyric andesite*

Subhedral phenocrystals of plagioclase are rotated and immersed within a fine-grained and foliated groundmass of quartz, plagioclase and biotite. The foliation is defined by sub-parallel clusters of fine-grained biotite. A 0.4 mm thick alkali feldspar-quartz veinlet crosscut this thin polished section oriented parallel to the foliation.

Alteration: clay and/or epidote: weak after plagioclase phenocrystals; epidote: subtle to weak.

Mineral	Alteration and Weathering Mineral	Modal %	Size Range (mm)
<b>Foliated andesite (~98% of PTS)</b>			
<i>Phenocrystals</i>			
Plagioclase (mostly albite)	Clay and/or epidote	3–5	up to 1.6 long
<i>Groundmass</i>			
Plagioclase (albite)		56–58	up to 0.15
Quartz		21–23	up to 0.1
Biotite		15–17	up to 0.1, up to 0.2 in the clusters
	Epidote	0.2–0.4	
<b>Alkali feldspar-quartz veinlet (~2% of PTS)</b>			
Alkali feldspar		1.5	up to 0.05
Quartz		0.5	up to 0.05

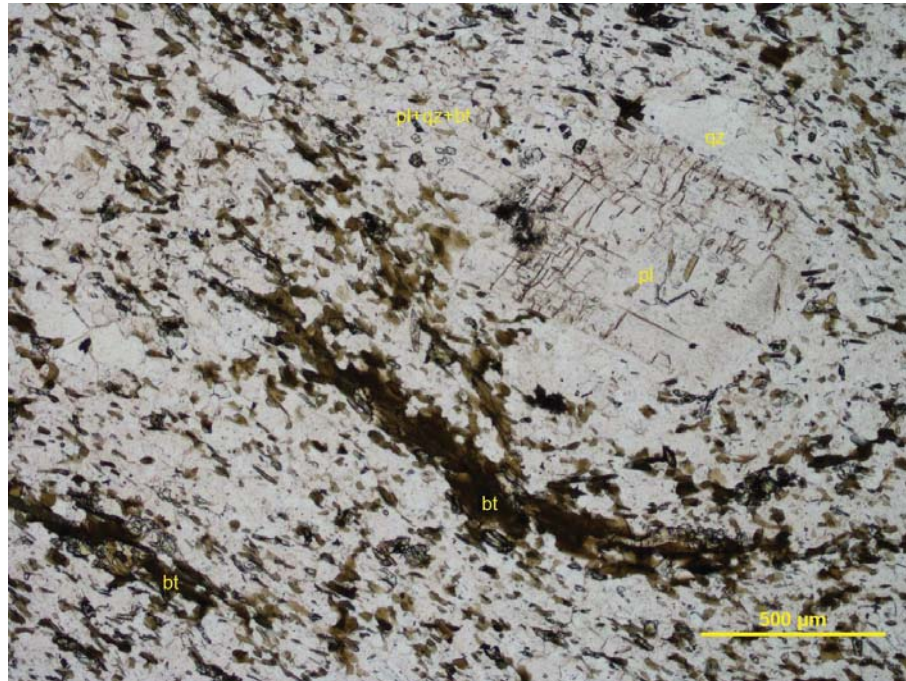
**Plagioclase** occurs as subhedral phenocrystals (up to 1.6 mm long), which are rotated in the fine-grained groundmass of quartz, plagioclase, and biotite, and are wrapped by the foliation defined by the biotite. Fine-grained anhedral crystals of plagioclase are the more abundant mineral in the groundmass, in which they are intergrown with subordinate crystals of quartz and fine-grained lamellae of biotite. The phenocrystals of plagioclase are fresh to weakly altered by a very fine-grained dispersion of unresolved material, likely clay and/or epidote. In most cases, the plagioclase show albite twinnings, and in some cases, the phenocrystals show euhedral growth zoning. The phenocrystal rims, and the fine-grained crystals in the groundmass show refractive indexes smaller than those of the quartz, therefore, most of the plagioclase in this thin polished section is albitic.

**Quartz** forms fine-grained anhedral to interlobate crystals, which are intergrown with the plagioclase within the groundmass.

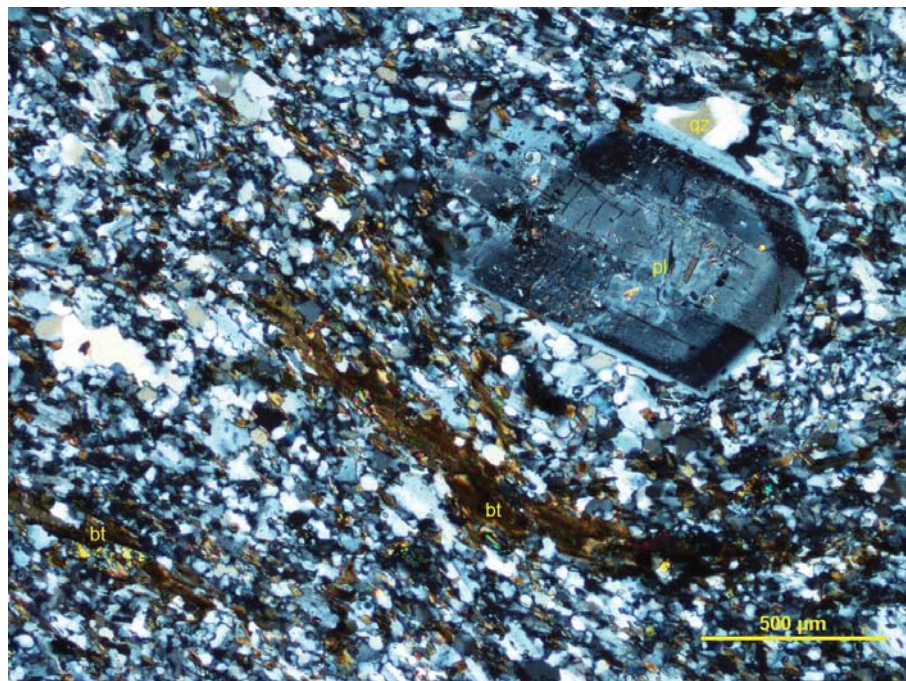
**Biotite** is dispersed in the plagioclase+quartz groundmass as fine-grained lamellae (up to 0.1 mm long). Slightly coarser lamellae and flakes (up to 0.2 mm across) are concentrated within sub-parallel clusters defining a sub-planar foliation. In some cases, the foliation wraps the plagioclase phenocrystals. I interpret this foliation as having formed during the emplacement and crystallization of the andesitic magma.

Fine-grained anhedral crystals of **epidote** are dispersed within the groundmass and overprinted some of the biotite lamellae.

Fine-grained crystals of **alkali feldspar** are associated with subordinate quartz within a 0.4 mm thick veinlet oriented parallel to the foliation. The veinlet can be observed in the image of the stained billet, in which the alkali feldspar is stained yellow.



**Photomicrograph 28a:** An euhedral phenocrystal of plagioclase (pl) is wrapped by the foliation defined by clustered biotite (bt) in a groundmass of plagioclase and quartz (pl+qz+bt). Plane-polarized transmitted light.



**Photomicrograph 28b:** Same area as shown in Photomicrograph 28a; under crossed polarizers transmitted light, the plagioclase shows a euhedral growth zoning, and the groundmass its fine-grained nature.

*IG\_BH03\_LG009*

*Rock Type: White mica-epidote-altered tonalite*

Subhedral crystals of plagioclase and anhedral crystals of quartz, and rare randomly oriented lamellae of biotite define an isotropic granular microstructure, in which the plagioclase is moderately altered by white mica, and the biotite is partially replaced by epidote.

Alteration: white mica: moderate after plagioclase; epidote: weak after biotite.

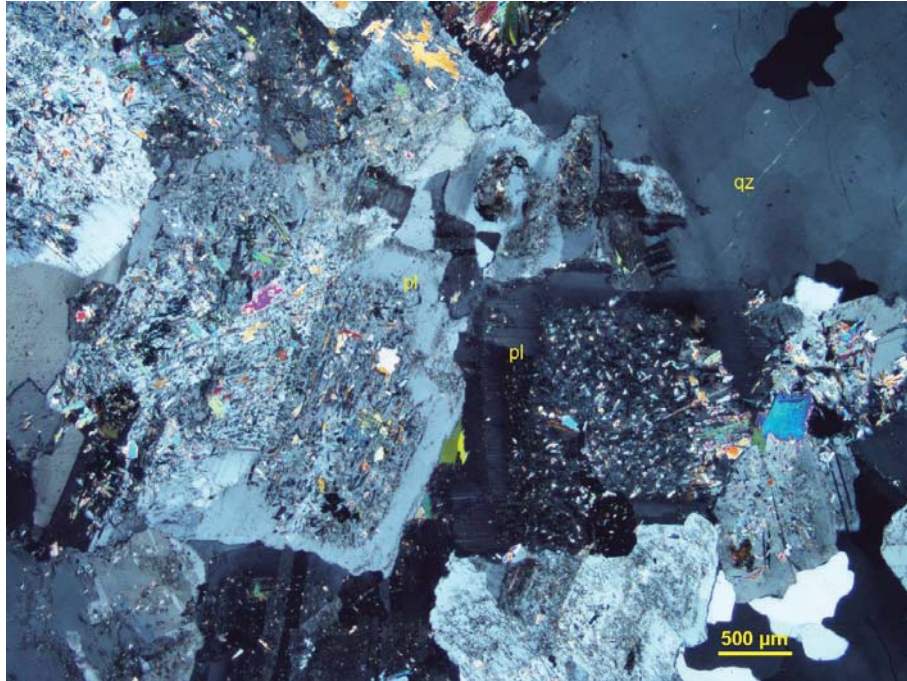
Mineral	Alteration and Weathering Mineral	Modal %	Size Range (mm)
Plagioclase	White mica	55–57	up to 2.5 long
Quartz		42–49	up to 3
Biotite	Epidote	1–1.5	up to 1 long
Ilmenite (?)		tr	up to 0.3 long
[Magnetite?]	Hematite	tr	~0.15

**Plagioclase** is medium- to coarse-grained and shows subhedral shapes. Its crystals are randomly oriented and are moderately altered by very fine- to fine-grained flakes of white mica. The alteration products are selectively dispersed within the core of the plagioclase crystals (Photomicrograph 29).

**Quartz** occurs as inequigranular crystals (0.2–3 mm) occupying the interstitial positions between the plagioclase. The coarser crystals of quartz show a moderate undulose extinction, and most of the crystals in the monomineralic interstitial aggregate show interlobate boundaries.

**Biotite** is rare, and its medium-grained lamellae (up to 1 mm long) are partially replaced by anhedral crystals of epidote (up to 1 mm long).

Very rare lamellae are dispersed within the quartz, and because of their shape and anisotropy under crossed-polarizers reflected light, I tentatively interpret them as **ilmenite**. Two crystals (up to 0.15 mm across) of **hematite** completely replaced euhedral crystals of probable magnetite (?).



**Photomicrograph 29:** Subhedral phenocrysts of plagioclase (pl) show a white mica altered core, and are associated with interstitial crystals of quartz (qz). Crossed polarizers transmitted light.

*IG\_BH03\_LG010*

*Rock Type: Amphibole-biotite schist*

A fine- to medium-grained xenoblastic aggregate of amphibole, biotite, plagioclase and epidote is relatively homogeneous and shows a weak schistosity defined by the preferred dimensional orientation of the tremolite-actinolite.

Alteration: iron oxides: strong after probable sulphide.

Mineral	Alteration and Weathering Mineral	Modal %	Size Range (mm)
Amphibole (hornblende and tremolite-actinolite)		70–72	up to 0.5
Biotite		20–22	up to 0.3
Plagioclase (albite)		3–5	up to 0.1
Epidote		3–5	up to 0.1, rare up to 0.2
Quartz		2–3	up to 0.1
	Iron oxides	tr	up to 0.1
Pyrite		tr	0.01

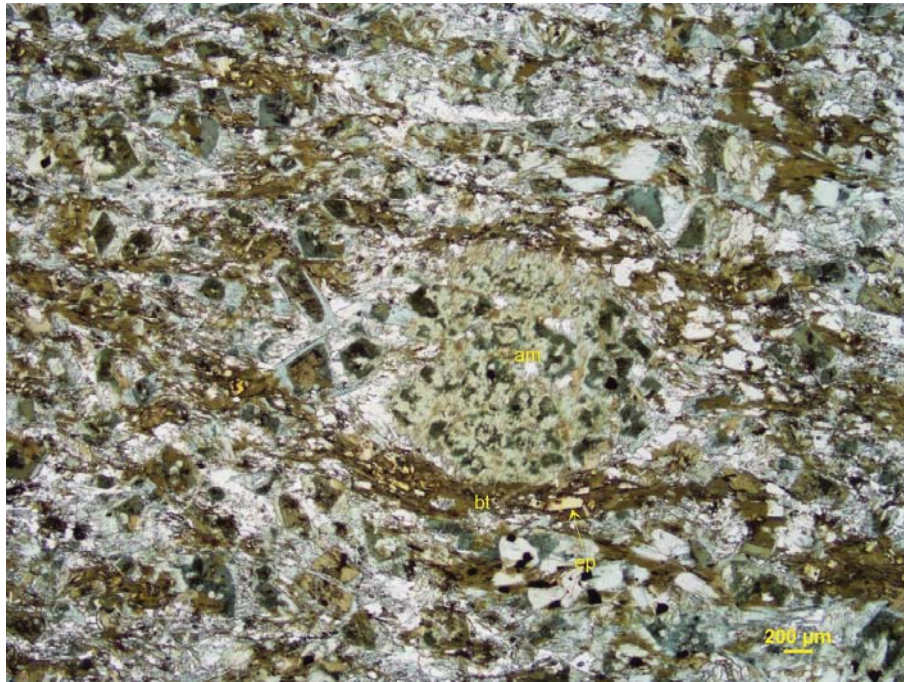
**Amphibole** occurs as relic porphyroblasts of **hornblende** and subidioblastic elongate prisms and rims of **tremolite-actinolite** around the hornblende. The hornblende shows its typical green and strong pleochroism (X: light yellow-green; Y: green; Z: green to gray-green) and forms medium-grained (up to 0.5 mm across) xenoblastic crystals rimmed by non-pleochroic amphibole. Tremolite-actinolite forms rims around the hornblende and elongate prisms, which show a preferred dimensional orientation, thus defining a weak schistosity in this rock. In rare cases, the less pleochroic tremolite-actinolite and the relic hornblende form sub-rounded porphyroblasts wrapped by the schistosity (Photomicrograph 30a). In other cases, the prismatic intergrowths of relic hornblende and tremolite-actinolite are rotated within the schistosity and are surrounded by quartz-rich strain shadows and subordinate fine-grained and non-pleochroic amphibole prisms (Photomicrograph 30d). The non-pleochroic amphibole shows extinction angles up to 15°, and this suggests that this type of amphibole belongs to the tremolite end-member of the tremolite-actinolite series.

**Biotite** is fine-to medium-grained, and its subidioblastic lamellae are preferentially iso-oriented and contribute to the schistosity. The biotite forms xenoblastic xenomorphs after probable amphibole, in which the fine-grained lamellae are randomly oriented (Photomicrograph 30c).

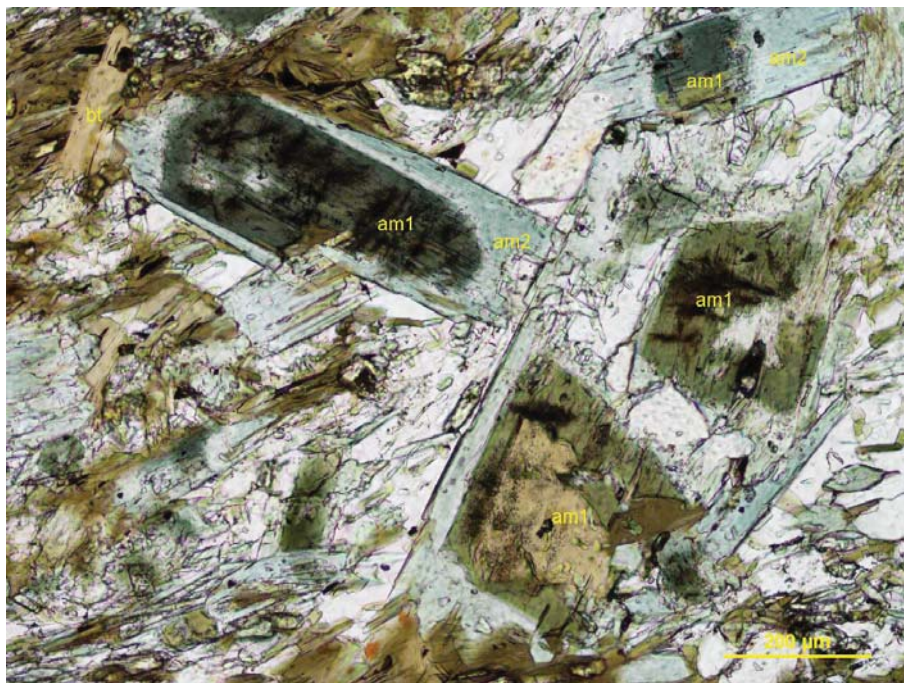
**Plagioclase** and **quartz** are fine-grained xenoblastic and occurs as interstitial crystal aggregates between the amphibole and the biotite.

**Epidote** forms fine-grained xenoblastic crystals, which overprinted and are spatially associated with the biotite.

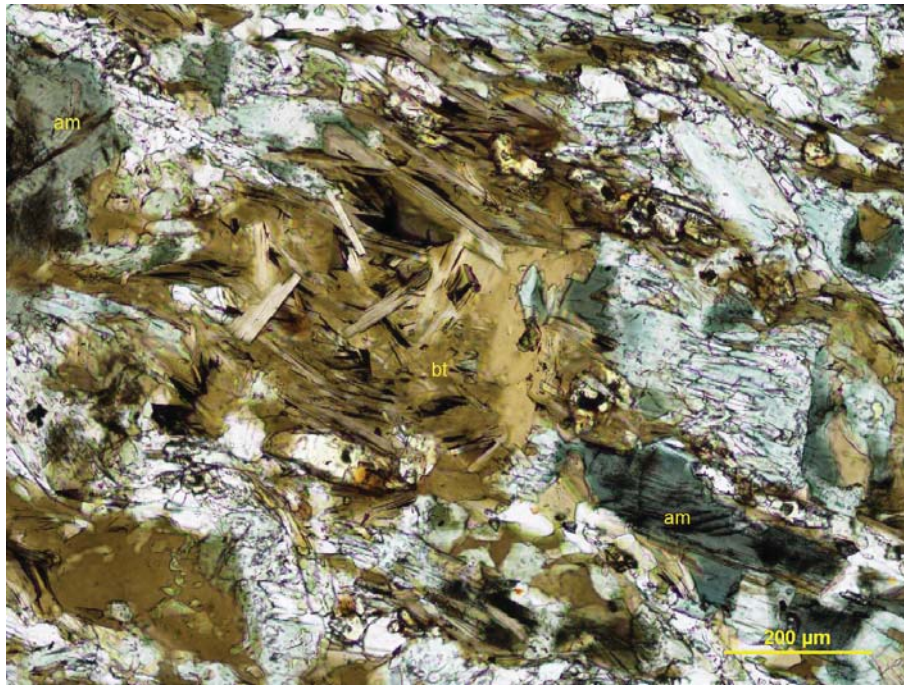
Fine-grained alteromorphs of **iron oxides**, probably after sulphide(s), occur within the tremolite and within the interstices between the tremolite and the biotite.  
 Very rare and very fine-grained crystals of **pyrite** occur within the rims of the relic crystals of hornblende.



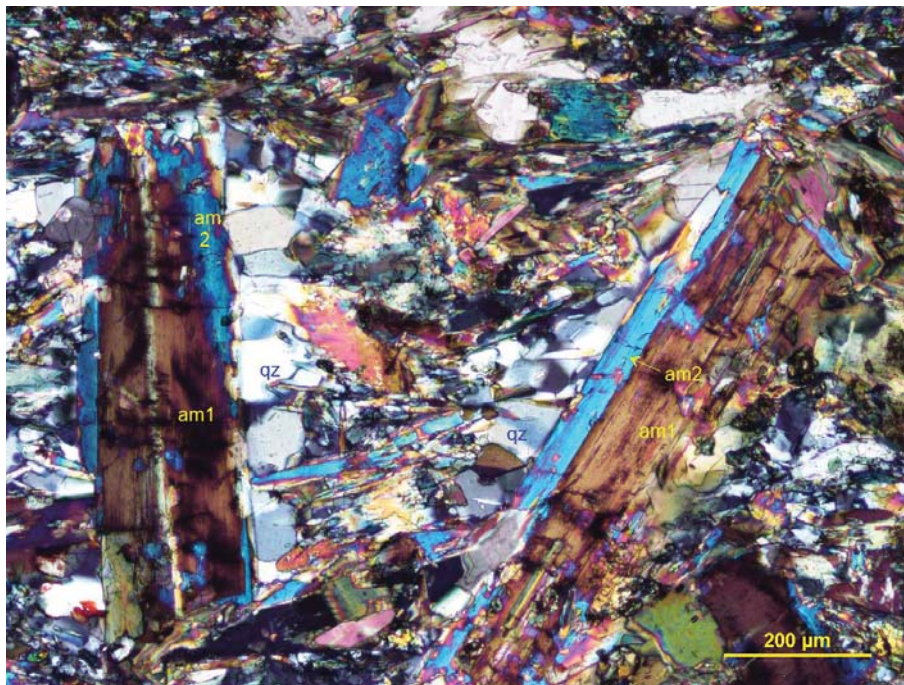
**Photomicrograph 30a:** A xenoblastic porphyroblast of amphibole is wrapped by the schistosity defined by biotite and amphibole. Plane-polarized transmitted light.



**Photomicrograph 30b:** Subidioblastic relics of hornblende (am1) are overgrown by less- to non-pleochroic tremolite-actinolite (am2). Plane-polarized transmitted light.



Photomicrograph 30c: A xenoblastic pseudomorph is made up of randomly oriented crystals of biotite (bt). Plane-polarized transmitted light.



Photomicrograph 30d: Two prismatic intergrowths of hornblende and tremolite-actinolite (am) are rotated within the schistosity and are surrounded by strain shadows of quartz (qz) and subordinate non-pleochroic tremolite. Crossed polarizers transmitted light.

*IG\_BH03\_LG011*

*Rock Type: White mica-epidote-altered tonalite*

Inequigranular subhedral crystals of plagioclase, anhedral crystals of quartz, and subordinate interstitial crystals of alkali feldspar define a coarse-grained granular microstructure, in which subordinate and subhedral lamellae of biotite are randomly oriented.

Alteration: white mica: weak to moderate after plagioclase; weak after biotite; epidote: weak; hematite: moderate after magnetite.

Mineral	Alteration and Weathering Mineral	Modal %	Size Range (mm)
Plagioclase	White mica	48–50	up to 5 long
Quartz		44–46	up to 2, rare up to 7 long
Alkali feldspar		5–7	up to 5 long
Biotite	Epidote	2–4	up to 1 long
	Epidote	1–1.5	up to 0.5
[Magnetite]	Hematite	tr	up to 0.25
Zircon		tr	0.01

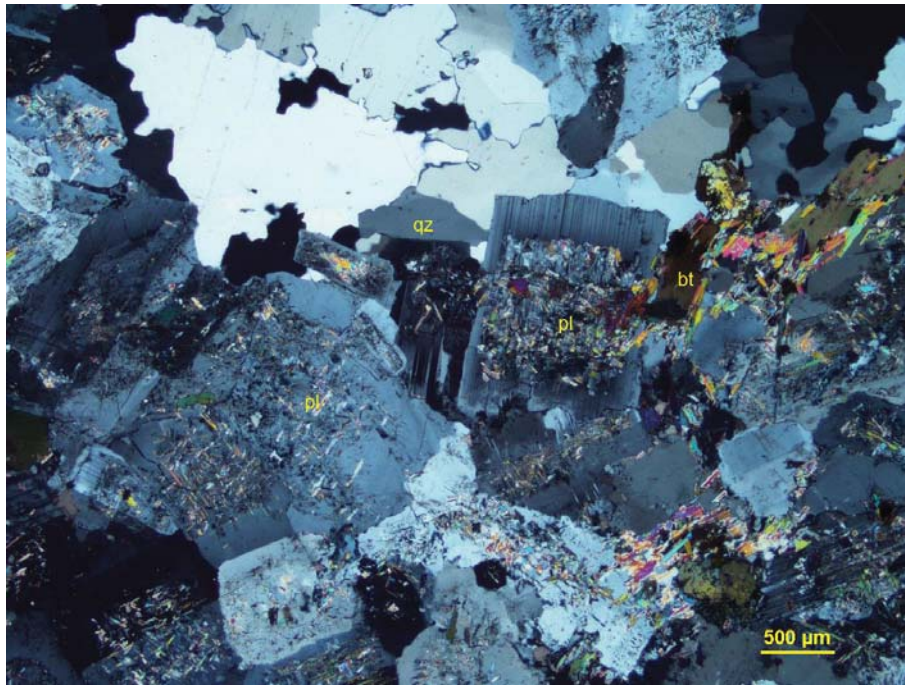
**Plagioclase** occurs as medium-to coarse-grained subhedral to euhedral crystals (up to 5 mm long). The plagioclase is weakly to moderately altered by very fine- to fine-grained flakes of white mica and lesser epidote. The alteration products are concentrated within the crystal core of plagioclase (photomicrograph 31). Some of the plagioclase crystals show continuous growth zoning. The crystal rim shows refractive indexes lower than those of the quartz, thus indicating that the rim composition is albitic.

**Quartz** forms inequigranular anhedral crystals (up to 2 mm in diameter, see Photomicrograph 31a) and crystal aggregates (up to 7 mm long) occupying the interstitial positions between the plagioclase.

**Alkali feldspar** occurs as anhedral and interstitial crystals (up to 1.2 mm across. In rare cases, the alkali feldspar forms coarse-grained poikilitic crystals up to 5 mm long (see Photomicrograph 31b), hosting subhedral inclusions of plagioclase and subordinate quartz. The alkali feldspar is fresh and shows Albite-Pericline twinnings.

**Biotite** occurs as medium-grained and randomly oriented crystals. The crystals are up to 1 mm long and are weakly to moderately altered by epidote and white mica.

Very rare anhedral crystals of **magnetite** (up to 0.25 mm in diameter) are hosted within epidote and are partially replaced by **hematite**.



**Photomicrograph 31:** Anhedral to subhedral crystals of plagioclase (pl) are weakly to moderately altered by white mica, and are associated with interstitial crystal aggregates of quartz (qz) and subordinate biotite (bt). Crossed polarizers transmitted light.

*IG\_BH03\_LG013*

*Rock Type: Biotite-plagioclase-phyric andesite  
Alkali feldspar veinlets*

Euhedral phenocrystals of plagioclase are dispersed within a fine-grained groundmass of plagioclase, biotite, and quartz. The fine-grained porphyritic microstructure is crosscut by intersecting and conjugated veinlets of alkali feldspar.

Alteration: epidote-chlorite: weak; chlorite: weak to moderate after biotite.

Mineral	Alteration and Weathering Mineral	Modal %	Size Range (mm)
<b>Andesite (~97% of PTS)</b>			
<i>Phenocrystals</i>			
Plagioclase	White mica	5–7	up to 1
[Biotite]	Chlorite+epidote	0.2–0.5	[up to 0.4 long]
<i>Groundmass</i>			
Plagioclase		5–57	up to 0.1
Biotite		20–22	up to 0.1
Quartz		15–20	up to 0.1
	Epidote	1–1.5	up to 0.1
	Chlorite	0.5–0.6	up to 0.15
<b>Alkali feldspar veinlets (~3% of PTS)</b>			
Alkali feldspar		3	up to 0.05

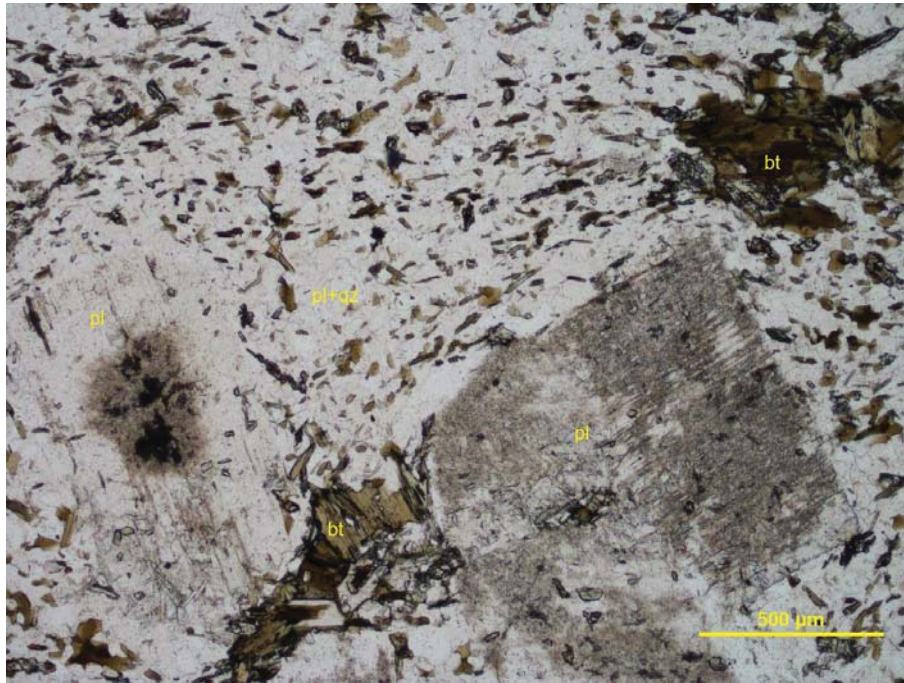
**Plagioclase** forms euhedral phenocrystals, which are weakly altered by a very fine-grained dispersion of white mica (see Photomicrograph 32b). The phenocrystals are dispersed within a fine-grained groundmass, in which fine-grained and, in some cases, subhedral crystals of plagioclase prevail over fine-grained lamellae of biotite and quartz. The phenocrystals of plagioclase and some of the fine-grained crystals dispersed within the groundmass show a growth zonation. The occurrence of growth zonation in the fine-grained crystals in the groundmass indicates that the plagioclase was not or was only slightly affected by the post-magmatic alteration.

**Biotite** is dispersed within the groundmass as fine-grained lamellae and sparse phenocrystals up to 0.4 mm long. In most cases, the biotite phenocrystals are weakly to moderately altered by chlorite. In some cases, the biotite forms fine-grained clusters, which I interpret as having replaced medium-grained phenocrystals. In most cases, the fine-grained lamellae of biotite are randomly oriented within the groundmass and define an isotropic microstructure.

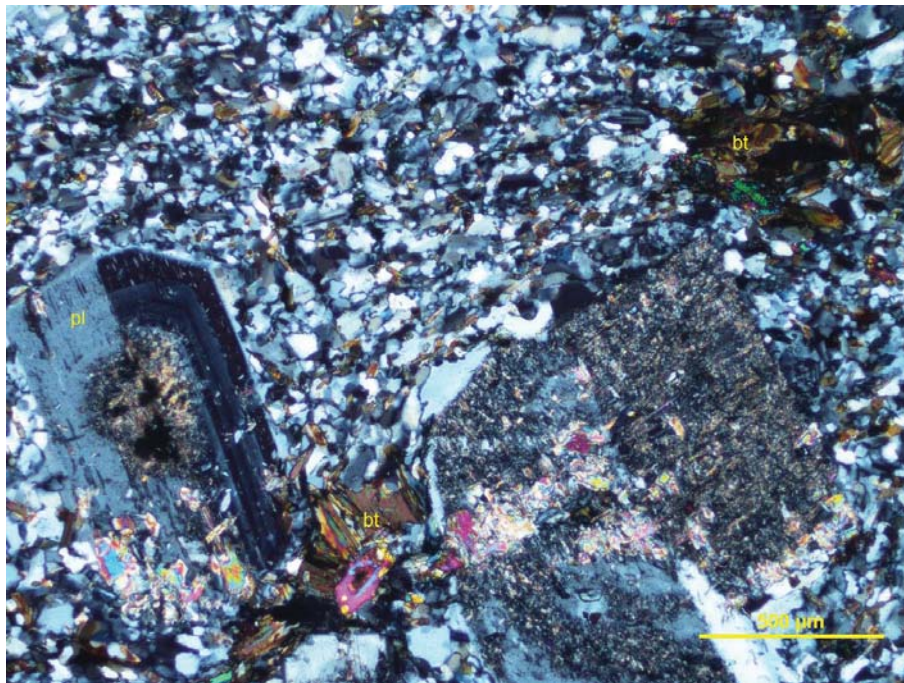
**Quartz** is subordinate to the plagioclase and the biotite in the groundmass, in which it forms fine-grained (up to 0.1 mm across) anhedral crystals.

**Alkali feldspar** filled in thin (up to 0.3 mm thick) intersecting and in some cases anastomosing veinlets crosscutting the porphyritic microstructure.

Very fine- to fine-grained crystals of **epidote** are dispersed within the groundmass and are spatially associated with the biotite lamellae. In some cases, the epidote and the chlorite form irregular replacement patches and discontinuous fillings.



**Photomicrograph 32a:** Subhedral phenocrysts of plagioclase (pl) are immersed within a fine-grained groundmass of plagioclase, biotite, and quartz (pl+bt+qz) and sparse clusters of biotite after magmatic biotite. Plane-polarized /Crossed polarizers transmitted /reflected light.



*IG\_BH03\_LG015*

*Rock Type: Leuco-monzogranite*

This thin polished section consists of an equigranular aggregate of subhedral crystals of plagioclase and anhedral crystals of quartz and alkali feldspar. Very rare lamellae and flakes of biotite are dispersed within the quartzofeldspathic aggregate and impart an isotropic nature to the microstructure.

Alteration: clay and/or epidote: weak after plagioclase; white mica-clay-epidote: subtle after biotite; epidote: subtle to weak; iron oxides: subtle.

Mineral	Alteration and Weathering Mineral	Modal %	Size Range (mm)
Plagioclase (albite)	Clay and/or epidote	40–42	up to 1.6 long
Quartz		37–39	up to 1
Alkali feldspar		20–25	up to 1
Biotite	White mica-clay-epidote	0.5–0.6	up to 0.3 long
	Epidote	0.2–0.4	up to 0.2
	Iron oxides	tr	up to 0.7 long

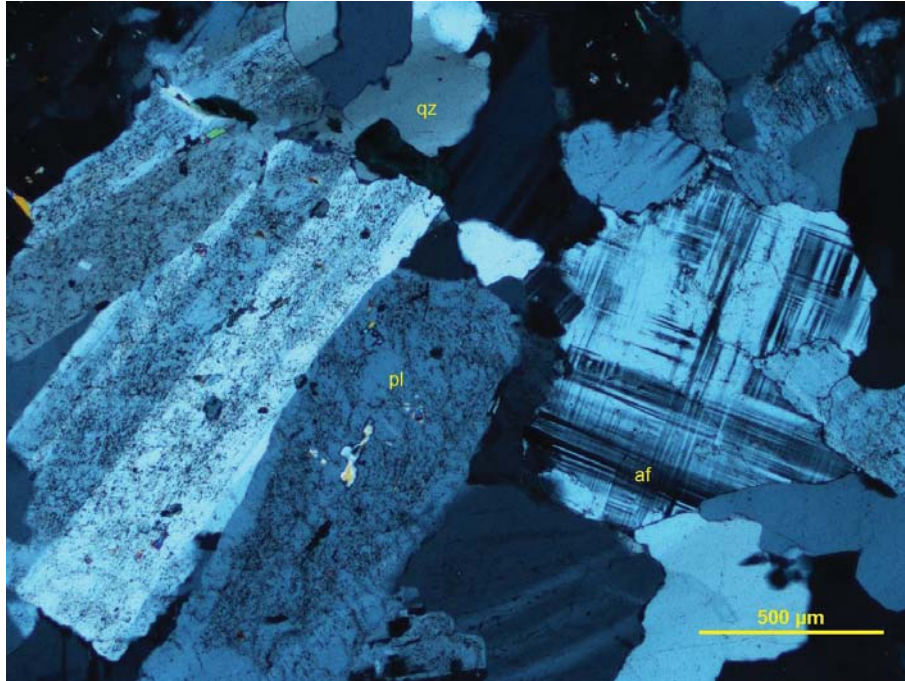
**Plagioclase** forms subhedral crystals (up to 1.6 mm long), which are randomly oriented and, in association with quartz and alkali feldspar, define a medium-grained granular microstructure (Photomicrograph 33). The plagioclase crystals are weakly altered by a very fine-grained dispersion of unresolved material (**clay** and/or **epidote**?). The plagioclase shows refractive indexes smaller than those of the quartz, and it is albite.

**Quartz** occurs as anhedral and interstitial crystals up to 1 mm across. Some of the crystals show undulose extinction and tend to form monomineralic and inclusion-free interstitial aggregates.

**Alkali feldspar** forms anhedral to interstitial crystals (up to 1 mm), which tend to occupy the interstitial positions between the plagioclase and the quartz. The alkali feldspar shows Albite-Pericline twinnings, and its distribution in the thin polished section is best appreciated in the image of the stained billet (the alkali feldspar is stained yellow).

**Biotite** is rare, and its lamellae are randomly oriented within the granular microstructure. Some of the lamellae are moderately altered by probable clay, and are overprinted by very rare flakes of white mica and anhedral crystals of **epidote**. The epidote is spatially associated with the rare lamellae of biotite.

**Iron oxides** completely replaced a 0.7 mm long pseudo-lamellar and unknown mineral.



**Photomicrograph 33:** A subhedral crystal of plagioclase (pl) and anhedral crystals of quartz (qz) and alkali feldspar (af) define a medium-grained granular microstructure. Crossed polarizers transmitted light.

*IG\_BH03\_LG016*

*Rock Type: Foliated plagioclase-phyric andesite*

Euhedral to subhedral phenocrystals of plagioclase are immersed and rotated within a fine-grained groundmass of plagioclase, biotite, and quartz. Thin and discontinuous clusters of biotite define a sub-planar foliation, which wraps the plagioclase phenocrystals.

Alteration: epidote: weak; white mica: subtle after plagioclase.

Mineral	Alteration and Weathering Mineral	Modal %	Size Range (mm)
<i>Phenocrystals</i>			
Plagioclase	White mica	5–7	up to 1.8 long
<i>Groundmass</i>			
Plagioclase		70–75	up to 0.1
Biotite		13–15	up to 0.1, rare up to 0.7 long
Quartz		10–20	up to 0.05
	Epidote	0.2–0.3	
Magnetite		tr	up to 0.3 long
	Chalcopyrite	tr	up to 0.1

**Plagioclase** occurs as subhedral to euhedral phenocrystals (up to 1.8 mm long), which are randomly oriented and rotated within the fine-grained groundmass. It is hard to distinguish the plagioclase from the quartz in the fine-grained groundmass; I tentatively interpret the plagioclase as the most abundant mineral within the groundmass. Some of the crystals are up to 0.1 mm across and show the typical Albite twinnings, and in rare cases, relics of growth zoning. The uncertain abundance of plagioclase and quartz in the groundmass is indicated by the wide range of modal percentages in the table above and would need to be determined by electron optic analysis.

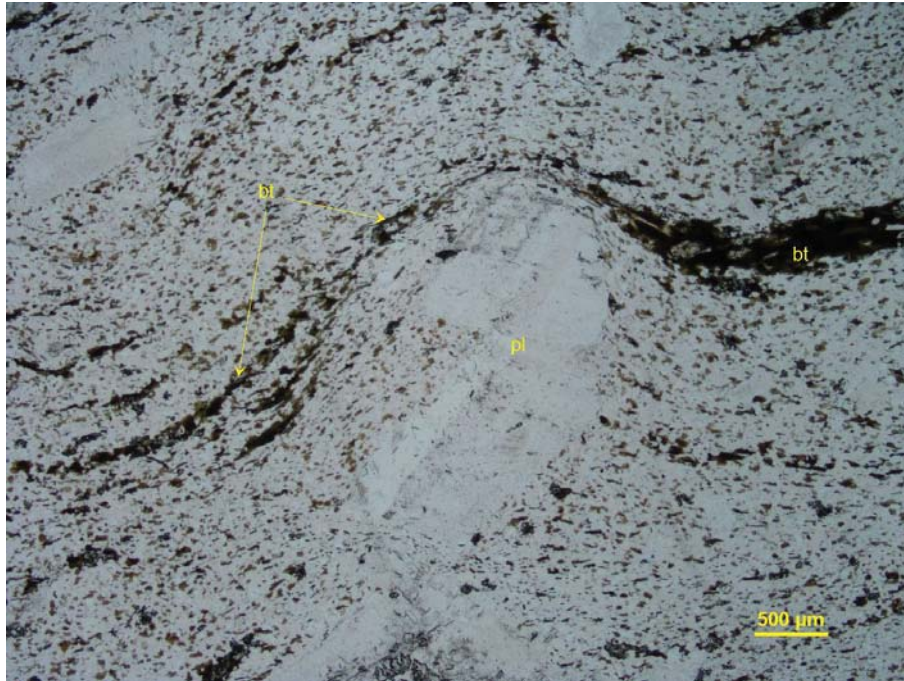
**Biotite** is dispersed within the groundmass as fine-grained flakes and lamellae (up to 0.1 mm long), and it is concentrated within discontinuous clusters defining a sub-planar foliation, which in some cases wraps the plagioclase phenocrystals (Photomicrograph 34a). Within the clusters, the biotite is preferentially iso-oriented, and in some cases, is up to 0.7 mm long. I interpret the clusters and the iso-orientation of the fine-grained lamellae dispersed within the groundmass as having occurred during the crystallization and emplacement of the magma; therefore, I classify this rock as a foliated magmatic rock—a foliated plagioclase-phyric andesite.

**Quartz** is fine-grained (up to 0.05 mm across), and its anhedral crystals are probably subordinate to the plagioclase in the groundmass.

Fine-grained anhedral crystals of epidote are spatially associated with and overprinted the biotite lamellae in the clusters. Sparse crystals of epidote are dispersed within the plagioclase--biotite-quartz groundmass.

**Magnetite** is very rare and its anhedral crystals are dispersed within the groundmass.

Very rare and fine-grained particles of **chalcopyrite** are spatially associated with the epidote dispersed within the groundmass.



**Photomicrograph 34a:** A cluster of fine-grained iso-oriented lamellae of biotite (bt) define the foliation, which wraps a plagioclase phenocrystal (pl) and are dispersed within the fine-grained groundmass. Plane-polarized /Crossed polarizers transmitted /reflected light.



**Photomicrograph 34b:** Same area as shown in Photomicrograph 34a. Under crossed polarizers transmitted light, the contrast between the subhedral phenocrystals of plagioclase (pl) and the fine-grained groundmass of plagioclase, biotite and quartz is more evident.

*IG\_BH03\_LG017*

*Rock Type: Chlorite-white mica-epidote-altered tonalite*

Anhedral to subhedral crystals of plagioclase and interstitial crystals of quartz define a medium-grained granular microstructure hosting less abundant and randomly oriented lamellae of biotite.

Alteration: Fe-chlorite: weak to moderate after biotite; white mica: weak to moderate after plagioclase; epidote: weak.

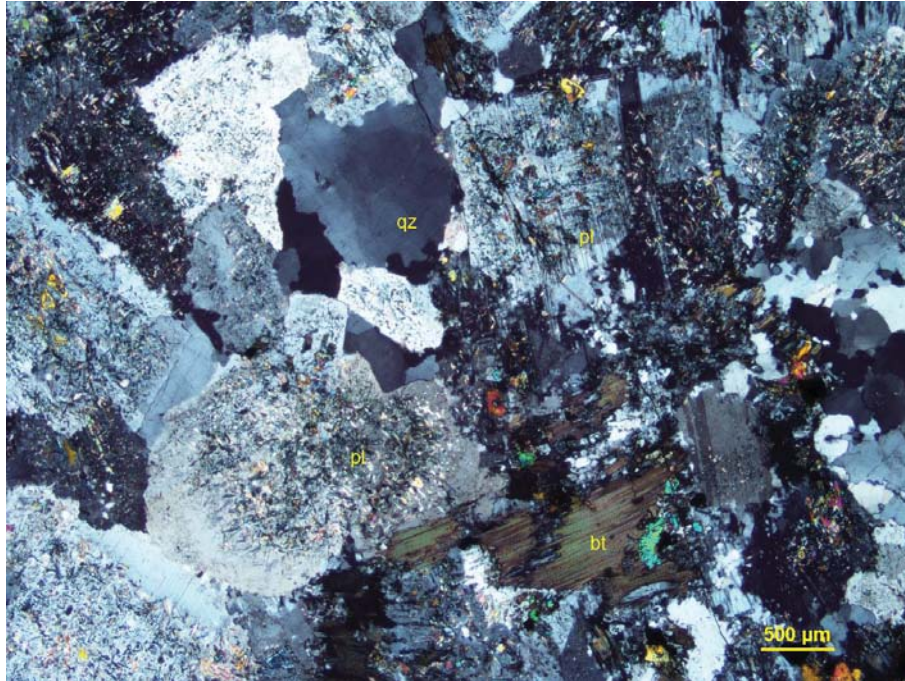
Mineral	Alteration and Weathering Mineral	Modal %	Size Range (mm)
Plagioclase	White mica>epidote	68–70	up to 2.5 long
Quartz		27–29	up to 2, rare up to 5 long
Biotite	Fe-chlorite>epidote	2–4	up to 1 long
[Magnetite]	Hematite	0.8–1	[up to 0.25]
Zircon		tr	~0.01

**Plagioclase** prevails over the quartz as anhedral to subhedral crystals (up to 2.5 mm long). The plagioclase crystals are randomly oriented and are weakly to moderately altered by fine-grained flakes of white mica and subordinate epidote. The alteration products are concentrated within the plagioclase cores. In some cases, the plagioclase crystals show a continuous growth zonation. The alteration-free rims show refractive indexes smaller than those of the quartz, thus indicating that the plagioclase's rim is albitic.

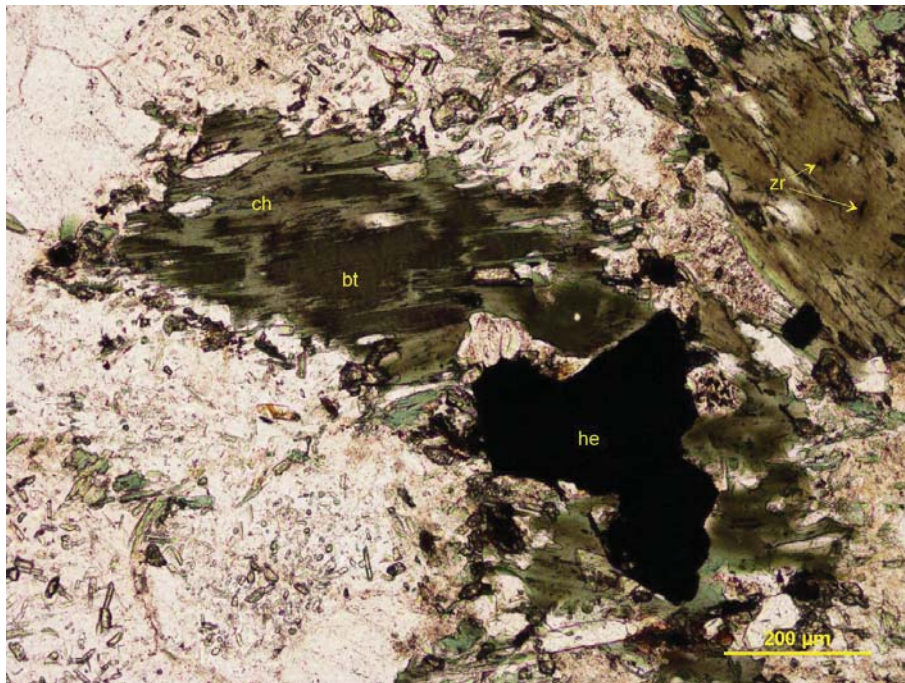
**Quartz** forms inequigranular anhedral crystals (up to 2 mm across, in rare cases up to 5 mm long). Most of the crystals of quartz in reciprocal contact show interlobate crystal boundaries, and in some cases, show a moderate undulose extinction.

**Biotite** is medium-grained and tends to form irregular clusters of randomly oriented lamellae. The biotite is weakly to strongly altered by Fe-chlorite and weakly altered by anhedral crystals of epidote.

Subhedral crystals of **magnetite** are spatially associated with the biotite clusters and are strongly altered by hematite.



**Photomicrograph 35a:** Anhedral to subhedral crystals of plagioclase (pl) are moderately altered by fine-grained white mica and subordinate epidote, and are associated with interstitial crystals and crystal aggregates of quartz (qz). Crossed polarizers transmitted light.



**Photomicrograph 35b:** Clusters of anhedral crystals of biotite (bt) are partially replaced by chlorite (ch). Subhedral alteromorphs of hematite (he) after magnetite are spatially associated with the biotite clusters. Plane-polarized transmitted light.

*IG\_BH03\_LG018*

*Rock Type: Amphibolite (metabasite?)*

This sample shows a medium-grained xenoblastic microstructure, in which crystals of amphibole, biotite is randomly oriented, and are associated with sparse and subordinate crystals of plagioclase (albite), epidote, and chlorite.

Mineral	Alteration and Weathering Mineral	Modal %	Size Range (mm)
Amphibole		86–88	up to 2 long
Biotite		5–10	up to 0.6
Plagioclase		4–5	up to 0.6
Epidote		2–4	up to 0.3
Chlorite		0.5–1	up to 0.4
Rutile		tr	up to 0.02 long
Pyrite		tr	up to 0.02

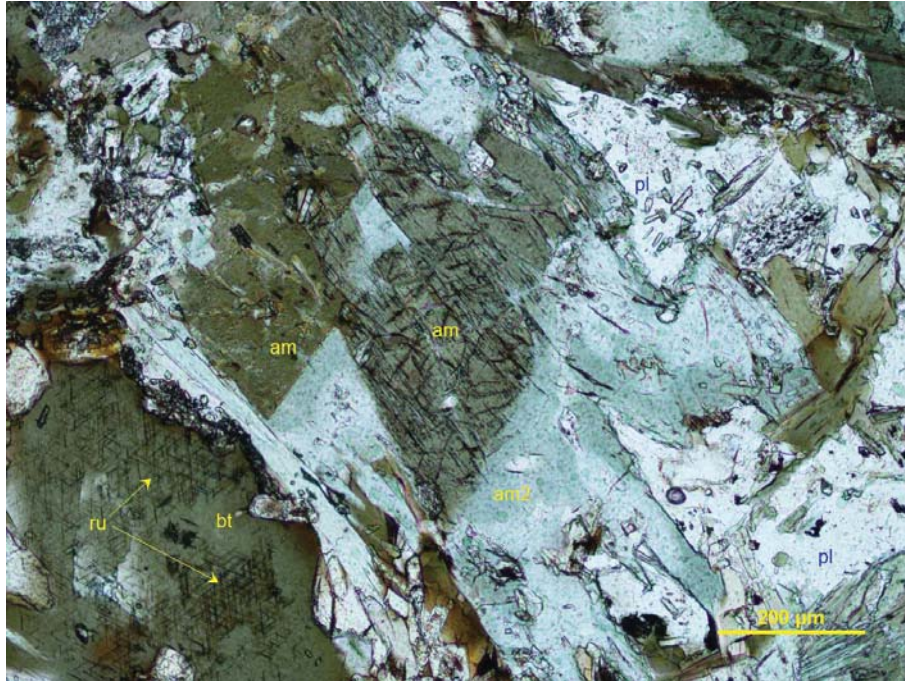
**Amphibole** dominates the composition of this sample as randomly oriented and xenoblastic crystals (up to 2 mm long). The amphibole occurs in at least two types of crystals: a strongly pleochroic one, and a subtly pleochroic one. The pleochroic crystals (X: light yellow-green; Y: light green; Z: light brownish green) are probably actinolite. The subtly pleochroic crystals show pale green colours, extinction angles up to 15°, and probably belong to the tremolite-actinolite series. The subtly pleochroic crystals form rims around the strongly pleochroic crystals and, in some cases, overprinted the strongly pleochroic crystals. In some cases are associated with the biotite.

**Biotite** is subordinate to the amphibole and occurs as xenoblastic lamellae (up to 0.6 mm long). The biotite is spatially associated with the subtly pleochroic amphibole and some of the biotite lamellae host inclusions of sagenitic rutile needles.

**Plagioclase** is medium-grained, and its xenoblastic crystals are heterogeneously dispersed. They are up to 0.6 mm long, and the fresh crystal show Albite twinnings.

**Epidote** forms irregular dispersions and clusters of fine-grained crystals, which are spatially associated with the biotite and chlorite lamellae.

Very rare and very fine-grained crystals of **pyrite** are dispersed within some of the less pleochroic crystals of amphibole.



**Photomicrograph 36:** Xenoblastic crystals of strongly pleochroic amphibole (am) are rimmed by a subtly pleochroic amphibole (am2) and are associated with xenoblastic crystals of biotite (bt) associated with sagenitic rutile (ru) and plagioclase (pl) hosting fine-grained crystals of epidote. Plane-polarized transmitted light.

*IG\_BH03\_LG019*

*Rock Type: White mica-epidote-altered tonalite*

Inequigranular subhedral crystals of plagioclase, anhedral crystals of quartz, and subordinate interstitial crystals of alkali feldspar define a coarse-grained granular microstructure. Subhedral lamellae of biotite are randomly oriented within the quartzofeldspathic aggregate.

Alteration: white mica: weak to moderate after plagioclase; weak after biotite; epidote: weak; hematite: moderate after magnetite.

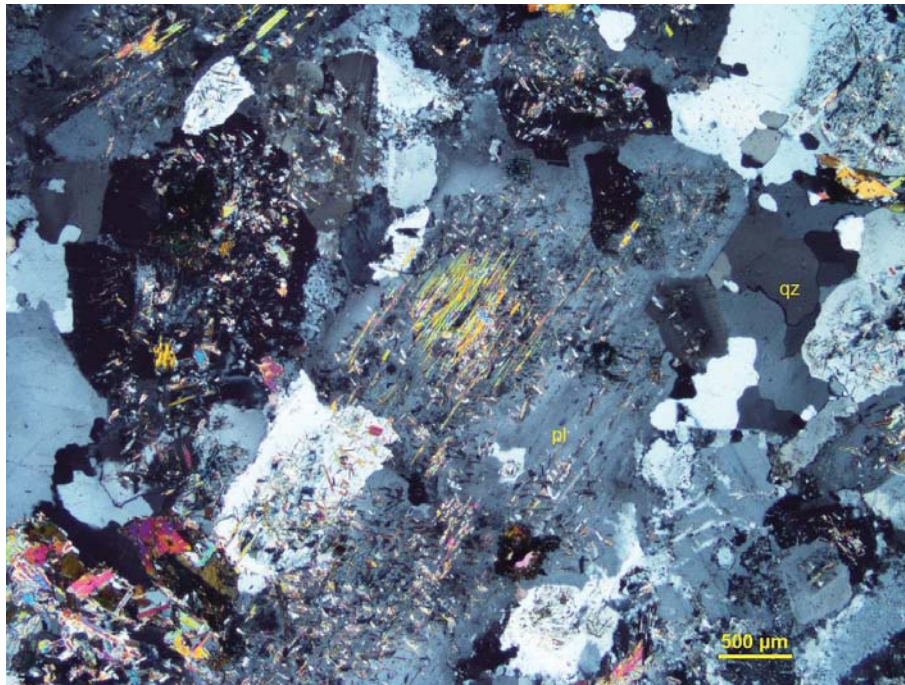
Mineral	Alteration and Weathering Mineral	Modal %	Size Range (mm)
Plagioclase	White mica	54–56	up to 2.5 rare up to 5 long
Quartz		40–42	up to 2, rare up to 5
Alkali feldspar		2–4	up to 2, rare up to 4 long
Biotite	Epidote	2–4	up to 1.5 long
	Epidote	0.5–1	up to 0.5
[Magnetite]	Hematite	tr	up to 0.25
Zircon		tr	0.01

**Plagioclase** occurs as anhedral to subhedral crystals (up to 2.5 mm across, rare up to 5 mm long). The plagioclase is randomly oriented, and define an isotropic granular microstructure. The plagioclase crystals are weakly to moderately altered by very fine-grained highly birefringent flakes of white mica and subordinate epidote (Photomicrograph 37a). The alteration products are concentrated within the subhedral core of the crystals (Photomicrograph 37c). The rims are alteration-free and show refractive indexes smaller than those of the quartz, thus indicating that the rim is albitic.

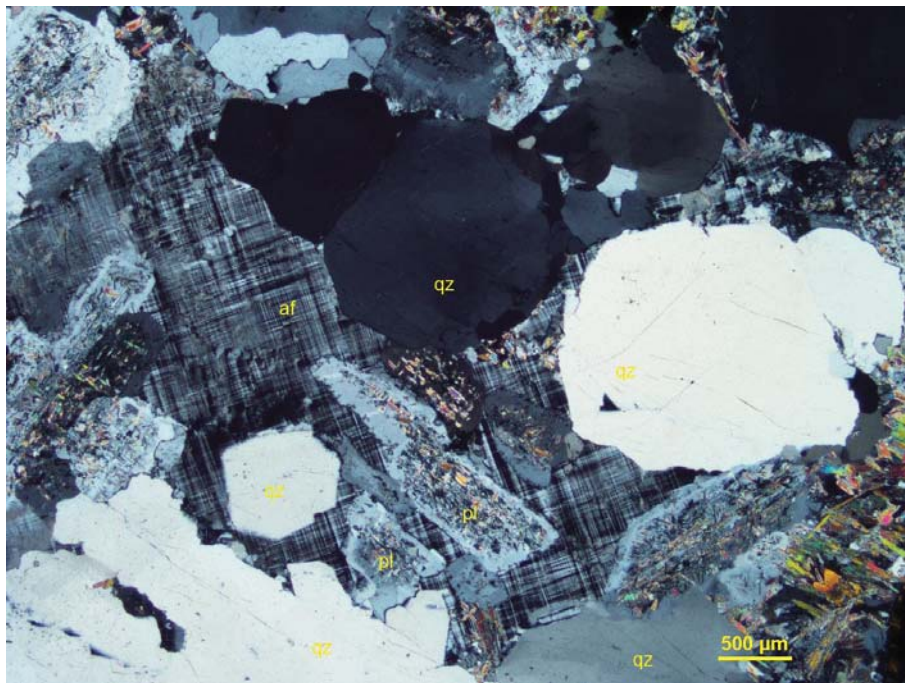
**Quartz** is inequigranular and occupies the interstitial positions between the plagioclase. Rare crystals are sub-rounded and are 5 mm in diameter. I interpret these crystals as relic phenocrystals.

**Alkali feldspar** forms anhedral to interstitial crystals up to 2 mm across, and in rare cases, up to 4 mm long. The alkali feldspar is fresh and shows Albite-Pericline twinnings. In some cases, the alkali feldspar is poikilitic and hosts subhedral crystals of plagioclase and quartz (Photomicrograph 37b).

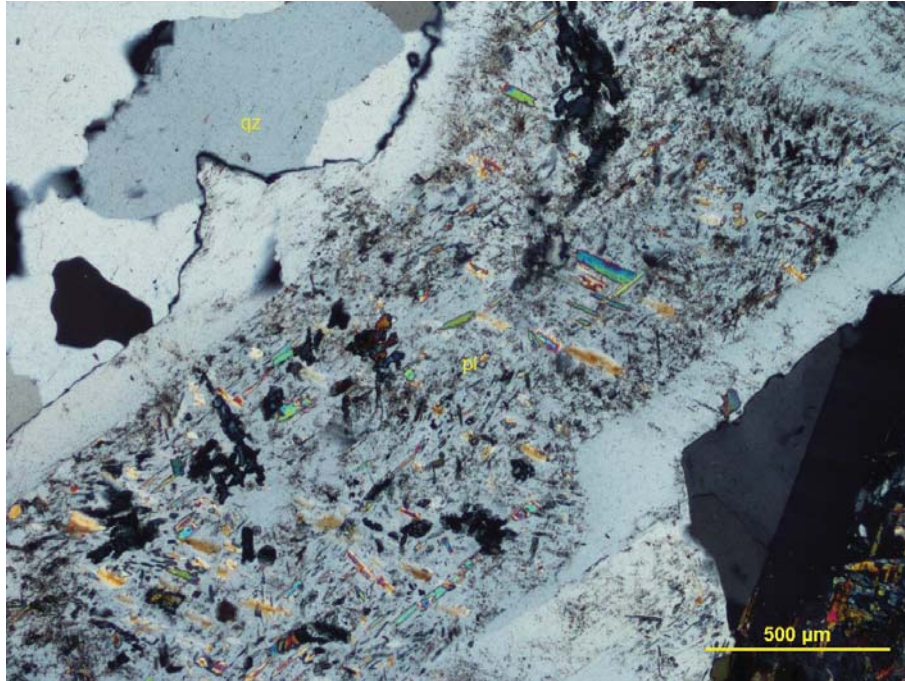
**Biotite** is fine- to medium-grained, and its anhedral to subhedral lamellae are randomly oriented within the mostly quartzofeldspathic aggregate. The biotite is weakly altered by fine-grained lamellae of white mica and anhedral crystals of epidote and hosts very fine-grained inclusions of **zircon**.



**Photomicrograph 37a:** A coarse-grained subhedral crystal of plagioclase is moderately altered by white mica within its core, and is immersed within interstitial crystal aggregates of quartz (qz). Crossed polarizers transmitted light.



**Photomicrograph 37b:** Sub-rounded crystals of quartz (qz) are intergrown with a coarse-grained poikilitic crystal of alkali feldspar (af). The poikilitic crystal host subhedral inclusions of plagioclase and quartz. Crossed polarizers transmitted light.



**Photomicrograph 37c:** A subhedral crystal of plagioclase (pl) shows a fresh albitic rim surrounding a moderately altered crystal core. Crossed polarizers transmitted light.

*IG\_BH03\_LG020*

*Rock Type: Tonalite  
Alkali feldspar breccia*

This thin polished section is microstructurally divided into two main domains. In the lower and middle part (Domain A), subhedral crystals of plagioclase, anhedral and interstitial crystals of quartz and alkali feldspar and randomly oriented lamellae of biotite define a relatively fresh assemblage and undisturbed microstructure. In the upper part, an irregular fault-filling micro-fault is filled mostly by alkali feldspar and divides Domain A from a fractured Domain B, in which plagioclase, quartz and alkali feldspar are filled in by alkali feldspar. In Domain A, biotite is relatively fresh. In Domain B, chlorite completely replaced the biotite.

Alteration: white mica: weak after plagioclase in Domain A; moderate in Domain B; Fe-chlorite: intense after biotite in Domain B, intense near the boundary with Domain B only in Domain A; epidote: subtle to weak in Domain A; weak in domain B

Mineral	Alteration and Weathering Mineral	Modal %	Size Range (mm)
<b>Domain A: tonalite (~83% of PTS)</b>			
Quartz		40–42	up to 2 long
Plagioclase	White mica>epidote	35–37	up to 3
Alkali feldspar		4–5	up to 15 long
Biotite	Chlorite-epidote	2–3	up to 2 long
	Epidote	0.2–0.3	up to 0.15
Zircon		tr	up to 0.01
<b>Domain B: alkali feldspar breccia (~15 of PTS)</b>			
Plagioclase	White mica	6–7	up to 2
Alkali feldspar		3–4	up to 2
Quartz		3–4	up to 0.5
[Biotite]	Chlorite	1–2	up to
	Epidote	0.2–0.4	up to 0.15
<b>Alkali feldspar ± calcite veinlets and fillings (~2% of PTS)</b>			
Alkali feldspar		2	up to 0.05
Calcite		tr	up to 0.05

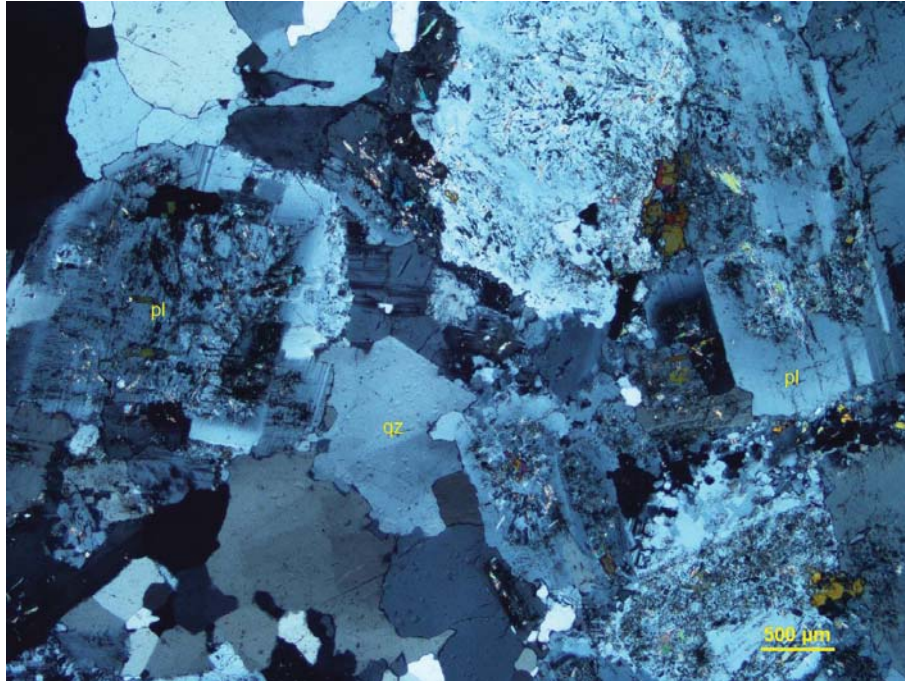
In Domain A, **plagioclase** is anhedral to subhedral, and its crystals (up to 2.5 mm across) are randomly oriented and define an isotropic granular microstructure. The plagioclase is weakly altered by very fine- to fine-grained flakes of white mica and less abundant epidote. The refractive indexes of the plagioclase indicate that it is Albitic. In domain B, the plagioclase is moderately altered, and its average grain is finer-grained due to the fracturing.

**Quartz** is medium-grained, and in Domain A occurs as anhedral crystals (up to 2 mm in diameter) and interstitial crystal aggregates of interlobate crystals. In Domain B, the quartz is concentrated in irregular pockets delimited by fractures.

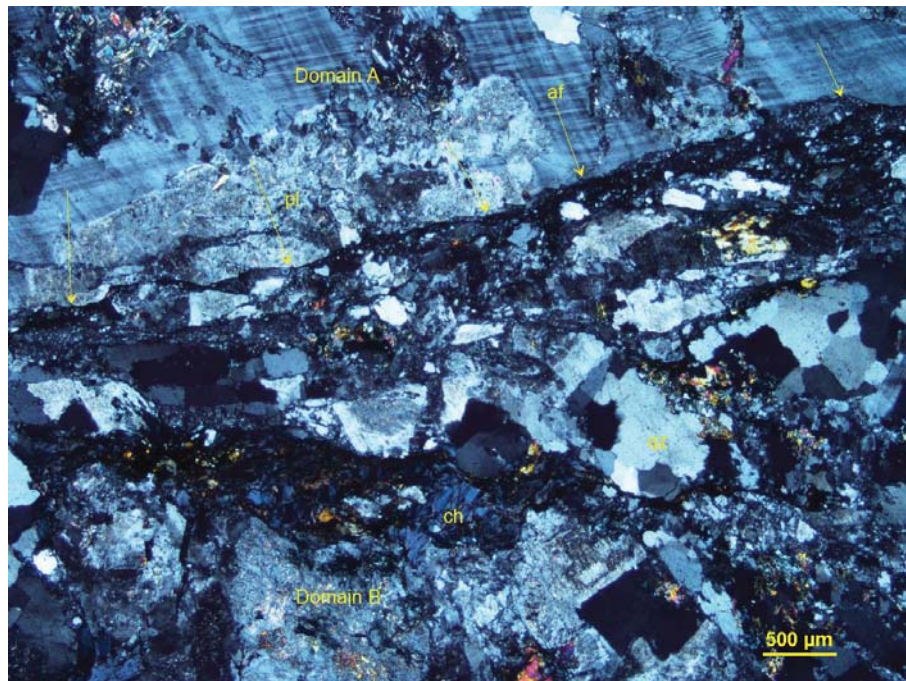
**Alkali feldspar** occurs as interstitial (up to 1 mm long) and, in some cases, poikilitic (up to 15 mm long) crystals in Domain A. In this domain, the alkali feldspar is fresh and shows Albite-Pericline twinnings. The orientation parallel to the boundary, and with it with most of the fractures in Domain B, of the 15 mm long crystal of alkali feldspar suggests that the fracturing of Domain B may have occurred during the final stages of the magmatic crystallization, that is to say, the crystallization of the alkali feldspar. This hypothesis would need to be tested in larger areas, and it is offered here as a tentative hypothesis only. In Domain B, the alkali feldspar is fine-to medium-grained interstitial to poikilitic, and because of the fracturing is up to 2 mm across. Very fine-grained flour dominated by alkali feldspar filled in the micro-fault fillings and the interstices between most of the crystal fragments (Photomicrograph 38b).

**Biotite** occurs as randomly oriented lamellae in Domain A. In most of Domain A, the biotite is relatively fresh, and is subtly to weakly altered by epidote; however, near the boundary with Domain B, some lamellae of biotite are entirely replaced by epitaxial Fe-chlorite. Within Domain B, a lenticular domain of iso-oriented lamellae of chlorite completely replaced the biotite and defines an irregular and incipient schistosity.

**Epidote** is spatially associated with the biotite in Domain A, and it is associated with the chlorite in Domain B in the alteromorphs after the biotite and forms irregular clusters filling the incipient fractures.



**Photomicrograph 38a:** Domain A—Subhedral crystals of plagioclase (pl) are weakly altered, and are associated with interstitial aggregates of quartz (qz). Crossed polarizers transmitted light.



**Photomicrograph 38b:** Domain B—Fractured crystals of plagioclase, quartz aggregates, and a lenticular domain of chlorite (ch) and epidote after biotite are divided from Domain A by an alkali feldspar filled micro-fault (yellow arrows). Crossed polarizers transmitted light.

*IG\_BH03\_LG021*

*Rock Type: Foliated plagioclase-phyric andesite*

Subhedral phenocrystals of plagioclase are randomly oriented within a fine-grained groundmass of plagioclase, quartz, and biotite. The biotite lamellae define sub-parallel clusters, which wrap the phenocrystals and define a foliated porphyritic microstructure.

Alteration: calcite-pyrite: weak; white mica: moderate after plagioclase phenocrystals.

Mineral	Alteration and Weathering Mineral	Modal %	Size Range (mm)
<i>Phenocrystals</i>			
Plagioclase	White mica	15–17	0.5–2.5
<i>Groundmass</i>			
Plagioclase		60–62	up to 0.3
Quartz		15–20	up to 0.1
Biotite		5–8	up to 0.1
	Calcite	2–3	up to 0.1
	Pyrite	1–2	up to 1.5
	Iron oxides	tr	up to 0.2 long

**Plagioclase** occurs as inequigranular phenocrystals (up to 2.5 mm long), which are randomly oriented within a fine-grained foliated groundmass. In the groundmass, the plagioclase is fine-grained (0.05–0.5 mm), and in some cases, it forms subhedral crystals intergrown with the quartz. The fine-grained crystals of plagioclase are fresh. The phenocrystals are moderately altered by very fine-grained flakes of white mica (Photomicrograph 39).

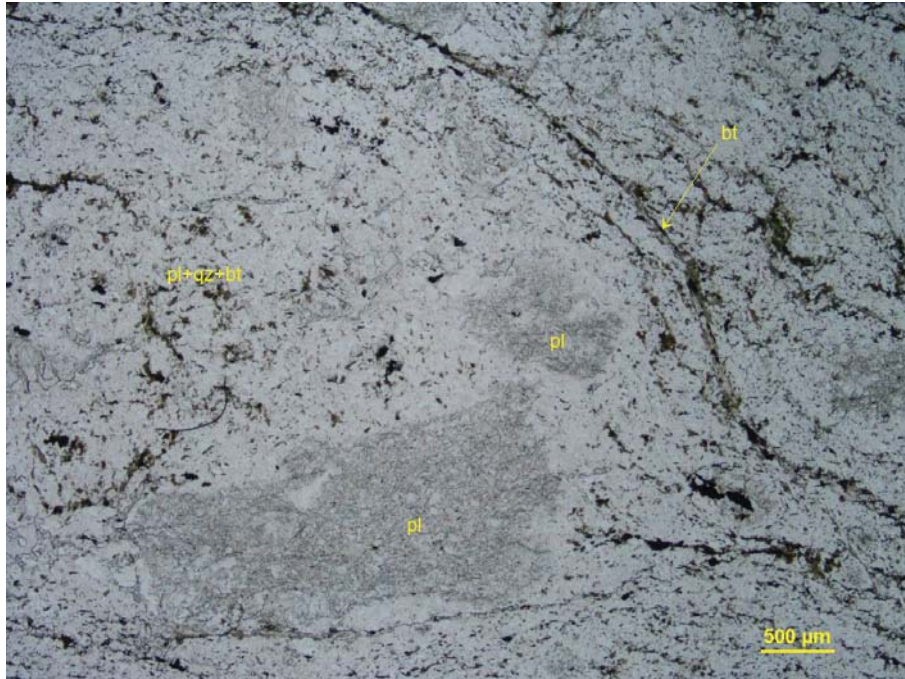
**Quartz** forms fine-grained anhedral crystals intergrown with the plagioclase and the biotite in the groundmass. The quartz and the plagioclase define an inequigranular

**Biotite** occurs as very fine- to fine-grained randomly oriented lamellae dispersed within the groundmass, and it is concentrated within undulose, discontinuous, and up to 0.2 mm thick clusters of preferentially oriented lamellae. The biotite clusters define an irregular foliation (Photomicrograph 39b), which wraps the plagioclase phenocrystals. The composition and grain size of the strain shadows surrounding the rotated phenocrystals of plagioclase are similar to the groundmass in the rest of the rock. I interpret this similarity as the suggestion that the deformation generating the foliation occurred during the final stages of the magmatic crystallization.

**Calcite** is fine-grained and forms irregularly shaped crystal aggregates, which are dispersed within the groundmass.

Rare and subhedral crystals of pyrite (up to 1.5 mm) are dispersed in the groundmass and, in some cases, surrounded by slightly crystals of plagioclase and quartz slightly coarser than the average grain size in the groundmass, and fine-grained crystals and crystal aggregates of calcite. Because of the pyrite's euhedral shape and the occurrence of strain shadow filling in with slightly larger crystals of

the groundmass (and calcite), I interpret the pyrite as having crystallized during the final stages of the deformation and magmatic crystallization.



**Photomicrograph 39a:** Undulating clusters of preferentially iso-oriented lamellae of biotite (bt) wrap the phenocrysts of plagioclase (pl) and define the foliation. Plane-polarized transmitted light.



**Photomicrograph 39b:** The phenocrysts of plagioclase (pl) are moderately altered by very fine-grained flakes of white mica, and are immersed within a fine-grained groundmass of plagioclase, quartz, and biotite (pl+qz+bt). Crossed polarizers transmitted light.

*IG\_BH03\_LG022*

Rock Type: *Leuco-granite*  
*Calcite veinlet*

Subhedral and randomly oriented crystals of plagioclase and anhedral crystals of quartz and alkali feldspar define a medium-grained granular microstructure, in which rare lamellae of biotite are dispersed. A ~0.02 mm thick calcite veinlet crosscut the granular microstructure.

Alteration: clay and/or epidote: subtle after plagioclase; white mica: subtle to strong after biotite; epidote: subtle.

Mineral	Alteration and Weathering Mineral	Modal %	Size Range (mm)
<b>Leucogranite</b> (~100% of PTS)			
Plagioclase	Clay and/or epidote	47–49	up to 2
Quartz		40–42	up to 1, rare up to 2 long
Alkali feldspar		11–15	up to 1
Biotite		0.2–0.3	up to 0.4 long
	White mica	0.1–0.15	up to 0.3 long
	Epidote	tr	up to 0.05
	Pyrrhotite	tr	up to 0.02
<b>Calcite veinlet</b> (tr)			
Calcite		tr	up to 0.05

**Plagioclase** forms subhedral to anhedral crystals up to 2 mm long. The plagioclase crystals are randomly oriented and, in association with anhedral crystals of quartz and alkali feldspar, define a medium-grained granular microstructure. The plagioclase crystals are subtly altered by a very fine-grained, earthy and unresolved material and show Albite twinnings. Most of the crystals show refractive indexes smaller than those of the quartz; therefore, the plagioclase is albite.

**Quartz** occurs as anhedral and inequigranular crystals. The quartz crystals vary from 0.1 mm up to 1 mm, and in rare cases, are up to 2 mm long. The quartz crystals tend to form interlobate crystal aggregates, which occupy the interstitial positions between the plagioclase crystals. In some cases, the medium-grained crystals show moderate undulose extinction.

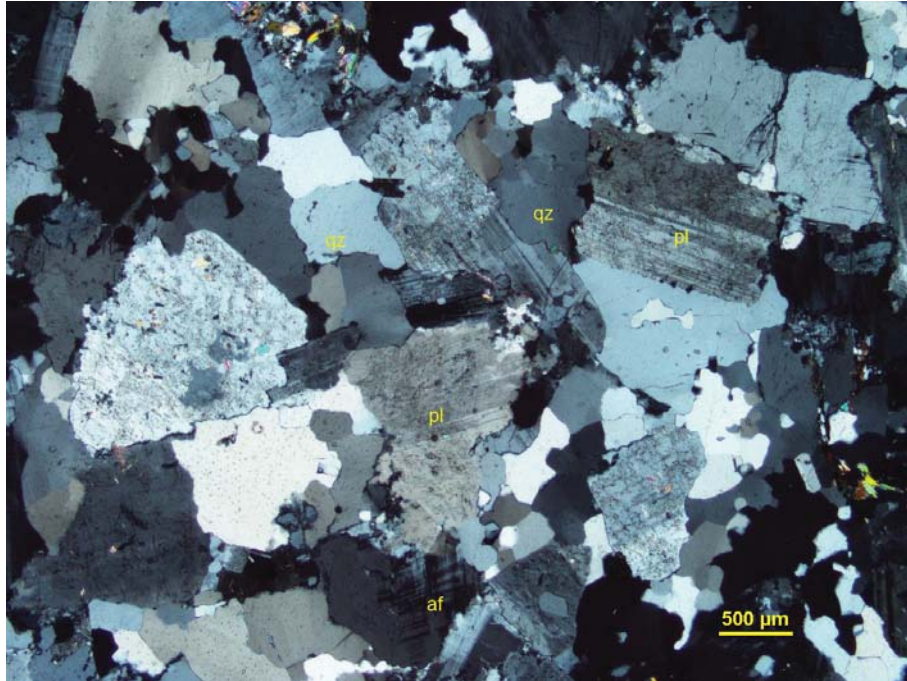
**Alkali feldspar** is medium-grained (up to 1 mm across) and occurs as anhedral crystals. The alkali feldspar crystals are fresh and some of them show Albite-Pericline twinnings.

**Biotite** is rare, and the fine-grained lamellae are randomly oriented in the granular microstructure. The very low amount of biotite, which is the only magmatic ferromagnesian mineral in this rock, is

noted in the pre-fix "leuco-" of the classification of this rock. For more details see (Gillespie & Styles, 1999).

Fine-grained anhedral crystals of **white mica** and subordinate and fine-grained crystals of **epidote** are spatially associated with and overprinted the biotite during the post-magmatic deuteritic or alteration stage. In some cases, the white mica epitaxially replaced medium-grained lamellae of biotite.

Rare and very fine-grained crystals of **pyrrhotite** are dispersed near the **calcite** veinlet.



**Photomicrograph 40:** Anhedral to subhedral crystals of plagioclase (pl) and anhedral crystals of quartz (qz) and subordinate alkali feldspar (af) define a granular microstructure. Crossed polarizers transmitted light.

Blank page.

## **2. Lithogeochemical Analysis**



Report No.: A20-05149 (i)  
 Report Date: 18-Jun-20  
 Date Submitted: 14-May-20  
 Your Reference: PF11654-Rev

Nuclear Waste Mgmt.Org.  
 22 St Clair Ave East, 6th floor  
 Toronto Ontario M4T 2S3  
 Canada

ATTN: Lindsay Waffle

## CERTIFICATE OF ANALYSIS

48 Core samples were submitted for analysis.

The following analytical package(s) were requested:		Testing Date:
14-Ra-226 (Solids)	QOP Ra-226 (Alpha Spectrometry)	2020-06-03 09:52:00
1B (3+)	QOP INAAGEO/QOP INAA-Short Lived (Nickel Sulphide INAA)	2020-05-21 19:45:31
4B-INAA(Lithores)	QOP INAAGEO (INAA)	2020-05-29 10:44:05
4F-B(0.5ppm)	QOP INAA - PGNA (PGNA)	2020-06-01 09:08:18
4F-C, S	Infrared	2020-05-22 19:04:13
4F-Cl	QOP INAA – Short Lived (INAA)	2020-05-29 08:56:11
4F-F	QOP Fluorine (Fusion Specific Ion Electrode-ISE)	
4F-Hg	QOP HgFIMS (Cold Vapour AA)	2020-05-21 20:01:03
4F-Total N	Total Nitrogen (Agriculture Dept)	2020-06-03 13:16:15
4LITHORES + 4B1 (11+)	QOP WRA/ QOP WRA 4B2/QOP Total (/Major/Trace Elements Fusion ICPOES/ICPMS/Total Digestion ICPOES)	2020-05-21 15:52:21
5S	QOP INAA – Short Lived (INAA)	2020-06-01 08:16:06
MLA Schedule 1	MLA Schedule 1	

REPORT **A20-05149 (i)**

This report may be reproduced without our consent. If only selected portions of the report are reproduced, permission must be obtained. If no instructions were given at time of sample submittal regarding excess material, it will be discarded within 90 days of this report. Our liability is limited solely to the analytical cost of these analyses. Test results are representative only of material submitted for analysis.

Notes:

Values which exceed the upper limit should be assayed for most accurate values.

Values which exceed Upper limit should be assayed for most accurate values.

We recommend using option 4B1 for accurate levels of the base metals Cu, Pb, Zn, Ni and Ag. Option 4B-INAA for As, Sb, high W >100ppm, Cr >1000ppm and Sn >50ppm by Code 5D. Values for these elements provided by Fusion ICP/MS, are order of magnitude only and are provided for general information. Mineralized samples should have the Quant option selected or request assays for values which exceed the range of option 4B1. Total includes all elements in % oxide to the left of total. Zr is now being reported from FUS-ICP instead of FUS-MS.

Footnote: INAA data may be suppressed due to high concentrations of some analytes.

CERTIFIED BY:



---

Emmanuel Esemé , Ph.D.  
Quality Control Coordinator

**ACTIVATION LABORATORIES LTD.**  
41 Bittern Street, Ancaster, Ontario, Canada, L9G 4V5  
TELEPHONE +905 648-9611 or +1.888.228.5227 FAX +1.905.648.9613  
E-MAIL [Ancaster@actlabs.com](mailto:Ancaster@actlabs.com) ACTLABS GROUP WEBSITE [www.actlabs.com](http://www.actlabs.com)

Analyte Symbol	Ra-226	Os	Ir	Ru	Rh	Pt	Pd	Au	Mass	Au	As	Br	Cr	Ir	Sc	Se	Sb	Mass	B	Mass	C-Total	Total S	Cl
Unit Symbol	Bq/g	ppb	g	ppb	ppm	ppm	ppm	ppb	ppm	ppm	ppm	g	ppm	g	%	%	%						
Lower Limit	0.01	2	0.1	5	0.2	5	2	0.5	2	0.5	0.5	0.5	5	5	0.1	3	0.2		0.5		0.01	0.01	0.01
Method Code	Alpha Spectroscopy	NI-FINA	INAA	INAA	INAA	INAA	INAA	INAA	INAA	INAA	INAA	PGNAA	PGNAA	CS	CS	INAA							
IG_BH02_LG001										< 2	< 0.5	< 0.5	17	< 5	2.7	< 3	< 0.2	32.3					
IG_BH02_LG002										< 2	< 0.5	< 0.5	28	< 5	1.9	< 3	1.0	31.2					
IG_BH02_LG003										< 2	< 0.5	< 0.5	17	< 5	2.0	< 3	< 0.2	30.8					
IG_BH02_LG004	0.03	< 2	< 0.1	6	0.2	< 5	2	0.8	25	< 2	< 0.5	< 0.5	19	< 5	1.9	< 3	< 0.2	1.07	4.9	1.07	< 0.01	< 0.01	0.02
IG_BH02_LG005										< 2	< 0.5	< 0.5	22	< 5	2.8	< 3	7.1	31.1					
IG_BH02_LG006	0.05	< 2	< 0.1	6	< 0.2	< 5	< 2	0.5	25	< 2	0.5	< 0.5	22	< 5	2.0	< 3	< 0.2	1.03	5.0	1.03	0.04	< 0.01	< 0.01
IG_BH02_LG007										< 2	< 0.5	18.1	14	< 5	2.9	< 3	< 0.2	32.3					
IG_BH02_LG008										< 2	< 0.5	1.2	20	< 5	1.8	< 3	< 0.2	29.6					
IG_BH02_LG009										< 2	< 0.5	11.7	35	< 5	2.1	< 3	< 0.2	28.1					
IG_BH02_LG010										< 2	0.5	< 0.5	23	< 5	2.9	< 3	< 0.2	31.1					
IG_BH02_LG011										< 2	< 0.5	< 0.5	29	< 5	1.8	< 3	0.4	30.7					
IG_BH02_LG012										< 2	< 0.5	1.1	30	< 5	2.2	< 3	< 0.2	30.4					
IG_BH02_LG013										< 2	< 0.5	< 0.5	22	< 5	2.2	< 3	< 0.2	30.5					
IG_BH02_LG014										< 2	< 0.5	< 0.5	22	< 5	1.0	< 3	< 0.2	32.5					
IG_BH02_LG015										< 2	< 0.5	< 0.5	668	< 5	34.5	< 3	< 0.2	30.2					
IG_BH02_LG016	0.02	< 2	< 0.1	6	< 0.2	< 5	< 2	0.5	25	< 2	< 0.5	11.2	13	< 5	2.1	< 3	< 0.2	1.04	5.8	1.04	< 0.01	< 0.01	0.02
IG_BH02_LG017										< 2	< 0.5	18.5	21	< 5	2.9	< 3	0.3	31.7					
IG_BH02_LG018										< 2	< 0.5	4.0	24	< 5	1.6	< 3	< 0.2	30.5					
IG_BH02_LG019	0.04	< 2	< 0.1	< 5	< 0.2	< 5	< 2	< 0.5	25	< 2	< 0.5	< 0.5	23	< 5	1.9	< 3	< 0.2	1.05	< 0.5	1.05	< 0.01	< 0.01	< 0.01
IG_BH02_LG020										2	< 0.5	1.7	23	< 5	3.8	< 3	< 0.2	30.0					
IG_BH02_LG021										< 2	1.0	1.4	376	< 5	19.0	< 3	0.4	33.1					
IG_BH02_LG022										3	1.7	6.8	22	< 5	2.0	< 3	< 0.2	30.3					
IG_BH02_LG023										< 2	< 0.5	14.3	< 5	< 5	2.3	< 3	0.2	30.8					
IG_BH02_LG024										< 2	< 0.5	5.1	21	< 5	1.7	< 3	< 0.2	31.2					
IG_BH02_LG025										< 2	< 0.5	13.6	24	< 5	1.9	< 3	< 0.2	32.0					
IG_BH02_LG026										< 2	< 0.5	13.7	21	< 5	1.9	< 3	< 0.2	29.2					
IG_BH03_LG001		< 2	< 0.1	< 5	< 0.2	< 5	< 2	1.3	25	< 2	< 0.5	< 0.5	27	< 5	2.0	< 3	< 0.2	1.06	< 0.5	1.06	< 0.01	< 0.01	0.02
IG_BH03_LG002		< 2	< 0.1	6	< 0.2	< 5	< 2	0.5	25	< 2	< 0.5	< 0.5	28	< 5	2.1	< 3	< 0.2	1.04	2.6	1.04	< 0.01	< 0.01	< 0.01
IG_BH03_LG003										< 2	0.9	< 0.5	369	< 5	16.6	< 3	< 0.2	34.0					
IG_BH03_LG004										< 2	0.9	< 0.5	18	< 5	1.2	< 3	< 0.2	32.7					
IG_BH03_LG005										< 2	0.6	< 0.5	21	< 5	4.0	< 3	< 0.2	36.4					
IG_BH03_LG006										< 2	< 0.5	6.5	17	< 5	2.2	< 3	< 0.2	34.0					
IG_BH03_LG007										< 2	< 0.5	1.7	20	< 5	0.7	< 3	< 0.2	32.5					
IG_BH03_LG008										< 2	< 0.5	< 0.5	46	< 5	4.1	< 3	< 0.2	34.2					
IG_BH03_LG009										3	< 0.5	< 0.5	26	< 5	2.0	< 3	< 0.2	34.4					
IG_BH03_LG010										< 2	< 0.5	< 0.5	949	< 5	20.2	< 3	< 0.2	35.6					
IG_BH03_LG011										< 2	< 0.5	< 0.5	18	< 5	2.0	< 3	< 0.2	33.3					
IG_BH03_LG012		< 2	< 0.1	< 5	< 0.2	< 5	< 2	< 0.5	25	< 2	1.3	< 0.5	21	< 5	2.0	< 3	0.2	1.06	5.7	1.09	< 0.01	< 0.01	< 0.01
IG_BH03_LG013										< 2	< 0.5	< 0.5	31	< 5	4.0	< 3	< 0.2	35.8					
IG_BH03_LG014		< 2	< 0.1	< 5	< 0.2	< 5	< 2	0.5	25	< 2	< 0.5	< 0.5	15	< 5	2.0	< 3	< 0.2	1.06	< 0.5	1.09	< 0.01	< 0.01	0.01
IG_BH03_LG015										< 2	< 0.5	17.6	20	< 5	1.2	< 3	< 0.2	34.8					
IG_BH03_LG016										< 2	1.5	< 0.5	30	< 5	2.3	< 3	< 0.2	34.9					
IG_BH03_LG017										< 2	1.0	< 0.5	27	< 5	2.0	< 3	< 0.2	34.7					
IG_BH03_LG018										< 2	< 0.5	< 0.5	650	< 5	28.6	< 3	< 0.2	39.7					
IG_BH03_LG019										< 2	< 0.5	12.2	30	< 5	2.2	< 3	< 0.2	33.9					
IG_BH03_LG020										< 2	< 0.5	12.0	16	< 5	2.1	< 3	< 0.2	32.9					
IG_BH03_LG021										< 2	< 0.5	< 0.5	23	< 5	3.5	< 3	< 0.2	36.8					
IG_BH03_LG022										< 2	< 0.5	5.5	21	< 5	0.6	< 3	< 0.2	33.2					

## Results

## Activation Laboratories Ltd.

Report: A20-05149

Analyte Symbol	F	Hg	Total N	SiO2	Al2O3	Fe2O3(T)	MnO	MgO	CaO	Na2O	K2O	TiO2	P2O5	LOI	Total	Sc	Be	V	Cr	Co	Ni	Cu	Zn
Unit Symbol	%	ppb	%	%	%	%	%	%	%	%	%	%	%	%	%	ppm	ppm	ppm	ppm	ppm	ppm	ppm	ppm
Lower Limit	0.01	5	0.1	0.01	0.01	0.01	0.001	0.01	0.01	0.01	0.01	0.001	0.01		0.01	1	1	5	20	1	1	1	1
Method Code	FUS-ISE	1G	Analyze r	FUS-ICP	FUS-ICP	FUS-ICP	FUS-ICP	FUS-ICP	FUS-ICP	FUS-ICP	FUS-ICP	FUS-ICP	FUS-ICP	GRAV	FUS-ICP	FUS-ICP	FUS-ICP	FUS-ICP	FUS-MS	FUS-MS	TD-ICP	TD-ICP	TD-ICP
IG_BH02_LG001				70.95	14.65	2.70	0.035	0.68	2.93	4.42	1.66	0.296	0.09	0.48	98.89	3	1	25	< 20	4	4	13	66
IG_BH02_LG002				72.86	13.56	2.11	0.036	0.33	1.86	4.20	2.58	0.220	0.07	0.58	98.41	2	1	14	30	2	4	10	57
IG_BH02_LG003				72.33	14.43	1.91	0.025	0.34	1.24	4.50	2.73	0.175	0.05	0.80	98.54	2	1	12	20	2	3	12	46
IG_BH02_LG004	< 0.01	< 5	< 0.1	74.01	14.09	1.73	0.033	0.32	1.74	4.39	3.01	0.160	0.03	0.45	99.96	2	1	10	20	2	2	7	44
IG_BH02_LG005				71.59	14.60	2.96	0.039	0.71	3.06	4.34	1.75	0.308	0.10	0.50	99.95	3	1	26	30	5	4	7	67
IG_BH02_LG006	0.02	< 5	< 0.1	74.22	14.18	1.86	0.036	0.37	2.02	4.53	2.47	0.174	0.04	0.68	100.6	2	2	12	20	2	1	12	48
IG_BH02_LG007				70.15	14.51	2.92	0.049	0.75	1.91	5.54	1.22	0.315	0.09	1.39	98.85	3	1	29	20	5	5	21	39
IG_BH02_LG008				72.63	14.02	1.70	0.028	0.32	1.58	4.47	2.90	0.154	0.04	1.65	99.49	2	1	10	< 20	2	2	9	39
IG_BH02_LG009				72.64	13.75	1.81	0.034	0.38	1.42	4.52	2.91	0.164	0.05	0.93	98.61	2	1	11	40	2	2	8	38
IG_BH02_LG010				71.82	14.62	2.74	0.032	0.65	3.09	4.50	1.71	0.306	0.10	0.37	99.92	3	< 1	24	20	5	4	15	64
IG_BH02_LG011				73.51	13.50	1.55	0.031	0.27	1.53	4.38	3.24	0.131	0.04	0.48	98.66	2	1	9	40	2	2	7	37
IG_BH02_LG012				73.34	13.55	1.88	0.037	0.42	1.56	4.40	2.81	0.160	0.05	0.87	99.06	2	1	12	30	2	2	8	39
IG_BH02_LG013				73.13	13.74	1.84	0.033	0.31	1.78	4.38	2.84	0.167	0.04	1.92	100.2	2	1	12	30	2	4	7	43
IG_BH02_LG014				75.78	13.04	0.78	0.015	0.06	0.59	4.30	4.59	0.038	0.01	0.19	99.41	1	1	< 5	< 20	< 1	< 1	2	14
IG_BH02_LG015				42.77	12.00	10.30	0.159	10.24	11.38	1.99	3.26	0.940	0.47	5.72	99.24	39	1	233	750	45	197	71	79
IG_BH02_LG016	< 0.01	< 5	< 0.1	74.50	14.07	1.88	0.034	0.34	1.84	4.47	2.97	0.165	0.04	0.46	100.8	2	1	13	< 20	2	2	6	42
IG_BH02_LG017				72.59	14.75	2.59	0.045	0.55	2.63	4.68	1.75	0.250	0.06	0.56	100.5	3	1	23	20	4	2	9	58
IG_BH02_LG018				74.38	13.74	1.43	0.026	0.32	1.06	4.11	4.51	0.130	0.04	0.68	100.4	2	< 1	10	30	2	2	25	21
IG_BH02_LG019	< 0.01	< 5	< 0.1	73.68	14.16	1.80	0.033	0.33	1.75	4.36	3.09	0.163	0.05	0.43	99.85	2	1	12	20	2	2	8	42
IG_BH02_LG020				72.90	13.25	2.65	0.037	0.68	2.70	3.93	1.75	0.260	0.07	1.13	99.37	4	< 1	29	20	5	6	15	48
IG_BH02_LG021				55.35	14.26	7.12	0.133	5.49	9.57	3.46	1.02	0.574	0.18	3.11	100.3	20	1	140	420	26	75	43	81
IG_BH02_LG022				74.15	13.99	1.82	0.033	0.36	1.86	4.46	2.63	0.167	0.04	0.66	100.2	2	1	14	20	2	2	9	48
IG_BH02_LG023				58.90	18.74	1.97	0.037	0.53	4.01	8.61	1.27	0.249	0.06	4.12	98.49	2	1	21	< 20	2	4	37	48
IG_BH02_LG024				75.04	13.86	1.62	0.029	0.25	1.62	4.64	2.93	0.130	0.03	0.47	100.6	2	1	9	< 20	2	1	8	35
IG_BH02_LG025				72.74	14.30	1.85	0.031	0.32	1.99	4.97	3.10	0.166	0.05	1.05	100.6	2	< 1	14	20	2	2	3	17
IG_BH02_LG026				73.11	14.25	1.97	0.027	0.42	1.44	4.70	2.69	0.188	0.05	1.66	100.5	2	1	14	20	2	3	13	21
IG_BH03_LG001	< 0.01	< 5	< 0.1	73.39	14.24	1.77	0.030	0.39	1.99	4.52	2.46	0.189	0.06	0.60	99.64	2	1	14	20	2	3	10	52
IG_BH03_LG002	< 0.01	< 5	< 0.1	72.92	13.84	1.77	0.032	0.38	1.99	4.54	2.21	0.183	0.05	0.59	98.51	2	1	13	20	2	2	10	51
IG_BH03_LG003				53.93	13.46	8.28	0.125	7.90	8.18	3.24	2.12	0.728	0.20	2.08	100.2	19	1	175	430	33	228	15	101
IG_BH03_LG004				77.01	12.83	0.90	0.022	0.17	0.50	4.14	4.61	0.077	0.01	0.27	100.5	1	2	< 5	< 20	1	1	11	27
IG_BH03_LG005				71.09	14.53	3.22	0.040	0.81	3.17	4.26	1.86	0.447	0.12	0.50	100.1	4	1	34	20	6	7	17	70
IG_BH03_LG006				72.26	14.69	1.67	0.023	0.37	1.31	4.27	3.33	0.164	0.05	1.27	99.40	2	1	18	< 20	2	2	18	38
IG_BH03_LG007				75.89	12.90	0.59	0.014	0.06	0.51	4.42	4.28	0.036	< 0.01	0.33	99.04	< 1	1	< 5	< 20	< 1	< 1	8	20
IG_BH03_LG008				71.43	14.98	3.01	0.041	0.85	3.32	4.41	1.64	0.331	0.10	0.54	100.6	4	< 1	36	50	6	7	16	66
IG_BH03_LG009				74.22	14.14	1.76	0.029	0.40	1.92	4.36	2.36	0.184	0.05	0.87	100.3	2	< 1	13	30	2	1	9	48
IG_BH03_LG010				51.35	12.14	8.67	0.144	10.19	8.32	2.67	2.63	0.629	0.18	3.32	100.3	23	1	179	1110	42	229	20	77
IG_BH03_LG011				74.49	14.17	1.85	0.032	0.41	2.10	4.45	2.38	0.195	0.05	0.67	100.8	2	1	16	20	3	3	27	53
IG_BH03_LG012	< 0.01	< 5	< 0.1	73.41	13.76	1.80	0.030	0.39	2.05	4.36	2.54	0.192	0.05	0.52	99.10	2	< 1	14	20	2	3	8	50
IG_BH03_LG013				70.92	14.61	2.95	0.040	0.84	3.38	4.31	1.62	0.328	0.09	0.62	99.70	4	< 1	35	40	6	5	19	67
IG_BH03_LG014	< 0.01	< 5	< 0.1	73.85	13.92	1.85	0.032	0.39	2.11	4.52	2.37	0.196	0.06	0.46	99.75	2	1	15	< 20	3	3	8	51
IG_BH03_LG015				77.24	12.93	0.60	0.022	0.05	0.41	4.47	4.47	0.034	0.01	0.28	100.5	1	< 1	< 5	20	< 1	< 1	3	13
IG_BH03_LG016				73.14	14.64	2.01	0.030	0.44	2.59	4.55	1.89	0.213	0.06	0.42	99.98	2	< 1	18	20	3	2	31	59
IG_BH03_LG017				73.91	14.32	1.87	0.032	0.45	2.14	6.01	0.74	0.200	0.05	0.85	100.6	2	1	15	30	3	3	48	39
IG_BH03_LG018				44.69	10.31	10.71	0.172	15.61	10.16	0.69	2.66	0.895	0.45	3.80	100.2	31	1	206	720	62	535	13	86
IG_BH03_LG019				73.70	14.16	1.91	0.028	0.47	2.03	4.84	1.79	0.209	0.05	1.57	100.8	2	1	15	20	3	4	25	34
IG_BH03_LG020				73.50	14.31	1.90	0.030	0.42	2.28	4.55	2.40	0.209	0.06	0.98	100.7	2	1	16	20	3	1	11	37
IG_BH03_LG021				70.13	14.33	3.02	0.037	0.79	3.08	4.65	1.52	0.407	0.10	1.52	99.58	4	1	32	30	6	7	23	68
IG_BH03_LG022				76.99	12.80	0.58	0.013	0.05	0.62	4.53	3.50	0.036	< 0.01	0.60	99.73	< 1	< 1	< 5	30	< 1	2	6	12

Analyte Symbol	Cd	S	Ga	Ge	As	Rb	Sr	Y	Zr	Nb	Mo	Ag	In	Sn	Sb	Cs	Ba	La	Ce	Pr	Nd	Sm	Eu
Unit Symbol	ppm	%	ppm	ppm	ppm	ppm	ppm	ppm	ppm	ppm	ppm	ppm	ppm	ppm	ppm	ppm	ppm	ppm	ppm	ppm	ppm	ppm	ppm
Lower Limit	0.5	0.001	1	0.5	5	1	2	0.5	1	0.2	2	0.3	0.1	1	0.2	0.1	2	0.05	0.05	0.01	0.05	0.01	0.005
Method Code	TD-ICP	TD-ICP	FUS-MS	FUS-MS	FUS-MS	FUS-MS	FUS-ICP	FUS-MS	FUS-ICP	FUS-MS	FUS-MS	TD-ICP	FUS-MS	FUS-MS	FUS-MS	FUS-MS	FUS-ICP	FUS-MS	FUS-MS	FUS-MS	FUS-MS	FUS-MS	FUS-MS
IG_BH02_LG001	< 0.5	0.003	19	1.0	< 5	50	258	4.2	145	4.0	< 2	< 0.3	< 0.1	1	0.3	2.4	390	16.2	31.1	3.08	11.1	1.90	0.614
IG_BH02_LG002	< 0.5	0.003	18	1.0	< 5	91	161	4.9	112	3.6	3	0.3	< 0.1	1	0.6	1.9	555	20.7	36.2	3.58	11.9	1.91	0.494
IG_BH02_LG003	< 0.5	0.003	19	1.0	< 5	87	198	5.3	88	3.8	< 2	< 0.3	< 0.1	1	< 0.2	2.6	505	16.9	29.3	2.99	10.5	2.08	0.412
IG_BH02_LG004	< 0.5	0.003	18	1.0	< 5	99	181	4.7	85	3.8	< 2	< 0.3	< 0.1	1	< 0.2	3.3	522	16.4	28.9	3.00	10.2	1.82	0.431
IG_BH02_LG005	< 0.5	0.004	18	1.0	< 5	52	244	4.3	134	4.2	< 2	< 0.3	< 0.1	1	4.0	2.3	419	21.7	38.3	3.88	13.8	2.17	0.675
IG_BH02_LG006	< 0.5	0.002	18	1.1	< 5	88	194	5.2	93	4.3	< 2	< 0.3	< 0.1	1	< 0.2	3.8	466	17.2	30.5	3.13	10.8	1.98	0.463
IG_BH02_LG007	< 0.5	0.003	20	1.0	< 5	58	238	5.5	152	4.0	< 2	0.4	< 0.1	1	< 0.2	1.3	348	18.4	37.5	3.45	12.5	2.26	0.746
IG_BH02_LG008	< 0.5	0.003	18	1.1	< 5	86	182	4.8	79	4.1	< 2	0.3	< 0.1	1	< 0.2	1.8	529	15.1	26.8	2.74	9.74	1.76	0.409
IG_BH02_LG009	< 0.5	0.002	18	1.1	< 5	86	163	5.0	86	4.1	2	< 0.3	< 0.1	1	< 0.2	1.5	603	16.5	29.5	3.01	10.5	1.91	0.444
IG_BH02_LG010	< 0.5	0.004	18	0.9	< 5	49	253	3.6	143	3.6	2	0.5	< 0.1	1	< 0.2	1.0	396	20.4	36.7	3.69	12.7	2.07	0.619
IG_BH02_LG011	< 0.5	0.003	18	1.1	< 5	105	155	6.0	74	3.4	< 2	< 0.3	< 0.1	1	< 0.2	2.2	481	14.1	25.4	2.62	9.47	1.97	0.401
IG_BH02_LG012	< 0.5	0.002	18	1.0	< 5	81	180	5.3	88	4.1	2	0.3	< 0.1	1	< 0.2	1.7	507	16.2	29.2	2.94	10.3	1.94	0.467
IG_BH02_LG013	< 0.5	0.014	18	1.1	< 5	90	222	5.2	88	4.3	< 2	< 0.3	< 0.1	1	< 0.2	1.9	565	18.1	31.0	3.15	11.1	1.99	0.408
IG_BH02_LG014	< 0.5	0.001	19	1.8	< 5	126	16	9.4	15	3.5	< 2	< 0.3	< 0.1	< 1	< 0.2	1.3	14	3.31	6.48	0.73	2.71	0.98	0.139
IG_BH02_LG015	< 0.5	0.067	14	1.4	< 5	104	789	20.2	125	6.4	< 2	< 0.3	< 0.1	1	< 0.2	6.4	655	45.9	101	12.4	49.4	8.86	2.42
IG_BH02_LG016	< 0.5	0.003	18	1.0	< 5	93	192	4.9	91	3.9	< 2	< 0.3	< 0.1	1	< 0.2	2.6	570	17.6	30.6	3.10	10.4	1.94	0.476
IG_BH02_LG017	< 0.5	0.003	19	0.8	< 5	73	307	5.6	105	4.7	< 2	< 0.3	< 0.1	1	< 0.2	2.9	330	19.6	34.5	3.41	11.6	1.81	0.478
IG_BH02_LG018	< 0.5	0.003	15	0.8	< 5	134	136	3.3	66	2.3	< 2	< 0.3	< 0.1	1	< 0.2	0.7	919	10.4	16.9	1.73	5.94	1.09	0.468
IG_BH02_LG019	< 0.5	0.003	18	1.0	< 5	98	193	4.5	89	4.1	< 2	< 0.3	< 0.1	1	< 0.2	2.1	668	16.8	29.4	2.93	10.1	1.86	0.478
IG_BH02_LG020	< 0.5	0.002	16	0.8	< 5	70	236	4.3	119	3.3	< 2	0.3	< 0.1	1	< 0.2	2.3	471	18.2	32.2	3.19	10.9	1.83	0.509
IG_BH02_LG021	< 0.5	0.004	17	1.8	< 5	37	1226	14.5	109	5.2	< 2	< 0.3	< 0.1	1	0.4	0.3	213	37.9	69.7	7.80	30.5	5.21	1.35
IG_BH02_LG022	< 0.5	0.002	18	0.9	< 5	83	206	4.4	93	4.1	< 2	< 0.3	< 0.1	1	< 0.2	1.6	561	17.1	29.9	2.98	10.5	1.77	0.464
IG_BH02_LG023	< 0.5	0.003	19	1.0	< 5	34	310	9.0	125	7.3	< 2	0.3	< 0.1	1	< 0.2	0.6	495	15.4	30.1	3.08	11.3	2.95	0.937
IG_BH02_LG024	< 0.5	0.003	17	1.0	< 5	86	153	4.0	70	3.3	< 2	< 0.3	< 0.1	1	< 0.2	1.9	391	12.7	22.3	2.25	7.80	1.40	0.381
IG_BH02_LG025	< 0.5	0.001	19	1.1	< 5	115	192	4.4	98	4.0	2	< 0.3	< 0.1	1	< 0.2	0.6	682	21.0	34.4	3.42	11.8	1.84	0.509
IG_BH02_LG026	< 0.5	0.022	17	0.9	< 5	108	203	4.6	108	3.7	< 2	< 0.3	< 0.1	1	< 0.2	2.8	711	16.8	28.5	2.87	9.86	1.79	0.399
IG_BH03_LG001	< 0.5	0.002	18	1.0	< 5	81	219	4.3	109	4.4	< 2	0.4	< 0.1	1	< 0.2	3.0	493	20.2	34.8	3.39	11.5	2.03	0.501
IG_BH03_LG002	< 0.5	0.004	18	1.0	< 5	76	208	5.2	111	4.7	< 2	< 0.3	< 0.1	1	< 0.2	2.8	453	19.4	34.1	3.40	11.5	1.99	0.440
IG_BH03_LG003	< 0.5	0.003	17	1.2	< 5	78	575	13.5	104	4.1	< 2	< 0.3	< 0.1	1	< 0.2	9.0	417	30.7	65.7	7.63	29.8	5.53	1.45
IG_BH03_LG004	< 0.5	0.002	19	1.8	< 5	172	21	8.5	22	4.2	< 2	< 0.3	< 0.1	1	< 0.2	3.9	46	2.83	6.25	0.68	2.53	0.87	0.114
IG_BH03_LG005	< 0.5	0.006	19	0.9	< 5	57	250	6.5	165	6.4	< 2	0.3	< 0.1	1	< 0.2	1.5	447	22.8	41.8	4.29	15.4	2.77	0.819
IG_BH03_LG006	< 0.5	0.003	20	0.9	< 5	109	171	3.6	101	4.9	< 2	< 0.3	< 0.1	1	< 0.2	1.8	930	15.1	27.9	2.70	8.96	1.61	0.323
IG_BH03_LG007	< 0.5	0.004	17	1.4	< 5	162	15	7.7	14	2.5	< 2	< 0.3	< 0.1	< 1	< 0.2	2.3	16	5.52	10.7	1.11	3.63	0.90	0.123
IG_BH03_LG008	< 0.5	0.005	18	0.8	< 5	49	253	4.9	140	4.2	< 2	0.4	< 0.1	1	< 0.2	1.3	400	19.3	34.2	3.51	12.7	2.14	0.621
IG_BH03_LG009	< 0.5	0.003	18	0.9	< 5	73	224	4.2	99	3.7	< 2	0.4	< 0.1	1	< 0.2	1.5	636	18.1	31.5	3.17	10.4	1.82	0.504
IG_BH03_LG010	< 0.5	0.006	14	1.3	< 5	82	519	13.8	91	5.2	< 2	< 0.3	< 0.1	1	< 0.2	4.8	656	25.0	52.4	6.21	25.0	4.77	1.30
IG_BH03_LG011	< 0.5	0.003	18	0.9	< 5	76	220	4.2	106	4.3	2	0.4	< 0.1	1	< 0.2	2.2	509	17.3	30.0	2.99	10.3	1.75	0.476
IG_BH03_LG012	< 0.5	0.002	18	0.9	< 5	78	218	4.1	106	4.0	< 2	0.3	< 0.1	1	< 0.2	2.0	605	19.7	33.9	3.36	11.2	1.84	0.446
IG_BH03_LG013	< 0.5	0.008	18	0.8	< 5	48	250	4.8	145	4.1	< 2	0.4	< 0.1	1	< 0.2	1.2	400	19.8	34.7	3.50	12.2	2.08	0.627
IG_BH03_LG014	< 0.5	0.003	18	0.9	< 5	83	222	4.2	109	4.6	< 2	< 0.3	< 0.1	1	< 0.2	2.6	500	19.7	33.8	3.31	11.4	1.92	0.456
IG_BH03_LG015	< 0.5	0.010	18	1.8	< 5	200	8	16.2	31	3.4	< 2	< 0.3	< 0.1	< 1	0.2	2.2	7	4.42	9.85	1.14	4.00	1.32	0.065
IG_BH03_LG016	< 0.5	0.006	17	0.8	< 5	69	245	3.5	111	3.3	< 2	0.4	< 0.1	1	< 0.2	1.9	513	17.1	29.1	2.79	9.29	1.50	0.432
IG_BH03_LG017	< 0.5	0.007	18	0.8	< 5	24	339	4.3	115	4.7	< 2	0.6	< 0.1	1	< 0.2	0.8	623	18.4	33.8	3.27	11.5	2.02	0.545
IG_BH03_LG018	< 0.5	0.020	12	1.4	< 5	73	416	17.7	118	6.2	< 2	< 0.3	< 0.1	1	< 0.2	4.5	629	46.0	102	12.2	49.1	8.62	2.20
IG_BH03_LG019	< 0.5	0.006	18	0.9	< 5	58	243	4.2	120	4.5	< 2	< 0.3	< 0.1	1	< 0.2	1.0	390	20.9	36.0	3.54	12.0	1.93	0.491
IG_BH03_LG020	< 0.5	0.004	18	0.9	< 5	69	242	3.9	122	4.5	< 2	0.4	< 0.1	1	< 0.2	1.1	574	20.0	34.5	3.34	11.3	1.88	0.521
IG_BH03_LG021	< 0.5	0.015	18	0.8	< 5	50	264	5.8	163	6.1	< 2	< 0.3	< 0.1	1	< 0.2	2.6	452	22.7	41.5	4.24	15.0	2.59	0.806
IG_BH03_LG022	< 0.5	0.054	16	1.3	< 5	99	49	5.1	23	2.8	< 2	< 0.3	< 0.1	< 1	< 0.2	1.1	62	5.85	11.1	1.17	4.06	0.96	0.168

## Results

## Activation Laboratories Ltd.

## Report: A20-05149

Analyte Symbol	Gd	Tb	Dy	Ho	Er	Tm	Yb	Lu	Hf	Ta	W	Tl	Pb	Li	Bi	Th	U	Re	I
Unit Symbol	ppm	ppm	ppm																
Lower Limit	0.01	0.01	0.01	0.01	0.01	0.005	0.01	0.002	0.1	0.01	0.5	0.05	5	1	0.1	0.05	0.01	1	0.5
Method Code	FUS-MS	TD-ICP	TD-ICP	FUS-MS	FUS-MS	FUS-MS	INAA	INAA											
IG_BH02_LG001	1.44	0.18	0.84	0.12	0.36	0.050	0.32	0.045	3.6	0.54	1.2	0.37	9	93	0.7	4.41	1.74		
IG_BH02_LG002	1.39	0.18	0.88	0.15	0.43	0.056	0.36	0.053	2.8	0.82	< 0.5	0.44	7	69	< 0.1	5.06	1.62		
IG_BH02_LG003	1.49	0.20	1.01	0.16	0.44	0.064	0.41	0.060	2.6	0.91	< 0.5	0.40	9	76	< 0.1	6.77	1.40		
IG_BH02_LG004	1.43	0.18	0.88	0.14	0.39	0.057	0.37	0.051	2.6	0.79	3.9	0.41	10	71	< 0.1	6.22	2.21	< 1	1.4
IG_BH02_LG005	1.62	0.19	0.92	0.14	0.42	0.055	0.34	0.045	3.4	0.61	< 0.5	0.31	< 5	77	0.1	4.73	1.30		
IG_BH02_LG006	1.52	0.21	1.01	0.16	0.45	0.059	0.39	0.056	2.8	0.90	0.7	0.39	8	80	< 0.1	6.70	2.85	1	0.5
IG_BH02_LG007	1.75	0.23	1.10	0.18	0.46	0.062	0.43	0.061	3.6	0.53	0.6	0.31	12	89	0.4	4.40	1.91		
IG_BH02_LG008	1.39	0.18	0.96	0.15	0.40	0.053	0.34	0.051	2.3	1.07	2.6	0.33	9	62	< 0.1	5.59	1.77		
IG_BH02_LG009	1.51	0.19	0.91	0.15	0.42	0.058	0.38	0.055	2.5	1.00	1.8	0.36	7	44	< 0.1	6.46	1.36		
IG_BH02_LG010	1.43	0.19	0.78	0.11	0.29	0.039	0.24	0.036	3.5	0.47	4.4	0.25	< 5	86	< 0.1	4.12	1.00		
IG_BH02_LG011	1.53	0.21	1.05	0.19	0.50	0.071	0.49	0.074	2.5	0.82	< 0.5	0.49	8	56	< 0.1	6.49	1.15		
IG_BH02_LG012	1.46	0.21	1.08	0.17	0.44	0.059	0.38	0.058	2.5	0.90	< 0.5	0.32	8	42	< 0.1	6.19	1.80		
IG_BH02_LG013	1.57	0.19	0.93	0.16	0.42	0.061	0.41	0.060	2.7	0.83	2.1	0.39	8	80	< 0.1	7.02	2.45		
IG_BH02_LG014	1.22	0.24	1.54	0.29	0.83	0.121	0.82	0.126	1.3	1.14	< 0.5	0.50	18	17	< 0.1	1.97	7.31		
IG_BH02_LG015	6.50	0.78	4.11	0.72	1.96	0.275	1.67	0.248	3.2	0.38	< 0.5	0.47	11	242	< 0.1	5.95	2.12		
IG_BH02_LG016	1.49	0.18	0.89	0.16	0.43	0.057	0.39	0.061	2.7	0.86	< 0.5	0.43	8	61	< 0.1	6.21	1.93	< 1	< 0.5
IG_BH02_LG017	1.34	0.18	1.03	0.18	0.49	0.073	0.47	0.067	2.8	1.28	< 0.5	0.37	8	71	< 0.1	4.34	2.54		
IG_BH02_LG018	0.89	0.12	0.58	0.09	0.23	0.034	0.23	0.031	1.8	0.39	< 0.5	0.55	7	25	< 0.1	3.05	1.37		
IG_BH02_LG019	1.27	0.18	0.83	0.14	0.38	0.054	0.32	0.048	2.6	0.90	0.7	0.46	8	65	0.2	5.78	2.71	< 1	< 0.5
IG_BH02_LG020	1.28	0.17	0.81	0.14	0.35	0.055	0.37	0.060	3.0	0.55	< 0.5	0.34	7	58	< 0.1	4.71	1.42		
IG_BH02_LG021	3.96	0.49	2.57	0.48	1.40	0.201	1.40	0.218	2.9	0.33	0.5	0.19	20	55	0.1	5.41	2.04		
IG_BH02_LG022	1.35	0.18	0.85	0.14	0.36	0.051	0.36	0.059	2.6	0.94	26.1	0.34	8	41	< 0.1	5.48	1.15		
IG_BH02_LG023	2.77	0.35	1.70	0.27	0.67	0.088	0.55	0.082	4.0	1.41	0.6	0.13	< 5	54	< 0.1	6.52	1.19		
IG_BH02_LG024	1.12	0.14	0.76	0.13	0.37	0.048	0.28	0.042	2.1	0.69	< 0.5	0.35	11	49	< 0.1	4.47	1.60		
IG_BH02_LG025	1.34	0.17	0.92	0.14	0.36	0.054	0.36	0.054	2.7	0.67	0.7	0.47	< 5	28	< 0.1	4.60	2.34		
IG_BH02_LG026	1.45	0.18	0.87	0.14	0.39	0.050	0.33	0.048	3.0	0.78	0.9	0.47	< 5	58	< 0.1	5.12	1.90		
IG_BH03_LG001	1.50	0.18	0.87	0.14	0.37	0.049	0.30	0.044	3.2	0.71	0.9	0.39	8	71	< 0.1	5.75	1.71	< 1	0.5
IG_BH03_LG002	1.54	0.19	1.01	0.16	0.44	0.062	0.36	0.050	3.2	0.84	< 0.5	0.34	6	66	< 0.1	6.20	2.63	< 1	0.5
IG_BH03_LG003	4.05	0.51	2.55	0.44	1.26	0.169	1.08	0.161	2.9	0.26	< 0.5	0.34	19	143	0.1	4.06	1.09		
IG_BH03_LG004	0.95	0.20	1.35	0.24	0.68	0.100	0.64	0.090	1.8	1.05	0.5	0.62	17	30	0.2	1.72	6.38		
IG_BH03_LG005	2.03	0.25	1.31	0.23	0.58	0.079	0.51	0.072	4.2	0.63	< 0.5	0.32	8	91	< 0.1	4.97	1.29		
IG_BH03_LG006	1.13	0.15	0.72	0.13	0.31	0.041	0.23	0.033	3.4	0.71	< 0.5	0.43	9	86	< 0.1	4.73	1.54		
IG_BH03_LG007	0.98	0.19	1.31	0.25	0.73	0.100	0.61	0.085	1.0	0.74	< 0.5	0.65	18	10	< 0.1	2.01	1.57		
IG_BH03_LG008	1.52	0.19	0.94	0.16	0.42	0.059	0.38	0.055	3.6	0.49	< 0.5	0.28	< 5	77	< 0.1	4.35	1.09		
IG_BH03_LG009	1.27	0.17	0.84	0.14	0.32	0.044	0.29	0.046	2.7	0.62	< 0.5	0.28	7	35	< 0.1	5.31	1.28		
IG_BH03_LG010	3.70	0.49	2.62	0.47	1.33	0.179	1.21	0.187	2.4	0.28	< 0.5	0.38	7	138	0.1	4.12	0.92		
IG_BH03_LG011	1.32	0.17	0.82	0.14	0.36	0.050	0.33	0.048	2.9	0.67	< 0.5	0.33	8	34	< 0.1	5.15	1.14		
IG_BH03_LG012	1.37	0.16	0.86	0.13	0.36	0.046	0.33	0.044	2.8	0.60	< 0.5	0.33	9	58	< 0.1	5.51	1.68	2	< 0.5
IG_BH03_LG013	1.43	0.19	0.99	0.16	0.43	0.063	0.40	0.057	3.7	0.45	< 0.5	0.23	6	73	< 0.1	4.30	1.15		
IG_BH03_LG014	1.33	0.17	0.85	0.13	0.37	0.053	0.33	0.050	3.2	1.21	< 0.5	0.35	7	53	< 0.1	5.60	2.43	< 1	0.5
IG_BH03_LG015	1.83	0.40	2.58	0.49	1.41	0.203	1.28	0.177	2.8	1.97	< 0.5	0.81	16	7	< 0.1	2.55	12.9		
IG_BH03_LG016	1.12	0.14	0.68	0.11	0.30	0.039	0.26	0.036	2.9	0.45	< 0.5	0.36	6	53	0.1	4.24	1.32		
IG_BH03_LG017	1.39	0.18	0.85	0.13	0.33	0.043	0.30	0.049	3.2	0.74	< 0.5	0.11	< 5	22	< 0.1	5.96	1.61		
IG_BH03_LG018	6.37	0.74	3.66	0.62	1.69	0.212	1.43	0.222	2.8	0.34	< 0.5	0.27	< 5	188	< 0.1	5.44	1.14		
IG_BH03_LG019	1.46	0.17	0.83	0.14	0.40	0.052	0.32	0.046	3.3	0.77	< 0.5	0.19	< 5	41	< 0.1	5.39	1.84		
IG_BH03_LG020	1.29	0.16	0.74	0.12	0.36	0.052	0.34	0.053	3.3	0.66	< 0.5	0.27	7	42	< 0.1	5.11	2.28		
IG_BH03_LG021	2.02	0.25	1.19	0.20	0.52	0.070	0.41	0.065	4.2	0.67	1.0	0.18	< 5	63	< 0.1	5.13	1.29		
IG_BH03_LG022	0.92	0.15	0.87	0.16	0.45	0.064	0.44	0.072	1.7	1.28	< 0.5	0.33	14	7	0.2	2.57	4.19		

Analyte Symbol	Os	Ir	Ru	Rh	Pt	Pd	Au	Mass	Au	As	Br	Cr	Ir	Sc	Se	Sb	Mass	B	Mass	C-Total	Total S	Cl	F
Unit Symbol	ppb	g	ppb	ppm	ppm	ppm	ppb	ppm	ppm	ppm	g	ppm	g	%	%	%	%						
Lower Limit	2	0.1	5	0.2	5	2	0.5		2	0.5	0.5	5	5	0.1	3	0.2		0.5		0.01	0.01	0.01	0.01
Method Code	NI-FINA	INAA	PGNAA	PGNAA	CS	CS	INAA	FUS-ISE															
NIST 694 Meas																							3.04
NIST 694 Cert																							3.2
DNC-1 Meas																							
DNC-1 Cert																							
GBW 07113 Meas																							
GBW 07113 Cert																							
SDC-1 Meas																							
SDC-1 Cert																							
SDC-1 Meas																							
SDC-1 Cert																							
MAG-1 (Depleted) Meas																							3.20
MAG-1 (Depleted) Cert																							3.10
TDB-1 Meas																							
TDB-1 Cert																							
SY-2 Meas																		86.5					
SY-2 Cert																		88.0					
SY-3 Meas																		107					
SY-3 Cert																		107					
BaSO4 Meas																						14.1	
BaSO4 Cert																						14.0	
NIST 1632c Meas																							0.10
NIST 1632c Cert																							0.110
W-2a Meas																							
W-2a Cert																							
Re 100 ppm Meas																							
Re 100 ppm Cert																							
Re 10 ppm Meas																							
Re 10 ppm Cert																							
DTS-2b Meas																							
DTS-2b Cert																							
SY-4 Meas																							
SY-4 Cert																							
Oreas 72a (4 Acid Digest) Meas																							
Oreas 72a (4 Acid Digest) Cert																							
Oreas 72a (4 Acid Digest) Meas																							
Oreas 72a (4 Acid Digest) Cert																							
BIR-1a Meas																							
BIR-1a Cert																							
ZW-C Meas																							
ZW-C Cert																							
SGR-1b Meas																					27.8	1.53	
SGR-1b Cert																					28	1.53	
OREAS 101b (Fusion) Meas																							
OREAS 101b (Fusion) Cert																							

Analyte Symbol	Os	Ir	Ru	Rh	Pt	Pd	Au	Mass	Au	As	Br	Cr	Ir	Sc	Se	Sb	Mass	B	Mass	C-Total	Total S	Cl	F	
Unit Symbol	ppb	g	ppb	ppm	ppm	ppm	ppb	ppm	ppm	ppm	g	ppm	g	%	%	%	%							
Lower Limit	2	0.1	5	0.2	5	2	0.5		2	0.5	0.5	5	5	0.1	3	0.2		0.5		0.01	0.01	0.01	0.01	
Method Code	NI-FINA	INAA	PGNAA	PGNAA	CS	CS	INAA	FUS-ISE																
OREAS 101b (4 Acid) Meas																								
OREAS 101b (4 Acid) Cert																								
OREAS 101b (4 Acid) Meas																								
OREAS 101b (4 Acid) Cert																								
OREAS 98 (4 Acid) Meas																								
OREAS 98 (4 Acid) Cert																								
OREAS 98 (4 Acid) Meas																								
OREAS 98 (4 Acid) Cert																								
OREAS 98 (4 Acid) Meas																								
OREAS 98 (4 Acid) Cert																								
NCS DC86318 Meas																								
NCS DC86318 Cert																								
SARM 3 Meas																								
SARM 3 Cert																								
DNC-1a Meas																								
DNC-1a Cert																								
DNC-1a Meas																								
DNC-1a Cert																								
OREAS 13b (4-Acid) Meas																								
OREAS 13b (4-Acid) Cert																								
OREAS 13b (Ni-S Fire Assay) Meas	13	17.1	72	40.1	188	139	208																	
OREAS 13b (Ni-S Fire Assay) Cert	12	17.9	78	43	204	134	201																	
USZ 42-2006 Meas																								
USZ 42-2006 Cert																								
GS311-4 Meas																					1.10	0.55		
GS311-4 Cert																					1.11	0.54		
OREAS 904 (4 ACID) Meas																								
OREAS 904 (4 ACID) Cert																								
OREAS 904 (4 ACID) Meas																								
OREAS 904 (4 ACID) Cert																								
SBC-1 Meas																								
SBC-1 Cert																								
SBC-1 Meas																								
SBC-1 Cert																								
I 100ppm Meas																								

Analyte Symbol	Os	Ir	Ru	Rh	Pt	Pd	Au	Mass	Au	As	Br	Cr	Ir	Sc	Se	Sb	Mass	B	Mass	C-Total	Total S	Cl	F
Unit Symbol	ppb	g	ppb	ppm	ppm	ppm	ppb	ppm	ppm	ppm	g	ppm	g	%	%	%	%						
Lower Limit	2	0.1	5	0.2	5	2	0.5		2	0.5	0.5	5	5	0.1	3	0.2		0.5		0.01	0.01	0.01	0.01
Method Code	NI-FINA	INAA	PGNAA	PGNAA	CS	CS	INAA	FUS-ISE															
I 100ppm Cert																							
I 100ppm Meas																							
I 100ppm Cert																							
OREAS 45d (4-Acid) Meas																							
OREAS 45d (4-Acid) Cert																							
OREAS 45d (4-Acid) Meas																							
OREAS 45d (4-Acid) Cert																							
AMIS 0367 (Ni-S) Meas					1860	903	198																
AMIS 0367 (Ni-S) Cert					1800.00	860.00	180.00																
REE-1 Meas																							
REE-1 Cert																							
AMIS 0414 (Ni-S) Meas					1930	1240																	
AMIS 0414 (Ni-S) Cert					2200	1370																	
OREAS 96 (4 Acid) Meas																							
OREAS 96 (4 Acid) Cert																							
OREAS 96 (4 Acid) Meas																							
OREAS 96 (4 Acid) Cert																							
OREAS 923 (4 Acid) Meas																							
OREAS 923 (4 Acid) Cert																							
OREAS 923 (4 Acid) Meas																							
OREAS 923 (4 Acid) Cert																							
OREAS 621 (4 Acid) Meas																							
OREAS 621 (4 Acid) Cert																							
OREAS 621 (4 Acid) Meas																							
OREAS 621 (4 Acid) Cert																							
Oreas 621 (Aqua Regia) Meas																							
Oreas 621 (Aqua Regia) Cert																							
OREAS 522 (4 Acid) Meas																							
OREAS 522 (4 Acid) Cert																							
OREAS 522 (4 Acid) Meas																							
OREAS 522 (4 Acid) Cert																							

Analyte Symbol	Os	Ir	Ru	Rh	Pt	Pd	Au	Mass	Au	As	Br	Cr	Ir	Sc	Se	Sb	Mass	B	Mass	C-Total	Total S	Cl	F
Unit Symbol	ppb	g	ppb	ppm	ppm	ppm	ppb	ppm	ppm	ppm	g	ppm	g	%	%	%	%						
Lower Limit	2	0.1	5	0.2	5	2	0.5		2	0.5	0.5	5	5	0.1	3	0.2		0.5		0.01	0.01	0.01	0.01
Method Code	NI-FINA	INAA	INAA	INAA	INAA	INAA	INAA	INAA	INAA	INAA	PGNAA	PGNAA	CS	CS	INAA	FUS-ISE							
OREAS 263 (Aqua Regia) Meas																							
OREAS 263 (Aqua Regia) Cert																							
DMMAS 122b Meas									760	1490		134		5.8		6.6							
DMMAS 122b Cert									715	1540		136		5.95		6.41							
GS316-3 Meas																				0.06	0.35		
GS316-3 Cert																				0.0600	0.340		
OREAS 130 (Aqua Regia) Meas																							
OREAS 130 (Aqua Regia) Cert																							
OREAS 153b (Aqua Regia) Meas																							
OREAS 153b (Aqua Regia) Cert																							
OREAS 153b (Aqua Regia) Meas																							
OREAS 153b (Aqua Regia) Cert																							
OREAS 153b (Aqua Regia) Meas																							
OREAS 153b (Aqua Regia) Cert																							
Oreas 623 (Aqua Regia) Meas																							
Oreas 623 (Aqua Regia) Cert																							
Oreas 623 (Aqua Regia) Meas																							
Oreas 623 (Aqua Regia) Cert																							
IG_BH02_LG015 Orig																							
IG_BH02_LG015 Dup																							
IG_BH02_LG023 Orig																							
IG_BH02_LG023 Dup																							
IG_BH03_LG006 Orig									< 2	< 0.5	6.8	15	< 5	2.2	< 3	< 0.2	35.0						
IG_BH03_LG006 Dup									< 2	1.4	6.2	19	< 5	2.1	< 3	< 0.2	33.0						
IG_BH03_LG008 Orig																							
IG_BH03_LG008 Dup																							
IG_BH03_LG012 Orig	< 2	< 0.1	< 5	< 0.2	< 5	< 2	< 0.5	25															
IG_BH03_LG012 Dup	< 2	< 0.1	< 5	< 0.2	< 5	< 2	0.5	25															
IG_BH03_LG014 Orig																							
IG_BH03_LG014 Dup																							



Analyte Symbol	Hg	SiO2	Al2O3	Fe2O3(T)	MnO	MgO	CaO	Na2O	K2O	TiO2	P2O5	Total	Sc	Be	V	V	Cr	Co	Ni	Ni	Cu	Cu	Zn
Unit Symbol	ppb	%	%	%	%	%	%	%	%	%	%	%	ppm	ppm	ppm	ppm	ppm	ppm	ppm	ppm	ppm	ppm	ppm
Lower Limit	5	0.01	0.01	0.01	0.001	0.01	0.01	0.01	0.01	0.001	0.01	0.01	1	1	5	5	20	1	20	1	1	10	1
Method Code	1G	FUS-ICP	FUS-ICP	FUS-ICP	FUS-ICP	FUS-ICP	FUS-ICP	FUS-ICP	FUS-ICP	FUS-ICP	FUS-ICP	FUS-ICP	FUS-ICP	FUS-ICP	FUS-MS	FUS-ICP	FUS-MS	FUS-MS	FUS-MS	TD-ICP	TD-ICP	FUS-MS	TD-ICP
NIST 694 Meas		11.25	1.88	0.73	0.010	0.34	43.02	0.88	0.55	0.120	30.22					1654							
NIST 694 Cert		11.2	1.80	0.790	0.0116	0.330	43.6	0.860	0.510	0.110	30.2					1740							
DNC-1 Meas		47.12	18.42	9.72	0.150	10.13	11.40	1.94	0.23	0.480	0.06		31			158							
DNC-1 Cert		47.15	18.34	9.97	0.150	10.13	11.49	1.890	0.234	0.480	0.070		31			148							
GBW 07113 Meas		70.52	12.66	3.18	0.140	0.14	0.58	2.48	5.41	0.280	0.04		5	4		< 5							
GBW 07113 Cert		72.8	13.0	3.21	0.140	0.160	0.590	2.57	5.43	0.300	0.0500		5.00	4.00		5.00							
SDC-1 Meas																					35	30	104
SDC-1 Cert																					38.0	30.000	103.00
SDC-1 Meas																					35	28	104
SDC-1 Cert																					38.0	30.000	103.00
MAG-1 (Depleted) Meas																							
MAG-1 (Depleted) Cert																							
TDB-1 Meas															475		250		90				340
TDB-1 Cert															471		251		92				323
SY-2 Meas																							
SY-2 Cert																							
SY-3 Meas																							
SY-3 Cert																							
BaSO4 Meas																							
BaSO4 Cert																							
NIST 1632c Meas																							
NIST 1632c Cert																							
W-2a Meas		54.27	15.73	10.93	0.170	6.45	11.29	2.30	0.64	1.090	0.13		36	< 1	270	286	90	43	70				100
W-2a Cert		52.4	15.4	10.7	0.163	6.37	10.9	2.14	0.626	1.06	0.140		36.0	1.30	262	262	92.0	43.0	70.0				110
Re 100 ppm Meas																							
Re 100 ppm Cert																							
Re 10 ppm Meas																							
Re 10 ppm Cert																							
DTS-2b Meas															20		> 10000	126	3630				
DTS-2b Cert															22.0		15500	120	3780				
SY-4 Meas		49.99	20.50	6.21	0.110	0.50	8.13	6.95	1.67	0.290	0.13		1	3		7							
SY-4 Cert		49.9	20.69	6.21	0.108	0.54	8.05	7.10	1.66	0.287	0.131		1.1	2.6		8.0							
Oreas 72a (4 Acid Digest) Meas																					6860	333	
Oreas 72a (4 Acid Digest) Cert																					6930.000	316	
Oreas 72a (4 Acid Digest) Meas																					6590	315	
Oreas 72a (4 Acid Digest) Cert																					6930.000	316	
BIR-1a Meas		47.92	15.63	11.28	0.170	9.57	13.52	1.83	0.02	0.970	0.03		44	< 1		339							
BIR-1a Cert		47.96	15.50	11.30	0.175	9.700	13.30	1.82	0.030	0.96	0.021		44	0.58		310							
ZW-C Meas																							
ZW-C Cert																							
SGR-1b Meas																							
SGR-1b Cert																							
OREAS 101b (Fusion) Meas															77			45					410
OREAS 101b															80			47					420

Analyte Symbol	Hg	SiO2	Al2O3	Fe2O3(T)	MnO	MgO	CaO	Na2O	K2O	TiO2	P2O5	Total	Sc	Be	V	V	Cr	Co	Ni	Ni	Cu	Cu	Zn
Unit Symbol	ppb	%	%	%	%	%	%	%	%	%	%	%	ppm	ppm	ppm	ppm	ppm	ppm	ppm	ppm	ppm	ppm	ppm
Lower Limit	5	0.01	0.01	0.01	0.001	0.01	0.01	0.01	0.01	0.001	0.01	0.01	1	1	5	5	20	1	20	1	1	10	1
Method Code	1G	FUS-ICP	FUS-ICP	FUS-ICP	FUS-ICP	FUS-ICP	FUS-ICP	FUS-ICP	FUS-ICP	FUS-ICP	FUS-ICP	FUS-ICP	FUS-ICP	FUS-ICP	FUS-MS	FUS-ICP	FUS-MS	FUS-MS	FUS-MS	TD-ICP	TD-ICP	FUS-MS	TD-ICP
(Fusion) Cert																							
OREAS 101b (4 Acid) Meas																					9	428	
OREAS 101b (4 Acid) Cert																					8.2	412	
OREAS 101b (4 Acid) Meas																					10	408	
OREAS 101b (4 Acid) Cert																					8.2	412	
OREAS 98 (4 Acid) Meas																					> 10000		1530
OREAS 98 (4 Acid) Cert																					14800	0.0	1360
OREAS 98 (4 Acid) Meas																					> 10000		1300
OREAS 98 (4 Acid) Cert																					14800	0.0	1360
OREAS 98 (4 Acid) Meas																					> 10000		1230
OREAS 98 (4 Acid) Cert																					14800	0.0	1360
NCS DC86318 Meas																							
NCS DC86318 Cert																							
SARM 3 Meas																							
SARM 3 Cert																							
DNC-1a Meas																					255	99	63
DNC-1a Cert																					247	100	70
DNC-1a Meas																					239	94	57
DNC-1a Cert																					247	100	70
OREAS 13b (4-Acid) Meas																					2290	2450	151
OREAS 13b (4-Acid) Cert																					2247.0	2327.0	133
OREAS 13b (Ni-S Fire Assay) Meas																					000	000	
OREAS 13b (Ni-S Fire Assay) Cert																							
USZ 42-2006 Meas															130			5	< 20				20
USZ 42-2006 Cert															115.00			7.89	13.18				27.37
GS311-4 Meas																							
GS311-4 Cert																							
OREAS 904 (4 ACID) Meas																					45	6380	27
OREAS 904 (4 ACID) Cert																					40.1	6120	26.3
OREAS 904 (4 ACID) Meas																					43	6410	28
OREAS 904 (4 ACID) Cert																					40.1	6120	26.3
SBC-1 Meas																					86	28	193
SBC-1 Cert																					83	31.0	186
SBC-1 Meas																					83	30	194

Analyte Symbol	Hg	SiO2	Al2O3	Fe2O3(T)	MnO	MgO	CaO	Na2O	K2O	TiO2	P2O5	Total	Sc	Be	V	V	Cr	Co	Ni	Ni	Cu	Cu	Zn	
Unit Symbol	ppb	%	%	%	%	%	%	%	%	%	%	%	ppm	ppm	ppm	ppm	ppm	ppm	ppm	ppm	ppm	ppm	ppm	
Lower Limit	5	0.01	0.01	0.01	0.001	0.01	0.01	0.01	0.01	0.001	0.01	0.01	1	1	5	5	20	1	20	1	1	10	1	
Method Code	1G	FUS-ICP	FUS-ICP	FUS-ICP	FUS-ICP	FUS-ICP	FUS-ICP	FUS-ICP	FUS-ICP	FUS-ICP	FUS-ICP	FUS-ICP	FUS-ICP	FUS-ICP	FUS-MS	FUS-ICP	FUS-MS	FUS-MS	FUS-MS	TD-ICP	TD-ICP	FUS-MS	TD-ICP	
SBC-1 Cert																					83	31.0	186	
I 100ppm Meas																								
I 100ppm Cert																								
I 100ppm Meas																								
I 100ppm Cert																								
OREAS 45d (4-Acid) Meas																					244	386	47	
OREAS 45d (4-Acid) Cert																					231.0	371	45.7	
OREAS 45d (4-Acid) Meas																					244	380	48	
OREAS 45d (4-Acid) Cert																					231.0	371	45.7	
AMIS 0367 (Ni-S) Meas																								
AMIS 0367 (Ni-S) Cert																								
REE-1 Meas																	290		30				80	
REE-1 Cert																	277		24.7				79.7	
AMIS 0414 (Ni-S) Meas																								
AMIS 0414 (Ni-S) Cert																								
OREAS 96 (4 Acid) Meas																						> 10000	434	
OREAS 96 (4 Acid) Cert																						39300	457	
OREAS 96 (4 Acid) Meas																						> 10000	458	
OREAS 96 (4 Acid) Cert																						39300	457	
OREAS 923 (4 Acid) Meas																						37	4540	353
OREAS 923 (4 Acid) Cert																						35.8	4230	345
OREAS 923 (4 Acid) Meas																						37	4530	363
OREAS 923 (4 Acid) Cert																						35.8	4230	345
OREAS 621 (4 Acid) Meas																						29	3670	> 10000
OREAS 621 (4 Acid) Cert																						26.2	3630	52200
OREAS 621 (4 Acid) Meas																						28	3590	> 10000
OREAS 621 (4 Acid) Cert																						26.2	3630	52200
Oreas 621 (Aqua Regia) Meas	3470																							
Oreas 621 (Aqua Regia) Cert	3930																							
OREAS 522 (4 Acid) Meas																						77	8830	28
OREAS 522 (4 Acid) Cert																						70.0	9160	30.2
OREAS 522 (4																						73	8880	30

Analyte Symbol	Hg	SiO2	Al2O3	Fe2O3(T)	MnO	MgO	CaO	Na2O	K2O	TiO2	P2O5	Total	Sc	Be	V	V	Cr	Co	Ni	Ni	Cu	Cu	Zn	
Unit Symbol	ppb	%	%	%	%	%	%	%	%	%	%	%	ppm	ppm	ppm	ppm	ppm	ppm	ppm	ppm	ppm	ppm	ppm	
Lower Limit	5	0.01	0.01	0.01	0.001	0.01	0.01	0.01	0.01	0.001	0.01	0.01	1	1	5	5	20	1	20	1	1	10	1	
Method Code	1G	FUS-ICP	FUS-ICP	FUS-ICP	FUS-ICP	FUS-ICP	FUS-ICP	FUS-ICP	FUS-ICP	FUS-ICP	FUS-ICP	FUS-ICP	FUS-ICP	FUS-ICP	FUS-MS	FUS-ICP	FUS-MS	FUS-MS	FUS-MS	TD-ICP	TD-ICP	FUS-MS	TD-ICP	
Acid) Meas																								
OREAS 522 (4 Acid) Cert																				70.0	9160		30.2	
OREAS 263 (Aqua Regia) Meas	179																							
OREAS 263 (Aqua Regia) Cert	170																							
DMMAS 122b Meas																								
DMMAS 122b Cert																								
GS316-3 Meas																								
GS316-3 Cert																								
OREAS 130 (Aqua Regia) Meas	688																							
OREAS 130 (Aqua Regia) Cert	670																							
OREAS 153b (Aqua Regia) Meas	66																							
OREAS 153b (Aqua Regia) Cert	66.0																							
OREAS 153b (Aqua Regia) Meas	67																							
OREAS 153b (Aqua Regia) Cert	66.0																							
Oreas 623 (Aqua Regia) Meas	793																							
Oreas 623 (Aqua Regia) Cert	830																							
Oreas 623 (Aqua Regia) Meas	779																							
Oreas 623 (Aqua Regia) Cert	830																							
IG_BH02_LG015 Orig		42.59	11.90	10.40	0.160	10.32	11.47	1.96	3.25	0.942	0.47	99.18	39	1	231	235	750	45	230				80	
IG_BH02_LG015 Dup		42.95	12.11	10.21	0.158	10.17	11.28	2.02	3.28	0.938	0.46	99.30	38	1	229	231	750	45	230				80	
IG_BH02_LG023 Orig																					5	37		48
IG_BH02_LG023 Dup																					4	37		48
IG_BH03_LG006 Orig		73.01	14.80	1.69	0.024	0.38	1.32	4.29	3.37	0.166	0.05	100.4	2	1	18	18	< 20	2	< 20				20	
IG_BH03_LG006 Dup		71.51	14.58	1.65	0.023	0.36	1.30	4.25	3.29	0.163	0.05	98.44	2	1	17	18	20	2	< 20				20	
IG_BH03_LG008 Orig																					7	15		63
IG_BH03_LG008 Dup																					6	16		70
IG_BH03_LG012 Orig																								
IG_BH03_LG012 Dup																								

Analyte Symbol	Hg	SiO2	Al2O3	Fe2O3(T)	MnO	MgO	CaO	Na2O	K2O	TiO2	P2O5	Total	Sc	Be	V	V	Cr	Co	Ni	Ni	Cu	Cu	Zn
Unit Symbol	ppb	%	%	%	%	%	%	%	%	%	%	%	ppm	ppm	ppm	ppm	ppm	ppm	ppm	ppm	ppm	ppm	ppm
Lower Limit	5	0.01	0.01	0.01	0.001	0.01	0.01	0.01	0.01	0.001	0.01	0.01	1	1	5	5	20	1	20	1	1	10	1
Method Code	1G	FUS-ICP	FUS-ICP	FUS-ICP	FUS-ICP	FUS-ICP	FUS-ICP	FUS-ICP	FUS-ICP	FUS-ICP	FUS-ICP	FUS-ICP	FUS-ICP	FUS-ICP	FUS-MS	FUS-ICP	FUS-MS	FUS-MS	FUS-MS	TD-ICP	TD-ICP	FUS-MS	TD-ICP
IG_BH03_LG014 Orig	< 5																						
IG_BH03_LG014 Dup	< 5																						
IG_BH03_LG021 Orig																					6	23	69
IG_BH03_LG021 Dup																					8	24	68
Method Blank	< 5																						
Method Blank	< 5																						
Method Blank	< 5																						
Method Blank	< 5																						
Method Blank		0.02	< 0.01	0.01	0.003	< 0.01	< 0.01	< 0.01	< 0.01	< 0.001	< 0.01		< 1	< 1	< 5	< 5	< 20	< 1	< 20				< 10
Method Blank		< 0.01	< 0.01	0.01	0.003	< 0.01	< 0.01	< 0.01	< 0.01	< 0.001	< 0.01		< 1	< 1	< 5								
Method Blank																							
Method Blank																							
Method Blank																					< 1	< 1	< 1
Method Blank																					< 1	< 1	< 1
Method Blank																					< 1	< 1	< 1
Method Blank																					< 1	< 1	< 1
Method Blank																					< 1	< 1	< 1
Method Blank																					< 1	< 1	< 1
Method Blank																					1	< 1	< 1
Method Blank																					< 1	< 1	< 1
Method Blank																							
Method Blank																							

Analyte Symbol	Zn	Cd	S	Ga	Ge	As	Rb	Sr	Sr	Y	Y	Zr	Nb	Mo	Ag	In	Sn	Sb	Cs	Ba	Ba	La	Ce
Unit Symbol	ppm	ppm	%	ppm	ppm	ppm	ppm	ppm	ppm	ppm	ppm	ppm	ppm	ppm	ppm	ppm	ppm	ppm	ppm	ppm	ppm	ppm	ppm
Lower Limit	30	0.5	0.001	1	0.5	5	1	2	2	0.5	1	1	0.2	2	0.3	0.1	1	0.2	0.1	3	2	0.05	0.05
Method Code	FUS-MS	TD-ICP	TD-ICP	FUS-MS	FUS-MS	FUS-MS	FUS-MS	FUS-MS	FUS-ICP	FUS-MS	FUS-ICP	FUS-ICP	FUS-MS	FUS-MS	TD-ICP	FUS-MS	FUS-MS	FUS-MS	FUS-MS	FUS-MS	FUS-ICP	FUS-MS	FUS-MS
NIST 694 Meas																							
NIST 694 Cert																							
DNC-1 Meas										144		16	35									108	
DNC-1 Cert										144.0		18.0	38									118	
GBW 07113 Meas										41		44	384									497	
GBW 07113 Cert										43.0		43.0	403									506	
SDC-1 Meas																							
SDC-1 Cert																							
SDC-1 Meas																							
SDC-1 Cert																							
MAG-1 (Depleted) Meas																							
MAG-1 (Depleted) Cert																							
TDB-1 Meas	150						21			34.6										233		18.3	41.8
TDB-1 Cert	155						23			36										241		17	41
SY-2 Meas																							
SY-2 Cert																							
SY-3 Meas																							
SY-3 Cert																							
BaSO4 Meas																							
BaSO4 Cert																							
NIST 1632c Meas																							
NIST 1632c Cert																							
W-2a Meas				17	1.5		20	194	201	20.7	20	92		< 2				0.8		172	182	10.9	23.2
W-2a Cert				17.0	1.00		21.0	190	190	24.0	24.0	94.0		0.600				0.790		182	182	10.0	23.0
Re 100 ppm Meas																							
Re 100 ppm Cert																							
Re 10 ppm Meas																							
Re 10 ppm Cert																							
DTS-2b Meas																							
DTS-2b Cert																							
SY-4 Meas	90			33			55	1160	1197	121	116	545	13.4						1.5	343	354	62.3	133
SY-4 Cert	93			35			55.0	1191	1191	119	119	517	13						1.5	340	340	58	122
Oreas 72a (4 Acid Digest) Meas			1.77																				
Oreas 72a (4 Acid Digest) Cert			1.74																				
Oreas 72a (4 Acid Digest) Meas			1.62																				
Oreas 72a (4 Acid Digest) Cert			1.74																				
BIR-1a Meas									109		14	14										8	
BIR-1a Cert									110		16	18										6	
ZW-C Meas	1030			91			> 1000						211				> 1000	4.4	261			32.4	
ZW-C Cert	1050			99			8500						198				1300	4.2	260			30.0	
SGR-1b Meas																							
SGR-1b Cert																							
OREAS 101b (Fusion) Meas										175				19								828	1330
OREAS 101b (Fusion) Cert										178				21								789	1331

Analyte Symbol	Zn	Cd	S	Ga	Ge	As	Rb	Sr	Sr	Y	Y	Zr	Nb	Mo	Ag	In	Sn	Sb	Cs	Ba	Ba	La	Ce
Unit Symbol	ppm	ppm	%	ppm	ppm	ppm	ppm	ppm	ppm	ppm	ppm	ppm	ppm	ppm	ppm	ppm	ppm	ppm	ppm	ppm	ppm	ppm	ppm
Lower Limit	30	0.5	0.001	1	0.5	5	1	2	2	0.5	1	1	0.2	2	0.3	0.1	1	0.2	0.1	3	2	0.05	0.05
Method Code	FUS-MS	TD-ICP	TD-ICP	FUS-MS	FUS-MS	FUS-MS	FUS-MS	FUS-MS	FUS-ICP	FUS-MS	FUS-ICP	FUS-ICP	FUS-MS	FUS-MS	TD-ICP	FUS-MS	FUS-MS	FUS-MS	FUS-MS	FUS-MS	FUS-ICP	FUS-MS	FUS-MS
OREAS 101b (4 Acid) Meas																							
OREAS 101b (4 Acid) Cert																							
OREAS 101b (4 Acid) Meas																							
OREAS 101b (4 Acid) Cert																							
OREAS 98 (4 Acid) Meas			18.9												48.8								
OREAS 98 (4 Acid) Cert			15.5												45.1								
OREAS 98 (4 Acid) Meas			15.8												41.3								
OREAS 98 (4 Acid) Cert			15.5												45.1								
OREAS 98 (4 Acid) Meas			14.8												38.7								
OREAS 98 (4 Acid) Cert			15.5												45.1								
NCS DC86318 Meas							379			> 10000												1960	413
NCS DC86318 Cert							369.42			17008												1960	432
SARM 3 Meas													> 1000										
SARM 3 Cert													978										
DNC-1a Meas																							
DNC-1a Cert																							
DNC-1a Meas																							
DNC-1a Cert																							
OREAS 13b (4-Acid) Meas			1.22												0.8								
OREAS 13b (4-Acid) Cert			1.2												0.86								
OREAS 13b (Ni-S Fire Assay) Meas																							
OREAS 13b (Ni-S Fire Assay) Cert																							
USZ 42-2006 Meas	480						63	5220		174			33.0	36						321		> 2000	> 3000
USZ 42-2006 Cert	469						67.12	4900		167			31.00	34.40						307		21100	27600
GS311-4 Meas																							
GS311-4 Cert																							
OREAS 904 (4 ACID) Meas			0.063												0.7								
OREAS 904 (4 ACID) Cert			0.0630												0.551								
OREAS 904 (4 ACID) Meas			0.061												0.6								
OREAS 904 (4 ACID) Cert			0.0630												0.551								
SBC-1 Meas		< 0.5																					
SBC-1 Cert		0.40																					
SBC-1 Meas		< 0.5																					
SBC-1 Cert		0.40																					
l 100ppm Meas																							

Analyte Symbol	Zn	Cd	S	Ga	Ge	As	Rb	Sr	Sr	Y	Y	Zr	Nb	Mo	Ag	In	Sn	Sb	Cs	Ba	Ba	La	Ce
Unit Symbol	ppm	ppm	%	ppm	ppm	ppm	ppm	ppm	ppm	ppm	ppm	ppm	ppm	ppm	ppm	ppm	ppm	ppm	ppm	ppm	ppm	ppm	ppm
Lower Limit	30	0.5	0.001	1	0.5	5	1	2	2	0.5	1	1	0.2	2	0.3	0.1	1	0.2	0.1	3	2	0.05	0.05
Method Code	FUS-MS	TD-ICP	TD-ICP	FUS-MS	FUS-MS	FUS-MS	FUS-MS	FUS-MS	FUS-ICP	FUS-MS	FUS-ICP	FUS-ICP	FUS-MS	FUS-MS	TD-ICP	FUS-MS	FUS-MS	FUS-MS	FUS-MS	FUS-MS	FUS-ICP	FUS-MS	FUS-MS
I 100ppm Cert																							
I 100ppm Meas																							
I 100ppm Cert																							
OREAS 45d (4-Acid) Meas			0.047																				
OREAS 45d (4-Acid) Cert			0.049																				
OREAS 45d (4-Acid) Meas			0.046																				
OREAS 45d (4-Acid) Cert			0.049																				
AMIS 0367 (Ni-S) Meas																							
AMIS 0367 (Ni-S) Cert																							
REE-1 Meas						116	> 1000	132		5640							498		1.1	103		1700	> 3000
REE-1 Cert						124	1050	129		5480							498		1.07	100.1		1661	3960
AMIS 0414 (Ni-S) Meas																							
AMIS 0414 (Ni-S) Cert																							
OREAS 96 (4 Acid) Meas			4.08													10.9							
OREAS 96 (4 Acid) Cert			4.19													11.5							
OREAS 96 (4 Acid) Meas			4.35													11.1							
OREAS 96 (4 Acid) Cert			4.19													11.5							
OREAS 923 (4 Acid) Meas		< 0.5	0.714													1.6							
OREAS 923 (4 Acid) Cert		0.420	0.691													1.60							
OREAS 923 (4 Acid) Meas		1.1	0.693													1.7							
OREAS 923 (4 Acid) Cert		0.420	0.691													1.60							
OREAS 621 (4 Acid) Meas		288	4.50													67.5							
OREAS 621 (4 Acid) Cert		284	4.48													69.0							
OREAS 621 (4 Acid) Meas		295	4.61													67.7							
OREAS 621 (4 Acid) Cert		284	4.48													69.0							
Oreas 621 (Aqua Regia) Meas																							
Oreas 621 (Aqua Regia) Cert																							
OREAS 522 (4 Acid) Meas			2.36													1.2							
OREAS 522 (4 Acid) Cert			2.50													1.31							
OREAS 522 (4 Acid) Meas			2.48													1.4							
OREAS 522 (4 Acid) Cert			2.50													1.31							

Analyte Symbol	Zn	Cd	S	Ga	Ge	As	Rb	Sr	Sr	Y	Y	Zr	Nb	Mo	Ag	In	Sn	Sb	Cs	Ba	Ba	La	Ce
Unit Symbol	ppm	ppm	%	ppm	ppm	ppm	ppm	ppm	ppm	ppm	ppm	ppm	ppm	ppm	ppm	ppm	ppm	ppm	ppm	ppm	ppm	ppm	ppm
Lower Limit	30	0.5	0.001	1	0.5	5	1	2	2	0.5	1	1	0.2	2	0.3	0.1	1	0.2	0.1	3	2	0.05	0.05
Method Code	FUS-MS	TD-ICP	TD-ICP	FUS-MS	FUS-MS	FUS-MS	FUS-MS	FUS-MS	FUS-ICP	FUS-MS	FUS-ICP	FUS-ICP	FUS-MS	FUS-MS	TD-ICP	FUS-MS	FUS-MS	FUS-MS	FUS-MS	FUS-MS	FUS-ICP	FUS-MS	FUS-MS
OREAS 263 (Aqua Regia) Meas																							
OREAS 263 (Aqua Regia) Cert																							
DMMAS 122b Meas																							
DMMAS 122b Cert																							
GS316-3 Meas																							
GS316-3 Cert																							
OREAS 130 (Aqua Regia) Meas																							
OREAS 130 (Aqua Regia) Cert																							
OREAS 153b (Aqua Regia) Meas																							
OREAS 153b (Aqua Regia) Cert																							
OREAS 153b (Aqua Regia) Meas																							
OREAS 153b (Aqua Regia) Cert																							
Oreas 623 (Aqua Regia) Meas																							
Oreas 623 (Aqua Regia) Cert																							
Oreas 623 (Aqua Regia) Meas																							
Oreas 623 (Aqua Regia) Cert																							
IG_BH02_LG015 Orig	80			14	1.4	< 5	103	818	789	20.2	19	125	6.3	< 2		0.1	1	< 0.2	6.4	638	653	46.3	102
IG_BH02_LG015 Dup	80			14	1.4	< 5	105	813	789	20.1	18	125	6.4	< 2		< 0.1	1	< 0.2	6.5	640	657	45.5	101
IG_BH02_LG023 Orig		< 0.5	0.003													0.3							
IG_BH02_LG023 Dup		< 0.5	0.003													0.4							
IG_BH03_LG006 Orig	30			20	0.9	< 5	108	167	172	3.6	3	106	5.5	< 2		< 0.1	1	< 0.2	1.7	889	937	15.0	27.5
IG_BH03_LG006 Dup	30			20	0.8	< 5	110	169	170	3.6	4	95	4.4	< 2		< 0.1	1	< 0.2	1.8	894	922	15.2	28.4
IG_BH03_LG008 Orig		< 0.5	0.005													0.4							
IG_BH03_LG008 Dup		< 0.5	0.005													0.4							
IG_BH03_LG012 Orig																							
IG_BH03_LG012 Dup																							
IG_BH03_LG014 Orig																							
IG_BH03_LG014 Dup																							

Analyte Symbol	Zn	Cd	S	Ga	Ge	As	Rb	Sr	Sr	Y	Y	Zr	Nb	Mo	Ag	In	Sn	Sb	Cs	Ba	Ba	La	Ce
Unit Symbol	ppm	ppm	%	ppm	ppm	ppm	ppm	ppm	ppm	ppm	ppm	ppm	ppm	ppm	ppm	ppm	ppm	ppm	ppm	ppm	ppm	ppm	ppm
Lower Limit	30	0.5	0.001	1	0.5	5	1	2	2	0.5	1	1	0.2	2	0.3	0.1	1	0.2	0.1	3	2	0.05	0.05
Method Code	FUS-MS	TD-ICP	TD-ICP	FUS-MS	FUS-MS	FUS-MS	FUS-MS	FUS-MS	FUS-ICP	FUS-MS	FUS-ICP	FUS-ICP	FUS-MS	FUS-MS	TD-ICP	FUS-MS	FUS-MS	FUS-MS	FUS-MS	FUS-MS	FUS-ICP	FUS-MS	FUS-MS
IG_BH03_LG021 Orig		< 0.5	0.017												0.3								
IG_BH03_LG021 Dup		< 0.5	0.013												< 0.3								
Method Blank																							
Method Blank																							
Method Blank																							
Method Blank																							
Method Blank	< 30			< 1	< 0.5	< 5	< 1	< 2	< 2	< 0.5	< 1	3	< 0.2	< 2		< 0.1	< 1	< 0.2	< 0.1	< 3	< 2	< 0.05	< 0.05
Method Blank									< 2		< 1	2										< 2	
Method Blank																							
Method Blank																							
Method Blank		< 0.5	0.001												< 0.3								
Method Blank		< 0.5	0.001												< 0.3								
Method Blank		< 0.5	< 0.001												< 0.3								
Method Blank		< 0.5	0.001												< 0.3								
Method Blank		< 0.5	0.005												< 0.3								
Method Blank		< 0.5	0.002												< 0.3								
Method Blank		< 0.5	< 0.001												< 0.3								
Method Blank		< 0.5	0.002												< 0.3								
Method Blank																							
Method Blank																							

Analyte Symbol	Pr	Nd	Sm	Eu	Gd	Tb	Dy	Ho	Er	Tm	Yb	Lu	Hf	Ta	W	Tl	Pb	Li	Bi	Th	U	Re	I
Unit Symbol	ppm	ppm	ppm																				
Lower Limit	0.01	0.05	0.01	0.005	0.01	0.01	0.01	0.01	0.01	0.005	0.01	0.002	0.1	0.01	0.5	0.05	5	1	0.1	0.05	0.01	1	0.5
Method Code	FUS-MS	TD-ICP	TD-ICP	FUS-MS	FUS-MS	FUS-MS	INAA	INAA															
NIST 694 Meas																							
NIST 694 Cert																							
DNC-1 Meas																							
DNC-1 Cert																							
GBW 07113 Meas																							
GBW 07113 Cert																							
SDC-1 Meas																	22	36					
SDC-1 Cert																	25.00	34					
SDC-1 Meas																	21	35					
SDC-1 Cert																	25.00	34					
MAG-1 (Depleted) Meas																							
MAG-1 (Depleted) Cert																							
TDB-1 Meas		25.1		2.10							3.20										2.70		
TDB-1 Cert		23		2.1							3.4										2.7		
SY-2 Meas																							
SY-2 Cert																							
SY-3 Meas																							
SY-3 Cert																							
BaSO4 Meas																							
BaSO4 Cert																							
NIST 1632c Meas																							
NIST 1632c Cert																							
W-2a Meas		12.8	3.40	1.10			3.80	0.76			1.90			0.47	0.5	0.05			< 0.1	2.30	0.51		
W-2a Cert		13.0	3.30	1.00			3.60	0.760			2.10			0.500	0.300	0.200			0.0300	2.40	0.530		
Re 100 ppm Meas																							100
Re 100 ppm Cert																							100
Re 10 ppm Meas																							11
Re 10 ppm Cert																							10.0
DTS-2b Meas																							
DTS-2b Cert																							
SY-4 Meas	15.2	58.4	13.1	2.02	13.8	2.66	17.5	4.34	13.7	2.28	14.9	2.22	10.4							1.30	0.80		
SY-4 Cert	15.0	57	12.7	2.00	14.0	2.6	18.2	4.3	14.2	2.3	14.8	2.1	10.6							1.4	0.8		
Oreas 72a (4 Acid Digest) Meas																							
Oreas 72a (4 Acid Digest) Cert																							
Oreas 72a (4 Acid Digest) Meas																							
Oreas 72a (4 Acid Digest) Cert																							
BIR-1a Meas																							
BIR-1a Cert																							
ZW-C Meas	9.90	26.5			4.50									84.2	319	34.0					19.2		
ZW-C Cert	9.5	25.0			4.70									82	320	34					20.0		
SGR-1b Meas																							
SGR-1b Cert																							
OREAS 101b (Fusion) Meas	128	388	50.0	8.03		5.05	30.4	6.10	18.7	2.77	17.3	2.66								36.1	390		
OREAS 101b (Fusion) Cert	127	378	48	7.77		5.37	32.1	6.34	18.7	2.66	17.6	2.58								37.1	396		

Analyte Symbol	Pr	Nd	Sm	Eu	Gd	Tb	Dy	Ho	Er	Tm	Yb	Lu	Hf	Ta	W	Tl	Pb	Li	Bi	Th	U	Re	I
Unit Symbol	ppm	ppm	ppm																				
Lower Limit	0.01	0.05	0.01	0.005	0.01	0.01	0.01	0.01	0.01	0.005	0.01	0.002	0.1	0.01	0.5	0.05	5	1	0.1	0.05	0.01	1	0.5
Method Code	FUS-MS	TD-ICP	TD-ICP	FUS-MS	FUS-MS	FUS-MS	INAA	INAA															
OREAS 101b (4 Acid) Meas																	23						
OREAS 101b (4 Acid) Cert																	23						
OREAS 101b (4 Acid) Meas																	21						
OREAS 101b (4 Acid) Cert																	23						
OREAS 98 (4 Acid) Meas																	363						
OREAS 98 (4 Acid) Cert																	345						
OREAS 98 (4 Acid) Meas																	311						
OREAS 98 (4 Acid) Cert																	345						
OREAS 98 (4 Acid) Meas																	293						
OREAS 98 (4 Acid) Cert																	345						
NCS DC86318 Meas	713	> 2000	> 1000	18.1	> 1000	456	> 1000	542	> 1000	256		244								64.6			
NCS DC86318 Cert	737	3429	1725	18.91	2168	468	3224	560	1750	271		264								67.0			
SARM 3 Meas																							
SARM 3 Cert																							
DNC-1a Meas																	< 5		5				
DNC-1a Cert																	6.3		5.2				
DNC-1a Meas																	< 5		5				
DNC-1a Cert																	6.3		5.2				
OREAS 13b (4-Acid) Meas																							
OREAS 13b (4-Acid) Cert																							
OREAS 13b (Ni-S Fire Assay) Meas																							
OREAS 13b (Ni-S Fire Assay) Cert																							
USZ 42-2006 Meas	> 1000	> 2000	535	88.0							16.9										991		
USZ 42-2006 Cert	2300	6500	539	87.22							17.85										946		
GS311-4 Meas																							
GS311-4 Cert																							
OREAS 904 (4 ACID) Meas																	8		16				
OREAS 904 (4 ACID) Cert																	10.6		16.7				
OREAS 904 (4 ACID) Meas																	7		16				
OREAS 904 (4 ACID) Cert																	10.6		16.7				
SBC-1 Meas																	30		159				
SBC-1 Cert																	35.0		163				
SBC-1 Meas																	29		154				
SBC-1 Cert																	35.0		163				
I 100ppm Meas																							98.8

Analyte Symbol	Pr	Nd	Sm	Eu	Gd	Tb	Dy	Ho	Er	Tm	Yb	Lu	Hf	Ta	W	Tl	Pb	Li	Bi	Th	U	Re	I
Unit Symbol	ppm	ppm	ppm																				
Lower Limit	0.01	0.05	0.01	0.005	0.01	0.01	0.01	0.01	0.01	0.005	0.01	0.002	0.1	0.01	0.5	0.05	5	1	0.1	0.05	0.01	1	0.5
Method Code	FUS-MS	TD-ICP	TD-ICP	FUS-MS	FUS-MS	FUS-MS	INAA	INAA															
I 100ppm Cert																							100
I 100ppm Meas																							101
I 100ppm Cert																							100
OREAS 45d (4-Acid) Meas																	22	22					
OREAS 45d (4-Acid) Cert																	21.8	21.5					
OREAS 45d (4-Acid) Meas																	21	22					
OREAS 45d (4-Acid) Cert																	21.8	21.5					
AMIS 0367 (Ni-S) Meas																							
AMIS 0367 (Ni-S) Cert																							
REE-1 Meas	454	1530	416	24.9	421	108	873	208	708	113	693		467							771	144		
REE-1 Cert	435	1456	381	23.5	433	106	847	208	701	106	678		479							719	137		
AMIS 0414 (Ni-S) Meas																							
AMIS 0414 (Ni-S) Cert																							
OREAS 96 (4 Acid) Meas																	91						
OREAS 96 (4 Acid) Cert																	101						
OREAS 96 (4 Acid) Meas																	97						
OREAS 96 (4 Acid) Cert																	101						
OREAS 923 (4 Acid) Meas																	85	32					
OREAS 923 (4 Acid) Cert																	83.0	31.4					
OREAS 923 (4 Acid) Meas																	81	32					
OREAS 923 (4 Acid) Cert																	83.0	31.4					
OREAS 621 (4 Acid) Meas																	> 5000	14					
OREAS 621 (4 Acid) Cert																	13600	14.2					
OREAS 621 (4 Acid) Meas																	> 5000	14					
OREAS 621 (4 Acid) Cert																	13600	14.2					
Oreas 621 (Aqua Regia) Meas																							
Oreas 621 (Aqua Regia) Cert																							
OREAS 522 (4 Acid) Meas																	25	16					
OREAS 522 (4 Acid) Cert																	12.5	16.2					
OREAS 522 (4 Acid) Meas																	21	16					
OREAS 522 (4 Acid) Cert																	12.5	16.2					

Analyte Symbol	Pr	Nd	Sm	Eu	Gd	Tb	Dy	Ho	Er	Tm	Yb	Lu	Hf	Ta	W	Tl	Pb	Li	Bi	Th	U	Re	I
Unit Symbol	ppm	ppm	ppm																				
Lower Limit	0.01	0.05	0.01	0.005	0.01	0.01	0.01	0.01	0.01	0.005	0.01	0.002	0.1	0.01	0.5	0.05	5	1	0.1	0.05	0.01	1	0.5
Method Code	FUS-MS	TD-ICP	TD-ICP	FUS-MS	FUS-MS	FUS-MS	INAA	INAA															
OREAS 263 (Aqua Regia) Meas																							
OREAS 263 (Aqua Regia) Cert																							
DMMAS 122b Meas																							
DMMAS 122b Cert																							
GS316-3 Meas																							
GS316-3 Cert																							
OREAS 130 (Aqua Regia) Meas																							
OREAS 130 (Aqua Regia) Cert																							
OREAS 153b (Aqua Regia) Meas																							
OREAS 153b (Aqua Regia) Cert																							
OREAS 153b (Aqua Regia) Meas																							
OREAS 153b (Aqua Regia) Cert																							
OREAS 153b (Aqua Regia) Meas																							
OREAS 153b (Aqua Regia) Cert																							
Oreas 623 (Aqua Regia) Meas																							
Oreas 623 (Aqua Regia) Cert																							
Oreas 623 (Aqua Regia) Meas																							
Oreas 623 (Aqua Regia) Cert																							
IG_BH02_LG015 Orig	12.4	49.8	8.94	2.45	6.49	0.78	4.05	0.70	2.01	0.289	1.74	0.248	3.2	0.38	< 0.5	0.43			< 0.1	5.97	2.10		
IG_BH02_LG015 Dup	12.3	49.1	8.78	2.39	6.51	0.78	4.16	0.73	1.91	0.260	1.61	0.249	3.2	0.38	0.5	0.51			< 0.1	5.94	2.14		
IG_BH02_LG023 Orig																	< 5	55					
IG_BH02_LG023 Dup																	6	54					
IG_BH03_LG006 Orig	2.69	8.85	1.56	0.326	1.10	0.15	0.74	0.12	0.31	0.041	0.25	0.038	4.1	0.73	< 0.5	0.41			< 0.1	4.58	1.53		
IG_BH03_LG006 Dup	2.70	9.07	1.65	0.320	1.17	0.14	0.70	0.13	0.32	0.040	0.22	0.028	2.7	0.68	< 0.5	0.45			< 0.1	4.89	1.56		
IG_BH03_LG008 Orig																	5	78					
IG_BH03_LG008 Dup																	< 5	77					
IG_BH03_LG012 Orig																							
IG_BH03_LG012 Dup																							
IG_BH03_LG014 Orig																							
IG_BH03_LG014 Dup																							

Analyte Symbol	Pr	Nd	Sm	Eu	Gd	Tb	Dy	Ho	Er	Tm	Yb	Lu	Hf	Ta	W	Tl	Pb	Li	Bi	Th	U	Re	I
Unit Symbol	ppm	ppm	ppm	ppm	ppm	ppm	ppm	ppm	ppm	ppm	ppm	ppm	ppm	ppm	ppm	ppm	ppm	ppm	ppm	ppm	ppm	ppm	ppm
Lower Limit	0.01	0.05	0.01	0.005	0.01	0.01	0.01	0.01	0.01	0.005	0.01	0.002	0.1	0.01	0.5	0.05	5	1	0.1	0.05	0.01	1	0.5
Method Code	FUS-MS	FUS-MS	FUS-MS	FUS-MS	FUS-MS	FUS-MS	FUS-MS	FUS-MS	FUS-MS	FUS-MS	FUS-MS	FUS-MS	FUS-MS	FUS-MS	FUS-MS	FUS-MS	TD-ICP	TD-ICP	FUS-MS	FUS-MS	FUS-MS	INAA	INAA
IG_BH03_LG021 Orig																	< 5	63					
IG_BH03_LG021 Dup																	5	63					
Method Blank																							
Method Blank																							
Method Blank																							
Method Blank																							
Method Blank	< 0.01	< 0.05	< 0.01	< 0.005	< 0.01	< 0.01	< 0.01	< 0.01	< 0.01	< 0.005	< 0.01	< 0.002	< 0.1	< 0.01	< 0.5	< 0.05			< 0.1	< 0.05	< 0.01		
Method Blank																							
Method Blank																							
Method Blank																							
Method Blank																	< 5	< 1					
Method Blank																	< 5	< 1					
Method Blank																	< 5	< 1					
Method Blank																	< 5	< 1					
Method Blank																	< 5	< 1					
Method Blank																	< 5	< 1					
Method Blank																	< 5	< 1					
Method Blank																	< 5	< 1					
Method Blank																	< 5	< 1					
Method Blank																	< 5	< 1					
Method Blank																	< 5	< 1					